UNIVERSITÉ DU QUÉBEC À MONTRÉAL

OCEANOGRAPHIC CHANGES OFF CANADIAN COASTS IN THE 20TH AND 21ST CENTURIES: GEOCHEMICAL PERSPECTIVES FROM DEEP-WATER CORALS

THESIS
PRESENTED
AS PARTIAL REQUIREMENT FOR THE DEGREE
OF DOCTOR OF PHILOSOPHY IN EARTH AND ATMOSPHERIC SCIENCES

PAR
SAMUEL DAVIN

JUIN 2019

UNIVERSITÉ DU QUÉBEC À MONTRÉAL

ÉTUDE DES CHANGEMENTS OCÉANOGRAPHIQUE CÔTIERS AU LARGE DU CANADA DURANT LES 20ÈME ET 21ÈME SIÈCLES : APPROCHE GÉOCHIMIQUE PAR LES CORAUX D'EAUX PROFONDES

THÈSE
PRÉSENTÉE
COMME EXIGENCE PARTIELLE
DU DOCTORAT EN SCIENCES DE LA TERRE ET DE L'ATMOSPHÈRE

PAR
SAMUEL DAVIN

JUIN 2019

ACKNOWLEDGEMENTS

First and foremost I wish to thank my supervisors, Claude Hillaire-Marcel and Evan Edinger, for their support and guidance during this project. From project conception to project completion they have always been available, in one form or another, to provide guidance on the subjects of life, chemistry, and the sea. I extend my gratitude to Yves Gelinas and Owen Sherwood for taking on roles as mentors, and for assisting with some of the more challenging aspects of my doctoral research. I would also like to thank my co-authors, Enno Schefuß and Carly Buchwald, for their assistance and patience as I found my feet in complex terrain.

Laboratory support at Geotop was provided Jean-François Hélie, Agnieszka Adamowicz, Bassam Ghaleb, and André Poirier. I extend my thanks to Michael Kucera for hosting me at MARUM (Universität Bremen) during my research stay in Germany, and to Moritz Lehmann for hosting me at the Universität Basel (Departement Umweltwissenschaften) during my research stay in Switzerland. I am especially grateful to Thomas Kuhn the many hours he spent working with me in the laboratory. I would be remiss to exclude Nicole Turcot, executive secretary of Geotop, from this list. Nicole, I would not have made it this far without your frequent assistance.

Numerous members of ArcticNet and VITALS, the captains and crews of the C.C.G.S. Amundsen and R/V Polarstern, and affiliated researchers and technicians have played critical roles in the acquisition of samples presented in this work. Similarly, I would also like to thank Jean-Éric Tremblay (Université Laval) for making available nutrient datasets collected during the C.C.G.S. Amundsen 2016 field season, which have provided context to my own work.

Beyond the scope of my academic work, there are a number of individuals who have made daily life in Montreal a pleasure. I am especially thankful for time spent outdoors with Charlie Beard, Chelsie Kadgien, Cornelia Roffeis, Julien Tremblay-Gravel, and toothy-snouted Balto. Where will I find such camaraderie again? Too late we met, too soon we part. To my understanding and equally delightful co-locators, Sophie Fiola and Mathieu Tremblay-Gravel, please know you are deeply appreciated. Renée Carter, Rebecca Paisley, and Coralie Zorzi: thank you for your friendship, advice, and wit.

To my family, to whom this work is dedicated, what can I say? You taught me that true wealth is found at the edges of fields and under pines. Thank you for your love and sacrifices.

This work was funded by scholarships to S.D. from ArcTrain, Geotop, VITALS, and by grants to C.H-M. and E.E. from the Natural Sciences and Engineering Research Council of Canada.

TABLE OF CONENTS

LIST OF FIGURES

LIST OF TABLES

RÉSUMÉ

En dépit de l'importance stratégique, économique et climatique des hautes latitudes de l'Hémisphère Nord, la compréhension de l'océanographie arctique et subarctique reste entravée par la rareté des archives instrumentales continues et leur brièveté, lorsqu'elles existent. Dans la présente étude, des proxy-données obtenues à partir de squelettes de coraux profonds ont été utilisées pour combler les lacunes des enregistrements instrumentaux. Deux genres d'octocoraliens d'eaux profondes ont été examinées : Primnoa et Keratoisis. Ces genres représentent deux des taxons de coraux dominants le long des marges canadiennes et ont été choisis pour leur abondance relative, leur longévité potentielle (à l'échelle de la centaines d'années) et pour la présence de stries de croissance protéiniques et carbonatées dans leur squelette, qui recèlent des informations distinctes et complémentaires sur les processus océanographiques gouvernant leur croissance. Alors que la composition isotopique des composants squelettiques protéiques de ces genres sont sensibles à l'écologie trophique des colonies, les éléments en traces et la composition isotopique de la calcite répondent aux propriétés de l'eau de mer ambiante. Dans les pages qui suivent, on trouvera trois chapitres focalisés sur l'interaction des processus biologiques, chimiques et physiques, autour des marges canadiennes, dans le but d'améliorer les connaissances sur les changements océanographiques des mers nordiques.

Le chapitre I présente une nouvelle approche méthodologique basée sur les teneurs en deutérium des stries protéiniques de croissance de cinq colonies de Primnoa prélevées dans le détroit de Georgie (sur la côte pacifique), le nord-ouest de l'Atlantique Nord et la mer du Labrador. Les teneurs en deutérium et la chimie de deux colonies proximales sont étroitement corrélées, tandis que des différences significatives de teneur en deutérium (> 30‰) sont observées entre les colonies issues de bassins éloignés. A l'aide d'analyses complémentaires des isotopes stables du carbone et de l'azote des spécimens étudiés, on a pu conclure que les teneurs en deutérium des anneaux protéiniques de croissance de Primnoa était liée à la teneur en deutérium de sa diète, elle-même dictée au moins partiellement par les teneurs en deutérium de l'eau de mer de surface. Le plus long enregistrement des teneurs en deutérium dans une colonie de P. pacifica du détroit de Georgie, âgée de 40 ans, démontre une corrélation étroite avec les enregistrements instrumentaux de la salinité de surface ($r = 0.67$, $p=0,0013$) et avec le contraste saisonnier ($r = 0,75$, $p <0,001$), conduisant à conclure que les teneurs en deutérium des coraux profonds être utilisées comme « proxy » de la salinité et de l'hydrographie des eaux de surface.

Le chapitre II est une étude des conditions hydrographiques à la hauteur du talus continental de Terre-Neuve au cours des 20^{e} et 21^{e} siècles, basée sur les composants calcite et protéinique de coraux bambous Keratoisis grayi. Dans cette étude, les mesures des rapports élémentaires Ba/Ca et Pb/Ca des segments calcitiques ds squelettes ont été couplées à l'analyse des teneurs en ^{15}N et ^{13}C des anneaux protéiniques de croissance des nœuds intermédiaires. Un bon accord s'observe entre les données extraites de deux colonies distinctes, démontrant la reproductibilité des enregistrements géochimiques dans Keratoisis. Dans les deux colonies, on observe une augmentation constante des teneurs en ^{15}N et ^{13}C avant 1960, i.e., avant les émissions anthropiques de CO_2 n'affectent de facçon importante la composition isotopique du carbone océanique. Les données Ba/Ca des deux colonies sont positivement corrélées à celles en 13C pendant l'intervalle précédant les changements d'origine anthropique ($r = 0,56$, $p <0,001$; $r = 0,71$, $p <0,001$), confirmant la validité du rapport Ba/Ca des squelettes coralliens comme indicateur de la productivité marine. Les deux colonies présentent des pics Pb/Ca synchrones, associés à l'utilisation maximale du plomb dans l'essence. Potentiellement un marqueur de l'âge des spécimens, le pic du rapport Pb/Ca présente un décalage temporel d'environ 20 ans, avec celui de l'utilisation maximale du Pb. L'enrichissement continu en ^{15}N des deux colonies de coraux est interprétée en relation avec l'intensification de la gyre subpolaire au cours du XX^{e} siècle, associée à des décalages modaux à long terme de la NAO. Nous concluons que les coraux bambous d'eau profonde recueillis vivants peuvent fournir un éventail d'importants indicateurs paléocéanographiques dans les sites de haute latitude septentrionale dépourvus d'enregistrements instrumentaux et qu'ils présentent en particulier des liens avec les oscillations climatiques à grande échelle.

Le chapitre III s'éloigne de l'étude directe sur les coraux d'eau profonde, mais a été entrepris dans le but de comprendre les mécanismes qui régissent la composition isotopique de l'azote fixé dans les squelettes coralliens profonds. Ce chapitre aborde les processus de recyclage de l'azote dans la mer du Labrador et le détroit de Davis, en particulier le long du plateau et du talus continentaux du Labrador. Les nitrates, un nutriment biolimitant dans l'Atlantique Nord, gouvernent la croissance du phytoplancton, qui constitue la base du réseau trophique marin et assure la majeure partie du régime alimentaire des coraux profonds. L'étude a consisté en mesure des compositions isotopiques des nitrates (^{15}N et ^{18}O) de l'eau de mer, à partir d'échantillons l'été et l'automne 2016, à travers de 11 profils bathymétriques, entre 53° à 68° de latitude nord. À partir de ces données, ainsi que informations complémentaires sur les concentrations en éléments nutritifs, on conclut à une limitation généralisée des nitrates dans la zone épipélagique le long de la côte du Labrador, bien que l'on relève également un taux de renouvellement des nitrates (fixation et/ou reminéralisation) par rapport aux pertes (dénitrification) variable géographiquement. Dans le détroit de Davis, le renouvellement des nitrates dans la zone épipélagique est limité par la stratification de la colonne d'eau, surmontée d'un couvert d'eau de mer froide et moins saumâtre. De ce fait, la disponibilité en nitrates dans le détroit de Davis est fortement

dépendante recyclage (reminéralisation et nitrification ultérieure) dans la partie supérieure de la colonne d'eau. Plus au sud, dans la mer du Labrador, les eaux sont moins stratifiées et le renouvellement des nitrates semble facilité. Un flux de nitrates isotopiquement légers, à la sortie du détroit d'Hudson, est notable. Il conduit à un enrichissement en à travers l'action combinée de la fixation de l'azote et des mélanges verticaux. En aval, le long de la péninsule du Labrador, la composition isotopique des nitrates dissous s'enrichit en ^{15}N par rapport aux eaux sortant du détroit d'Hudson. On en conclut que l'apport de nitrates complémentaires est spécifique du détroit d'Hudson. Alors que le nord du plateau du Labrador bénéficie de l'apport de ces nitrates frais, la composition isotopique des nitrates sur le talus du Labrador suggère que le mélange entre les eaux du plateau et celles du talus est minime. Ces résultats apportent une information importante en ce qui a trait à l'écologie trophique de l'Atlantique du Nord-Ouest.

Mots clés: Corail, Arctique, géochimie

ABSTRACT

Despite the strategic, economic, and climatic significance of the northern high latitudes, our contextual understanding of Arctic and sub-Arctic oceanography is hampered by the scarcity of continuous, long-term instrumental records. Here, oceanographic proxy data from the skeletons of deep-water corals has been used to extend and supplement gaps in the instrumental record. Two genera of deep-water octocoral are discussed in this work: *Primnoa* and *Keratoisis*. These genera represent two of the dominant coral taxa on the Eastern and Western Canadian Margin, and were chosen for their relative prevalence, potential longevity (on the scale of hundreds of years), and for the incremental growth secretions expressed in both the proteinaceous and calcium carbonate components of their hybrid skeletons, which harbor distinct and complementary records of oceanographic processes: While the isotopic compositions of the proteinaceous skeletal components of these genera are sensitive to the trophic ecology of the coral, the calcite chemical and trace element compositions are sensitive to properties of ambient seawater. In this work I present three chapters which focus on the interplay of biological, chemical, and physical processes on and around the Canadian margins in an effort to enhance our understanding of northern oceanography.

Chapter I is a method development piece which explores the deuterium content of annual proteinaceous growth rings of five Primnoa colonies collected from the Strait of Georgia, the northwestern North Atlantic, and the Labrador Sea. The deuterium content and general trend of proximal colonies are closely matched, while significant differences in deuterium content (>30‰) are noted between distal colonies. Coupled with stable carbon and nitrogen isotope measurements, we conclude that deuterium content in the proteinaceous growth rings of Primnoa is related to the dietary deuterium content, which in turn is at least partially dictated by the deuterium content of surface seawater. The longest coral deuterium record, extracted from a 40-year old P. pacifica colony in the Strait of Georgia, shares a strong relationship with instrumental records of annual sea surface salinity (SSS) ($r=0.67$, $p=0.0013$) and with the strength of annual SSS seasonality ($r=0.75$, $p<0.001$), indicating the potential for coral deuterium content to be used as a proxy for SSS and hydroclimatic variability.

Chapter II is a proxy study of oceanographic conditions on the Newfoundland Slope during the 20th and 21st centuries based on the calcite and proteinaceous skeletal components of two ~80 year-old colonies of the deep-water bamboo coral Keratoisis grayi. In this study measurements of skeletal calcite Ba/Ca and Pb/Ca are coupled with $\delta^{15}N$ and $\delta^{13}C$ in proteinaceous growth rings. We find generally good agreement between data extracted from the two distinct colonies, demonstrating the reproducibility of geochemical records in Keratoisis. In both colonies a steady increase in the $\delta^{15}N$ and $\delta^{13}C$ is observed prior to 1960, before $\delta^{13}C$ began to decline in response to anthropogenic CO_2 emissions. Ba/Ca measurements of both colonies show a positive correlation with δ13C prior to the onset of these recent anthropogenically-driven changes ($r=0.56$, $p < 0.001$; $r=0.71$, $p < 0.001$), supporting the use of Ba/Ca in coral skeletons as a proxy for marine productivity. Both colonies exhibit two synchronous Pb/Ca peaks associated with anthropogenic lead use. In addition to serving as a method of age validation, the temporal lag of ~20 years between periods of high Pb production and the appearance of heightened Pb concentrations in the corals supports a decadal-scale residence time of Pb on the northwestern North Atlantic Slope. Continuous (lifelong) $\delta^{15}N$ enrichment in both corals provides support for intensification of the sub-polar gyre during the 20th century associated with long-term NAO modal shifts. It is concluded that live-collected deep-water bamboo corals can provide an array of important paleoceanographical proxies at high northern latitude sites lacking instrumental recordings, and of linkages with large scale climate oscillations.

Chapter III departs from the direct study of deep-water corals but was undertaken in order to get a better insight into the mechanisms governing the isotopic composition of nitrogen ultimately fixed in deep coral skeletons. It investigates the nitrogen cycling processes in the Labrador Sea and Davis Strait, with a strong focus on the Labrador Shelf and Slope. Nitrate, a biolimiting nutrient in the North Atlantic, constrains the growth of phytoplankton, which are the foundation of the marine food web and make up the bulk of deep-water coral diet. This study is centered on the dual isotopic composition of nitrate ($\delta^{15}N$ and $\delta^{18}O$) in seawater collected in summer and autumn 2016 from 11 depth profiles spanning from 53 to 68°N. From these data, as well as from supporting nutrient concentration data, we find widespread nitrate limitation of the epipelagic zone in the Labrador Sea Corridor, though we note the rate of nitrate renewal (fixation and/or remineralization) relative to nitrate loss (denitrification) to vary spatially. In the Davis Strait nitrate renewal in the epipelagic zone is limited by stratification of the water column, topped by a confining cap of cold, fresh seawater. As a result, nitrate renewal in the Davis Strait is apparently highly dependent on nitrate recycling (remineralization and subsequent nitrification) in the upper water column. Further south, conditions in the Labrador Sea are less stratified, and nitrate renewal appears to be marginally enhanced. Of special interest is the appearance of isotopically light nitrate exiting the Hudson Strait, indicating enhanced rates of nitrate renewal through the combined actions of nitrogen fixation and vertical mixing. Downstream, along the Labrador Peninsula, the isotopic composition of dissolved nitrate becomes enriched relative to waters exiting the Hudson Strait, suggesting that enhanced nitrate renewal is a feature unique to the Hudson Strait. While the northern Labrador Shelf benefits from the introduction of fresh nitrate via the Hudson Strait, the isotopic composition of nitrate on the Labrador Slope suggests that mixing between the

Labrador Shelf and Slope is minimal. These findings provide important context to the trophic ecology of the northwestern North Atlantic.

Key words : Coral, Arctic, geochemistry

INTRODUCTION

0.1 General problem

At the time of this writing approximately 110 years have passed since the expeditionary parties of Frederick Cook and Robert Peary attained the North Pole, 108 years since the party of Roald Amundsen attained the South Pole, and perhaps 100 years since the end of the so-called "Heroic Age of Polar Exploration". The world, which even then was at the cusp of massive environmental and social reorganization, has since changed dramatically. Rapid, global industrialization since the 19th century has expanded the human diet to include an ever-growing demand for metals, coal, oil, gas, rare earth elements, and other extractables; wealth associated with this economic revolution has spurred an increasing demand for animal products and consumer goods. Rising to meet consumer demand, humans have released enormous quantities of sequestered fossil carbon into the atmosphere, while simultaneously enacting large-scale land use changes. These actions have driven atmospheric CO_2 levels from a preindustrial concentration of 280 ppm to the present concentration of >400 ppm. Now, in the face of abrupt anthropogenic climate change, the high latitudes have again risen to the forefront of public consciousness.

Perhaps no region is more sensitive to climate change than the Arctic and sub-Arctic (e.g., IPCC, 2014). Despite the importance of the North in regulating the global climate system through such mechanisms as the snow and ice albedo effect, the uptake of atmospheric gases into the ocean through deep-water formation, the sequestration of carbon in permafrost, and the role of landfast ice in regulating global sea level, instrumental records in the North are sparse and often short. This poses a critical issue, as historical records of environmental variability are key to adapting to and planning for anthropogenic climate change. In this regard northern communities are, and will continue to be the most impacted as they attempt to adapt cultural, social, economic, and nutritional practices to a rapidly changing environment. Here, geoscientists have developed proxies to supplement instrumental records. Through several decades of concerted proxy development work and the advent of increasingly advanced mathematical models, the major northern climate transitions since the Pleistocene have been reasonably well-established. Thus, the priority of proxy-based studies has shifted towards two goals: (1) establishing proxy records from high-resolution (sub-decadal) natural archives which may, ideally, be integrated with existing instrumental records; and (2) establishing proxy records near transitional, or otherwise highly dynamic, hydrographic boundaries.

0.2 Research theme

This is a biogeochemistry thesis. Thus, it follows that the works presented herein sit at the intersection of multiple disciplines. While the scope of the three chapeters is broad, I suggest that this breadth provides insight into the dynamic interplay between the biosphere, hydrosphere, lithosphere, and atmosphere which fundamentally shape marine environments and ecosystems. The central theme of this work is the development and assessment of isotopic and geochemical methods for proxy-record reconstruction of the chemical and biological oceanographic variability along the sub-Arctic Canadian margins during the 20th and 21st centuries, based on deep-water coral skeleton recordings. Inspired by the rarity and brevity of instrumental records in the high northern latitudes, this work has been undertaken to infer past environmental variability where instrumental records are lacking. In the face abrupt anthropogenic climate change, this work is intended to contextualize present and future coastal conditions by characterizing environmental variability of the recent past. This thesis addresses three complementary topics: (1) development of deuterium content in deep-water coral skeletons as a proxy for hydroclimatic variability, (2) application of multiple coral-based geochemical proxies of paleoproductivity changes, and (3) exploration of isotopic tracers of nitrate cycling with implications for biological productivity in the northwest North Atlantic. While these studies cover a range of methods, timescales, and locations, the unifying feature of this work is the link between marine trophic ecology and environmental variability. As a result, these studies serve not only as proxy records of environmental change, but as a resource on the trophic health of northern marine environments and on the biology of deep-water corals.

0.3 Oceanographic context

Three study regions, located east and west of Canada, are discussed in this work: (1) The Newfoundland Slope, (2) The Labrador Sea Corridor, and (3) The Strait of Georgia. These locations are discussed in greater depth within the subsequent chapters to which they are pertinent, however, a general overview is provided here. Since the Labrador Sea Corridor and the Newfoundland Slope belong to the northwestern North Atlantic regime, they are discussed together.

0.3.1 North Atlantic

Located between the Labrador Peninsula and western Greenland, the Labrador Sea is a critically important branch of the North Atlantic Ocean: In addition to hosting productive offshore fisheries, the Labrador Sea serves as Canada's strategic gateway from the Atlantic to the Arctic. It also plays a key role in the global climate system as the site of North Atlantic deep-water formation and is one of the few regions where the deep ocean exchanges gases with the atmosphere (Clarke and Coote, 1988; Azetsu-Scott et al., 2003; DeGrandpre et al., 2006).

The Labrador Current originates on the northern Labrador Shelf where the Baffin Current and the West Greenland Current converge. From its origin, the Labrador Current flows south past the Hudson Strait. Here, a portion of Labrador Sea Water enters the Strait and is modified via intense mixing with Hudson Bay and Foxe Basin Water, and waters sourced from the Canadian Island Archipelago to form Labrador Shelf Water (Dunbar, 1951; Kollmeyer et al., 1967). The Labrador Current and its associated shelf and slope flows are advected southwards along the Labrador Peninsula towards Newfoundland. Circulation on the shelf and slope of Newfound is generally characterized by a southeastern advection of the Labrador Current with associated slope and shelf flows (Smith et al., 1937). However, the dominance of the Labrador Current off Newfoundland is impacted by modal fluctuations of the North Atlantic Oscillation (NAO) (Petrie 2007). Positive NAO modal shifts are associated with a simultaneous expansion of the subtropical gyre and an intensification of the subarctic gyre, extending the northern extremity of the Gulf Stream and strengthening the Labrador Current (Han et al., 2010). Under these conditions warm slope water associated with the Gulf Stream is introduced onto the continental slope from Georges Bank to southwestern Newfoundland (Petrie 2010) and colder, more saline waters associated with the Labrador Current occur off northeastern Newfoundland and Labrador. During negative NAO modal shifts the trend is reversed and colder conditions prevail between Georges Bank to the Grand Banks of Newfoundland (Petrie 2007).

0.3.2 Strait of Georgia

The Strait of Georgia (SOG) is a shallow basin located between the Coast Range of British Columbia and Vancouver Island. It is connected to the Pacific Ocean via the Juan de Fuca Strait and by both the Johnstone and Queen Charlotte Straits to the North. It is approximately 240 km long and varies between approximately 20 and 58 km wide;

the basin is relatively shallow, having a maximum depth of 448 m and a mean depth of 157 m. Circulation within the basin is cyclonic. The Fraser River opens into the SOG, and it is from here that the majority of freshwater entering the SOG originates. Hydrographic seasonality in the SOG is strong, and sea surface salinity content changes by up to 6 parts per thousand over the course of a single year. Surface water conditions are generally characterized by warm, saline features during the summer, and cold and fresh conditions in winter and spring, associated with meltwater discharge from the Fraser River (Davenne and Masson, 2001). Warming air temperatures in British Columbia since at least the mid-20th century have affected the timing and intensity of the Fraser River spring freshet (Masson and Cummins 2004).

0.4 Coral

Coral is a term oft used, broadly interpreted, and rarely defined. The general understanding of coral is typically based on a set of presuppositions biased towards tropical-to-subtropical, shallow, reef-building organisms. Such assumptions, while based in truth, are not representative of the diverse collection of organisms actually encompassed by the term. Indeed, coral is a polyphyletic term describing an assemblage of animals found in every ocean basin, which may belong to either of the classes Anthozoa or Hydrozoa. Broadly defined, corals are sessile, marine cnidarians (invertebrates having specialized stinging cells used for prey capture and/or defense) with horn-like or calcium carbonate (aragonitic or calcitic) skeletal components.

Of the more than 5,000 species considered to be coral, only about a third live in waters shallower than 50 m (Cairns 2007). Thus, despite the common assumption that corals are exclusive to shallow and warm marine environments, the majority of coral actually live in deeper water. Furthermore, while shallow species are typically host to photosynthetic symbiotes (zooxanthellae), which supplement the energy requirements of the host coral, deep-water corals (also known as cold-water or deep-sea corals) are heterotrophic. These corals feed opportunistically upon small animals (e.g., zooplankton, small crustaceans) as well asnsinking and/or resuspended particulate organic matter (POM). POM is largely composed of dead phytoplankton, zooplankton, copepods, and bacteria (Griffin & Druffel 1989; Gili & Coma, 1998; Roark et al. 2005; Sherwood et al., 2005a; Sherwood et al., 2008; Williams and Grottoli 2010; Salvo et al., 2018). Coral genera without zooxanthellae are termed azooxanthellate corals. Prey and POM consumed by corals are captured by the array of tentacles (which are equipped with cnidocytes) surrounding the mouth of the polyp and digested in the stomach.

Deep-water corals of the Canadian Margin are ahermatypic, meaning they do not build reefs (Freiwald et al., 1999). They do, however, often grow in aggregations referred to as "gardens" or "thickets" found on the continental shelf and slope within a depth range of 50 to 5000 m on both muddy and hard substrate (Zibrowius and Taviani, 2005; Edinger at al., 2011). Thickets are biological hotspots which play a critical role in the life cycles of many marine organisms, including commercially viable wild fish stock (Dawson et al., 2002). Accordingly, deep-water corals are habitat-forming species critical to the health of the marine ecosystem. Concern has been expressed over the potential economic and social impacts of coral mortality on Canadian communities: In 2017 Canadian fisheries employed 76,400 people and exported $6,864,988 of fish and seafood (Fisheries and Oceans, 2017). As is often the case with organisms living in harsh environments (e.g., alpine vegetation), deep-water corals are long-lived and slow growing (e.g., Andrews et al., 2002; Roark et al., 2005; Noé et al., 2008; Sherwood and Edinger, 2009; Hill et al., 2011). Due to their slow growth and having adapted to live in generally stable conditions year-round (relative to their shallow-water counterparts), deep-water corals are susceptible to rapid environmental change and to physical damage. At present, they are threatened by bottom trawling practices of commercial fishing vessels (Roberts 2002; Edinger et al., 2007; Fuller et al., 2008) and by ongoing ocean acidification brought on by the uptake of anthropogenic CO_2 by the global ocean (Davies et al., 2007; Roberts and Cairns, 2014).

0.4.1 Proxy records from corals

Proxy-based reconstructions of historical and paleo-environmental conditions must begin with an understanding of environmental archives and the types of data which may be obtained from them. Of consideration are the temporal length, time-step resolution, prevalence, and accessibility of the archives from which proxy data is extracted. While an ideal environmental archive will be affected by as few confounding variables as possible, it is understood that all proxy data carries inherent uncertainty due to the multitude of processes operating within the natural environment, as well as from complications associated with the field collection and laboratory handling of physical samples. To date, the principal sources of proxy data for paleoenvironmental reconstructions include the chemical and physical characteristics of ice cores, biogenic and inorganic sediments, geomorphological features, incremental growth layers of some organisms (e.g., trees, mollusk shells, coral, coralline algae), and biological assemblages (e.g., micro- and macrofossils), as well as written records. Historically, paleoceanographic reconstructions have often been based on proxy data from marine sediment cores, which are capable of capturing exceptionally long records spanning millions of years. However, the depositional rates in marine settings (with the notable exception of some fjords) are quite low and are subject to bioturbation, making it difficult to assess short-term oceanographic variability through the study of marine sediments. In recent decades, particularly since the beginning of the 21st century, proxy data extracted from coral skeletons have gained significant interest from the marine science community. Broadly, some corals are valuable as archives of paleoceanographic data due to their longevity, sensitivity to hydrographic variability, geographic prevalence (including the high latitudes), and incremental growth secretions.

Deep-water corals are advantageous for proxy-based oceanographic studies due to their feeding habits and habitats. Deep marine environments are relatively insulated from seasonal variability, and as a result deep-water corals tend to inhabit more stable environments their shallow water counterparts.Similarly, because deep-water corals are azooxanthellate they are not subject to the direct biochemical signatures of photosynthesis. Neither of these benefits are shared by shallow corals or coralline algae. As a result, chemical proxy data extracted from the skeletons of deep-water corals are more apt to reflect long-term environmental and ecological shifts than seasonality or abrupt events. Previous proxy-based studies of boreal, deep-water coral skeletons generally fall into one of two categories: those which focus on the mineralized skeletal components, and those which focus on the proteinaceous skeletal components. A major exception are studies which estimate the reservoir age of water masses by contrasting the radiocarbon age of proteinaceous skeletal growth (representing a surface ocean ^{14}C age due to the trophic link to exported POM) with mineralized skeletal growth (representing a ^{14}C age of water at depth) (e.g. Roark et al., 2005; Sherwood et al., 2008).

The calcium carbonate skeletal components of corals are sensitive to the properties of seawater, which can be expressed as variations in skeletal trace element composition (e.g. Lea et al., 1989b; Serrato-Marks et al., 2017). Accordingly, the mineralized skeletal components of deep-water corals have attracted interest for their potential to yield well-resolved records of deep-sea water mass variability (summarized in Sinclair et al., 2011). Advancements in laser ablation inductively coupled plasma mass spectrometry (LA-ICP-MS) have allowed researchers to create high-resolution measurements of trace element variability across the radial growth of mineralized coral skeletons (e.g., Sinclair et al., 1998). Of the deep-water corals found along the

Canadian margins, bamboo corals, such as *Keratoisis sp.,* are excellent candidates for trace element studies conducted by LA-ICP-MS because the calcite internodes of bamboo corals are not interrupted by interbedded proteinaceous growth as they are in some corals (e.g., *Primnoa sp.*). Although biological effects can influence geochemical records in deep-water corals (Thresher et al., 2007), the variability of some trace elements have been found to have a good level of reproducibility and may be used to interpret environmental signals (Sinclair et al., 2011). Presently, some trace elements of special interest in corals are barium, magnesium, strontium, and lead: Mg/Ca has been interpreted as a paleotemperature proxy in calcitic corals (Thresher et al., 2004, 2010; Sinclair et al., 2005). The usefulness of paleotemperature proxies in deep-water corals may be limited due to the relatively cold and stable environments they inhabit. Sr partitioning in calcite is dependant on precipitation rate (Zhong and Mucci, 1989), wherein evevated Sr/Ca correspond to rapid precipitation. As such, Sr/Ca has been interpreted as a proxy for coral growth rate (Hill et al., 2005; Roark et al., 2005; Thresher et al., 2007). Pb/Ca is typically interpreted as a proxy for lead contamination from anthropogenic sources such as the combustion of coal, and the use of leaded paint and gasoline (e.g. Shen and Boyle, 1987). Measurements of bioaccumulated Pb in corals can be related to historical documentation of lead production, thus allowing researchers to estimate the residence time of anthropogenic lead in marine environments. Ba/Ca in corals has been linked to the barium content of seawater (Lea et al., 1989b; LaVigne et al., 2016; Serrato-Marks et al., 2017). Ba in the marine system is associated with organic matter and exhibits “nutrient-like” behavior, in that Ba concentrations are depleted in surface waters and enriched at depth (Dehairs et al., 1980). Recently, heightened Ba/Ca ratios in crustose coralline algae on the Newfoundland Shelf has been linked to periods of decreased biological utilization (Chan et al., 2017). At present Ba/Ca in deep-water corals is of interest as a potential proxy for biological productivity.

The stable carbon ($\delta^{13}C$) and nitrogen ($\delta^{15}N$) isotopic composition of animal tissues reflect diet and trophic level (DeNiro et al., 1981; Fry and Sherr, 1989). The diet of deep-water corals is largely composed of sinking and resuspended POM exported from the epipelagic zone (Sherwood et al., 2005a). Since the $\delta^{13}C$ and $\delta^{15}N$ values of POM undergo minimal alteration with depth (Altabet and Francois, 1994; Muzuka and Hillaire-Marcel, 1999), it follows that the $\delta^{13}C$ and $\delta^{15}N$ compositions of proteinaceous coral skeletal tissue can be used to track surface ocean processes related to trophic dynamics (Heikoop et al., 2002; Sherwood et al., 2005a). Bulk $\delta^{15}N$ and $\delta^{13}C$ of incremental growth rings in boreal, deep-water genera including *Primnoa* and *Keratoisis* are used to reconstruct time-resolved trends in primary productivity. While the $\delta^{13}C$ and $\delta^{15}N$ values of proteinaceous coral growth are closely tied to trophic ecology, the two isotope systems have differing sensitivities. $\delta^{15}N$ is more sensitive to changes in trophic level —$\delta^{13}C$ increases by ~1.1‰ and $\delta^{15}N$ increases by approximately 3.4‰ with each increase in trophic level (DeNiro and Epstein, 1981)— and $\delta^{13}C$ is sensitive to the community assemblage and lipid content of phytoplankton (Fry and Sherr, 1989). Furthermore, compound specific analysis of individual amino acids has been demonstrated as a method of deconvolving trophic level versus nitrogen source effects on the $\delta^{15}N$ value of coral tissue (Sherwood et al., 2011). These results suggest that bulk $\delta^{15}N$ in coral tissue may in some cases be interpreted as a proxy for the isotopic composition of bioavailable ("fixed") nitrate rather than trophic level variability.

Two genera of deep-water octocoral are discussed in this work: *Primnoa* and *Keratoisis*. These genera represent two of the dominant coral taxa on the Canadian Margin, and were chosen for longevity and for the incremental growth secretions expressed in both the proteinaceous and calcium carbonate components of their hybrid skeletons.

0.4.2 *Primnoa*

Primnoa is dominant genus of deep-water gorgonian octocoral (corals featuring eight-fold symmetry) characterized by an arborescent skeleton with inner calcium carbonate structures interbedded amongst annual proteinaceous growth rings composed of the compound *gorgonin.* Gorgonin constitues the proteinaceous skeletal growth of Primnoa, and serves to provide colonies with a degree of dynamic strength. Mature colonies are found to develop a massive carbonate outer cortex. *Primnoa* is found in boreal and cold northern temperate waters at depths from 50 to 3500 m (Cairns and Bayer, 2005). It is of particular interest due to its longevity (on the scale of tens to hundreds of years) and its *annual* gorgonin growth rings (Sherwood et al., 2005). Primnoa is azooxanthellate and is known to feed primarily upon exported POM (Griffin & Druffel 1989, Roark et al. 2005, Sherwood et al. 2005a).

Two species of *Primnoa* are confronted in the first chapter of this work: *P. pacifica* and *P. resedaeformis*. *P. pacifica* is distributed throughout the Eastern and Western Pacific and has been reported as far north as Glacier Bay, Alaska (60°N) (Cairns et al., 2007), and as far south as off La Jolla, California (33°N) (Cimberg et al., 1981). *P. resedaeformis* is distributed throughout the Eastern and Western Atlantic. It has been reported from as far North as coastal Norway (70°N) (Kramp, 1939) to as far south as Virginia Beach, Virginia (37°N) (Heikoop et al., 2002).

0.4.3 *Keratoisis*

Keratoisis grayi is the sole species of *Keratoisis* discussed in this work. *K. grayi* is an arborescent "bamboo" octocoral, named for its resemblance to bamboo, belonging to the family *Isididae*. *Keratoisis* skeletons are arborescent and feature proteinaceous growth nodes connected to massive internodal calcitic growth via a hollow central growth axis (Figure 1). Distribution of *K. grayi* includes muddy shelf and slope environments in the North Atlantic, including off Nova Scotia, Newfoundland, and Labrador (Gass and Willison, 2005; Wareham and Edinger, 2007; Buhl Mortensen et al., 2015; Neves et al., 2015; Cordeiro et al. 2018*)*. It is observed to grow in dense thickets and is curiously noted for bioluminesent polyps, which are sparse in comparison to the densely-packed polyps of *Primnoa*.

0.5 Marine nitrogen cycling

The marine food web is founded on the primary production of phytoplankton dwelling within the epipelagic zone of the ocean. Dead and dying phytoplankton sink and aggregate, forming the basis of POM (commonly known as *marine snow*). Sessile heterotrophs, including deep-water corals, depend on exported POM as a primary food source (e.g., Sherwood et al., 2005) and may be impacted by changes in phytoplankton abundance, community assemblage, and the timing of peak phytoplankton blooms. Perhaps the greatest constraint on marine phytoplankton growth is the availability of bioavailable ("fixed") nitrogen in the epipelagic zone (e.g., Kilham and Hecky, 1988; Antia et al., 1991 ; Seitzinger and Sanders, 1999).

Despite requiring nitrogen, the bulk of planktonic marine organisms lack nitrogenase enzymes and cannot directly assimilate the most prevalent N species, dinitrogen (N_2). In unpolluted environments, phytoplankton rely upon diazotrophs to convert N_2 into ammonium (NH_4^+), nitrifying bacteria for the production of nitrate (NO_3^-), nitrite (NO_2^-), and upon the remineralization of organic N from decomposing organic matter (Howarth et al., 1988). Of these species, NO_3^- is the predominant form of fixed nitrogen present in the ocean. Once assimilated by an organism, NO_3^- may be recycled back into the marine system via *remineralization* and subsequent *nitrification* or lost via *denitrification.* During remineralization decaying organic matter breaks down into organic forms of N and NH_4^+. The organic N is eventually returned to the dissolved inorganic nitrogen (DIN) pool and the remineralized NH_4^+ undergoes nitrification wherein it is oxidized back to NO_3^-. Denitrification is the primary sink of fixed N in marine environments (Seitzinger, 1988; Zehr and Ward, 2002), wherein NO_3^- is reduced by bacteria to N_2 gas through a series of intermediate products, then lost to dissolved and atmospheric nitrogen.

Marine nitrogen cycling is highly dynamic and the effects of fixation, assimilation, remineralization, nitrification, and denitrification can overprint one another. By studying the coupled stable nitrogen and oxygen isotopic compositions ($\delta^{15}N$ and $\delta^{18}O$) of NO_3^-, it is possible to infer information about the biogeochemical transformations NO_3^- has undergone and to determine the relative rates of fixation and denitrification (e.g., Sigman et al., 2001; Casciotti et al. 2002; Granger et al. 2004). Byidentifying zones of net fixation/denitrification, it becomes possible to demarcate the ocations and processes which are responsible for supporting the phytoplankton and, by extension, the marine food web.

0.6 A note on authorship

Each chapter presented here is a collaborative work of which I am the primary author. Accordingly, statements are made from the collective standpoint of "we". Similarly, materials, results, and conclusions are posessively referred to as "ours". In addition to having composed each manuscript, I have played the lead role in all laboratory analyses and subsequent data manipulations, as well as a major role in sample collection. Of notable exception are coral samples obtained prior to 2014 (provided by Evan Edinger, The Memorial University of Newfoundland), the radiometric dates of coral specimen 2452 presented in Chapter II (attributable to Sherwood and Edinger, 2009), and some of the nutrient concentration data presented in Chapter III (collected by ArcticNet staff aboard the CCGS Amundsen and recovered from the Polar Data Catalogue with permission from Professor Jean-Éric Tremblay). Professor Claude Hillaire-Marcel, a co-author of all three manuscripts, provided expert advice concerning all topics pertaining to geochemistry, as well on North Atlantic oceanography. Additionally, Professor Hillaire-Marcel played a significant role in the conception of Chapters I and

II. Professor Evan Edinger, co-author of Chapters I and II, provided expert advice regarding the biology of deep-water corals, as well as general insight into marine trophic ecology. Dr. Enno Schefuß, a co-author of Chapter I, provided extensive laboratory assistance measuring the deuterium content of coral samples, and expert council on the stable isotopes of hydrogen. Professor Owen Sherwood, co-author of Chapter III, assisted with seawater sampling in 2016 aboard the CCGS Amundsen, and with the interpretation of nitrate isotope data. Professor Carolyn Buchwald, also a co-author of Chapter III, provided expert advice on the behavior of nitrogen and oxygen isotopes in dissolved nitrate. All co-authors contributed to the editing of the manuscripts on which they are listed as co-authors.

0.7 References

Altabet, M. A., & Francois, R. (1994). Sedimentary nitrogen isotopic ratio as a recorder for surface ocean nitrate utilization. *Global Biogeochemical Cycles*, 8(1), 103-116.

Andrews, A. H., Cordes, E. E., Mahoney, M. M., Munk, K., Coale, K. H., Cailliet, G. M., & Heifetz, J. (2002). Age, growth and radiometric age validation of a deep-sea, habitat-forming gorgonian (Primnoa resedaeformis) from the Gulf of Alaska. *Hydrobiologia*, 471(1-3), 101-110.

Antia, N. J., Harrison, P. J., & Oliveira, L. (1991). The role of dissolved organic nitrogen in phytoplankton nutrition, cell biology and ecology. *Phycologia*, 30(1), 1-89

Azetsu-Scott, K., Jones, E. P., Yashayaev, I., & Gershey, R. M. (2003). Time series study of CFC concentrations in the Labrador Sea during deep and shallow convection regimes (1991–2000). *Journal of Geophysical Research: Oceans*, 108(C11).

Buhl-Mortensen, L., Olafsdottir, S. H., Buhl-Mortensen, P., Burgos, J. M., & Ragnarsson, S. A. (2015). Distribution of nine cold-water coral species (Scleractinia and Gorgonacea) in the cold temperate North Atlantic: effects of bathymetry and hydrography. *Hydrobiologia*, 759(1), 39-61.

Cairns, S. D., & Bayer, F. M. (2005). A review of the genus Primnoa (Octocorallia: Gorgonacea: Primnoidae), with the description of two new species. *Bulletin of Marine Science*, 77(2), 225-256.

Cairns, S. D. (2007). Deep-water corals: an overview with special reference to diversity and distribution of deep-water scleractinian corals. *Bulletin of Marine Science*, 81(3), 311-322.

Casciotti, K. L., Sigman, D. M., Hastings, M. G., Böhlke, J. K., & Hilkert, A. (2002). Measurement of the oxygen isotopic composition of nitrate in seawater and freshwater using the denitrifier method. *Analytical Chemistry*, 74(19), 4905-4912.

Chan, P., Halfar, J., Adey, W., Hetzinger, S., Zack, T., Moore, G. W. K., Wortmann, U.G,, Williams, B., & Hou, A. (2017). Multicentennial record of Labrador Sea primary productivity and sea-ice variability archived in coralline algal barium. *Nature Communications*, 8, 15543.

Cimberg, R. L., Gerrodette, T., & Muzik, K. (1981). Habitat requirements and expected distribution of Alaska coral. Final Report, Research Unit, 601, 207-308.

Clarke, R. A., & Coote, A. R. (1988). The formation of Labrador Sea Water. Part III: The evolution of oxygen and nutrient concentration. *Journal of Physical Oceanography*, 18(3), 469-480.

Cordeiro, R., van Ofwegen, L., & Williams, G. (2018). World List of Octocorallia. Keratoisis grayi Verrill, 1878. Accessed through: World Register of Marine Species at: http://www.marinespecies.org/aphia.php?p=taxdetails&id=158285.

Davenne E. & Masson D. (2001). Water properties in the Straits of Georgia and Juan de Fuca. Fisheries and Oceans Canada. Retrieved from www.sci.pac.dfo-mpo.gc.ca/osap/projects/straitofgeorgia/JdFG_e.pdf.

Davies, A. J., Roberts, J. M., & Hall-Spencer, J. (2007). Preserving deep-sea natural heritage: emerging Issues in offshore conservation and management. *Biological* Conservation, 138(3), 299-312.

Dawson, J. (2002). Biogeography of azooxanthellate corals in the Caribbean and surrounding areas. *Coral Reefs*, 21(1), 27-40.

DeGrandpre, M. D., Körtzinger, A., Send, U., Wallace, D. W., & Bellerby, R. G. J. (2006). Uptake and sequestration of atmospheric CO2 in the Labrador Sea deep convection region. *Geophysical Research Letters*, 33(21).

Dehairs, F., Chesselet, R. & Jedwab, J. (1980).Discrete suspended particles of barite and the barium cycle in the open ocean. *Earth and Planetary Science Letters*, 49, 528–550.

DeNiro, M. J., & Epstein, S. (1981). Influence of diet on the distribution of nitrogen isotopes in animals. *Geochimica et Cosmochimica Acta*, 45(3), 341-351.

Dunbar M. J., (1951). Eastern Arctic Waters, Canada. *Fisheries Research Board Bulletin*, 88, 1-131.

Edinger, E., Baker, K., Devillers, R., & Wareham, V. (2007). Coldwater corals off Newfoundland and Labrador: distribution and fisheries impacts. *WWF-Canada.*

Fisheries and Oceans Canada, Communications (2018). Facts on Canadian Fisheries. www.dfo-mpo.gc.ca. Retrieved 2018-12-09.

Freiwald, A., Wilson, J. B., & Henrich, R. (1999). Grounding Pleistocene icebergs shape recent deep-water coral reefs. *Sedimentary Geology*, 125(1), 1-8.

Fry, B., & Sherr, E. B. (1989). δ13C measurements as indicators of carbon flow in marine and freshwater ecosystems. In *Stable isotopes in ecological research* (pp. 196-229). Springer, New York, NY.

Fuller, S. D., Picco, C., Ford, J., Tsao, C. F., Morgan, L. E., Hangaard, D., & Chuenpagdee, R. (2008). *How We Fish Matters: Addressing the Ecological Impacts of Canadian Fishing Gear. Ecology Action Centre, Living Oceans Society and Marine Conservation Biology Institute, Canada*. ISBN 978-0-9734181-7-0.

Gass, S. E., & Willison, J. M. (2005). An assessment of the distribution of deep-sea corals in Atlantic Canada by using both scientific and local forms of knowledge. In *Cold-water corals and ecosystems* (pp. 223-245). Springer, Berlin, Heidelberg.

Gili J. M., & Coma R. (1998). Benthic suspension feeders: their paramount role in littoral marine food webs. *Trends in Ecology & Evolution*, 13(8), 316-321.

Granger, J., Sigman, D. M., Needoba, J. A., & Harrison, P. J. (2004). Coupled nitrogen and oxygen isotope fractionation of nitrate during assimilation by cultures of marine phytoplankton. *Limnology and Oceanography*, 49(5), 1763-1773.

Griffin, S., & Druffel, E. R. (1989). Sources of carbon to deep-sea corals. *Radiocarbon*, 31(3), 533-543.

Han, G., Ohashi, K., Chen, N., Myers, P. G., Nunes, N., & Fischer, J. (2010). Decline and partial rebound of the Labrador Current 1993–2004: Monitoring ocean currents from altimetric and conductivity-temperature-depth data. *Journal of Geophysical Research: Oceans*, 115(C12).

Heikoop J. M., Hickmott D. D., Risk M. J., Shearer C. K., & Atudorei V. (2002). Potential climate signals from the deep-sea gorgonian coral Primnoa resedaeformis. *Hydrobiologia*, 471, 117–124.

Hill, T. M., Spero, H. J., Guilderson, T., LaVigne, M., Clague, D., Macalello, S., & Jang, N. (2011). Temperature and vital effect controls on bamboo coral (Isididae) isotope geochemistry: a test of the "lines method". *Geochemistry, Geophysics, Geosystems*, 12(4).

Kilham, P., & Hecky, R. E. (1988). Comparative ecology of marine and freshwater phytoplankton 1. *Limnology and Oceanography*, 33, 776-795.

Kollmeyer R. C., McGill D.A., & Corwin N. (1967). Oceanography of the Labrador Sea in the vicinity of Hudson Strait in 1965. U.S. Coast Guard Oceanographic Rep. No. CG373-12, Washington, D.C, 92.

Kramp, P.L. (1939). Octocorallia. *The Zoology of Iceland,* 2(7), 1–13.

LaVigne, M., Grottoli, A. G., Palardy, J. E., & Sherrell, R. M. (2016). Multi-colony calibrations of coral Ba/Ca with a contemporaneous in situ seawater barium record. *Geochimica et Cosmochimica Acta*, 179, 203-216.

Lea, D., Shen, G. T. & Boyle, E. A (1989b). Coralline barium records temporal variability in equatorial Pacific upwelling. *Nature*, 340, 373–376.

Masson D. & Cummins P. F. (2004). Observations and modeling of seasonal variability in the Straits of Georgia and Juan de Fuca. *Journal of Marine Research*, 62(4), 491-516.

Muzuka, A. N., & Hillaire-Marcel, C. (1999). Burial rates of organic matter along the eastern Canadian margin and stable isotope constraints on its origin and diagenetic evolution. *Marine Geology*, 160(3-4), 251-270.

Neves, B., Edinger, E., Hillaire-Marcel, C., Saucier, E. H., France, S. C., Treble, M. A., & Wareham, V. E. (2015). Deep-water bamboo coral forests in a muddy Arctic environment. *Marine Biodiversity*, 45(4), 867-871.

Noé, S. U., Lembke-Jene, L., & Dullo, W. C. (2008). Varying growth rates in bamboo corals: sclerochronology and radiocarbon dating of a mid-Holocene deep-water gorgonian skeleton (Keratoisis sp.: Octocorallia) from Chatham Rise (New Zealand). *Facies*, 54(2), 151-166.

Petrie, B. (2007). Does the North Atlantic Oscillation affect hydrographic properties on the Canadian Atlantic continental shelf? *Atmosphere and Ocean*, 45(3), 141-151.

Roark, E. B., Guilderson, T. P., Flood-Page, S., Dunbar, R. B., Ingram, B. L., Fallon, S. J., & McCulloch, M. (2005). Radiocarbon-based ages and growth rates of bamboo corals from the Gulf of Alaska. *Geophysical Research Letters*, 32(4).

Roberts, C. M. (2002). Deep impact: the rising toll of fishing in the deep sea. *Trends in Ecology & Evolution*, 17(5), 242-245.

Roberts, J. M., & Cairns, S. D. (2014). Cold-water corals in a changing ocean. *Current Opinions in Environmental Sustainability*, 7, 118-126.

Salvo, F., Hamoutene, D., Hayes, V. E. W., Edinger, E. N., & Parrish, C. C. (2018). Investigation of trophic ecology in Newfoundland cold-water deep-sea corals using lipid class and fatty acid analyses. *Coral Reefs*, 37(1), 157-171.

Seitzinger, S. P. (1988). Denitrification in freshwater and coastal marine ecosystems: ecological and geochemical significance. *Limnology and Oceanography*, 33, 702-724.

Seitzinger, S. P., & Sanders, R. W. (1999). Atmospheric inputs of dissolved organic nitrogen stimulate estuarine bacteria and phytoplankton. *Limnology and Oceanography*, 44(3), 721-730.

Serrato-Marks, G., LaVigne, M., Hill, T. M., Sauthoff, W., Guilderson, T. P., Roark, E. B., Dunbar, R. B., & Horner, T. J. (2017). Reproducibility of Ba/Ca variations recorded by northeast Pacific bamboo corals. *Paleoceanography*, 32(9), 966-979.

Shen, G. T., & Boyle, E. A. (1987). Lead in corals: reconstruction of historical industrial fluxes to the surface ocean. *Earth and Planetary Science Letters*, 82(3-4), 289-304.

Sherwood O. A., Heikoop J. M., Scott D. B., Risk M. J., Guilderson T. P., & McKinney R.A. (2005a). Stable isotopic composition of deep-sea gorgonian corals Primnoa spp.: A new archive of surface processes. *Marine Ecology Progress Series*, 301, 135–148

Sherwood, O. A., Jamieson, R. E., Edinger, E. N., & Wareham, V. E. (2008). Stable C and N isotopic composition of cold-water corals from the Newfoundland and Labrador continental slope: Examination of trophic, depth and spatial effects. *Deep Sea Research Part I: Oceanographic Research Papers*, 55(10), 1392-1402.

Sherwood, O. A., & Edinger, E. N. (2009). Ages and growth rates of some deep-sea gorgonian and antipatharian corals of Newfoundland and Labrador. *Canadian Journal of Fisheries and Aquatic Sciences*, 66(1), 142-152.

Sherwood O. A., Lehmann M. F., Schubert C. J., Scott D. B., & McCarthy M. D. (2011). Nutrient regime shift in the western north atlantic indicated by compound-specific δ15N of deep-sea gorgonian corals. *Proceedings of the National Academy of Sciences*, 108(3), 1011–1015.

Sigman, D. M., Casciotti, K. L., Andreani, M., Barford, C., Galanter, M. B. J. K., & Böhlke, J. K. (2001). A bacterial method for the nitrogen isotopic analysis of nitrate in seawater and freshwater. *Analytical Chemistry*, 73(17), 4145-4153.

Sinclair, D. J., Sherwood, O. A., Risk, M. J., Hillaire-Marcel, C., Tubrett, M., Sylvester, P., ... & Kinsley, L. (2005). Testing the reproducibility of Mg/Ca profiles in the deep-water coral Primnoa resedaeformis: putting the proxy through its paces. In *Cold-water Corals and Ecosystems* (pp. 1039-1060). Springer, Berlin, Heidelberg.

Sinclair, D. J., Williams, B., Allard, G., Ghaleb, B., Fallon, S., Ross, S. W., & Risk, M. (2011). Reproducibility of trace element profiles in a specimen of the deep-water bamboo coral Keratoisis sp. *Geochimica et Cosmochimica Acta*, 75(18), 5101-5121.

Sinclair, D. J., Kinsley, L. P., & McCulloch, M. T. (1998). High resolution analysis of trace elements in corals by laser ablation ICP-MS. *Geochimica et Cosmochimica Acta*, 62(11), 1889-1901.

Smith, E. H., Soule, F. M., & Mosby, O. (1937). The Marion and General Greene Expeditions to Davis Strait and Labrador Sea, Under Direction of the United States Coast Guard: 1928-1931-1933-1934-1935: Scientific Results, Part 2: Physical Oceanography. US Government Printing Office.

Thresher R., Rintoul S. R., Koslow A. J., Weidman C., Adkins J. F., & Proctor C. (2004) Oceanic evidence of climate change in southern Australia over the last three centuries. *Geophysical Research Letters*, 31, L07212. doi: 10.1029/2003GL018869.

Thresher R., MacRae C., Wilson N., & Gurney R. (2007) Environmental effects on the skeletal composition of deep- water gorgonians (Keratoisis spp.; Isididae). *Bulletin of Marine Science*, 81, 409–422.

Thresher R. E., Wilson N. C., MacRae C. M., & Neil H. (2010) Temperature effects on the calcite skeletal composition of deep- water gorgonians (Isididae). *Geochimica et Cosmochimica Acta*, 74(16), 4655–4670.

Wareham, V. E., & Edinger, E. N. (2007). Distribution of deep-sea corals in the Newfoundland and Labrador region, Northwest Atlantic Ocean. *Bulletin of Marine Science, 81*(3), 289-313.

Williams, B., & Grottoli, A. G. (2010). Recent shoaling of the nutricline and thermocline in the western tropical Pacific. *Geophysical Research Letters*, 37(22).

Zehr, J. P., & Ward, B. B. (2002). Nitrogen cycling in the ocean: new perspectives on processes and paradigms. *Applied and Environmental Microbiology*, 68(3), 1015-1024.

Zhong, S., & Mucci, A. (1989). Calcite and aragonite precipitation from seawater solutions of various salinities: Precipitation rates and overgrowth compositions. *Chemical Geology*, 78(3-4), 283-299.

Zibrowius, H., & Taviani, M. (2005). Remarkable sessile fauna associated with deep coral and other calcareous substrates in the Strait of Sicily, Mediterranean Sea. In *Cold-water corals and ecosystems* (pp. 807-819). Springer, Berlin, Heidelberg.

CHAPTER I

STABLE HYDROGEN ISOTOPE VARIABILITY IN THE COLD-WATER CORAL GENUS *PRIMNOA*: IMPLICATIONS FOR PALEOCEANOGRAPHIC RECONSTRUCTIONS

Samuel Davin[1], Claude Hillaire-Marcel[1], Enno Schfuß[2], Evan Edinger[3]

[1]Geotop – Université du Québec à Montréal, Montreal, Canada

[2]MARUM– Center for Marine Environmental Sciences, University of Bremen, Bremen, Germany

[3]Departments of Biology, Geography, and Earth Sciences, Memorial University of Newfoundland, St. John's, Newfoundland, Canada

Submitted to *Geochimica et Cosmochimica Acta*

Abstract

Geographically ubiquitous and living on centennial timescales, deep-sea corals have the potential to provide paleoceanographic proxies at well-resolved spatial and temporal resolutions. So far no previously published work has explored the hydrogen isotopic composition of deep-sea corals, which are globally distributed and whose skeletons have the potential to provide paleoceanographic proxies at well-resolved spatial and temporal resolutions. We describe the process of measuring the non-exchangeable hydrogen isotopic composition of gorgonin (δD_{gorg}), the proteinaceous component of gorgonian coral skeletons, and present results from five Primnoa colonies, collected on the eastern and western Canadian margins. Our results indicate that δD_{gorg} is sensitive to regional marine environmental conditions, as evidence by reproducible δD_{gorg} values amongst proximal colonies and by the significant correlation between annually-resolved δD_{gorg} values and historical sea-surface salinities.

Keywords: Deuterium, proxy, geochemistry, climate, coral, Strait of Georgia, Atlantic

1.1 Introduction

The sensitivity of the northern high latitudes to climate change and its associated impacts on northern communities has increased scientific and public interest in these regions. As a result, monitoring the recent evolution of the North has become a topic of economic, social, and environmental concern (e.g., Årthun et al., 2017). However, the rarity and shortness of instrumental records in the North result in a lack of information regarding the pre-anthropogenic state and natural variability of environmental conditions. Here, the geoscience community has developed means to extract proxy data from natural archives. Historically, sediment cores and their constituents, molecular or otherwise, have been the most commonly studied form of marine record. However, the temporal resolution of marine sediments are generally insufficient to document abrupt, modern environmental variability. On the other hand, high-resolution bioarchives with an annual resolution or better, such as deep-sea corals (e.g., Heikoop et al., 2002), offer new research possibilities.

Deep-sea corals have emerged as promising bioarchives owing to their longevity (decadal to centennial timescales), widespread geographic and depth distributions along marine topographic highs, and to the incremental growth patterns of their skeletons (Goldberg, 1991). *Primnoa*, a dominant genus of deep-sea gorgonian octocorals found in boreal and cold northern temperate waters at depths from 50 to 3500 m (Cairns and Bayer, 2005), is of particular interest due to the annual growth rings of its hybrid gorgonin-calcite skeleton (Sherwood et al., 2005). Primnoa is azooxanthellate and is known to feed on phytodetrital matter, zooplankton, and bacteria (Gili & Coma, 1998; Sherwood et al., 2005).

Previous work has linked the carbon and nitrogen isotopic composition of annual gorgonin growth rings to the diet and trophic level of individual *Primnoa* colonies, with implications for inferring changes to the structure of local marine food webs (Heikoop et al., 2002; Kiriakoulakis et al., 2005; Sherwood et al., 2005; Williams et al., 2006; Sherwood et al., 2006; Risk et al., 2009; Baker et al., 2010; Sherwood et al. 2011; Sherwood et al., 2014; Williams et al., 2017). Other works on the gorgonin component of *Primnoa* skeletons have been dedicated to the study of growth rates and colony longevity (Andrews et al., 2002; Risk et al., 2002; Mortensen & Buhl-Mortensen 2005; Sherwood et al., 2005). However, much of the recent research dedicated to *Primnoa*, as well as other northern deep-sea corals, has focused on the mineralized components of the skeletons (Smith et al, 2000; Heikoop et al., 2002; Bond et al. 2005; Sinclair et al., 2005; Sherwood et al. 2005b; Grottoli and Williams et al., 2011).

Despite the widespread use of stable nitrogen and carbon isotopes in gorgonin for documenting food web variability (e.g., Heikoop et al., 2002) and the growing body of work on the elemental composition of deep sea coral skeletons (e.g., Sinclair 2005), no work to date has explored hydrogen isotopes in gorgonin. Herein we discuss an approach for determining the non-exchangeable hydrogen isotopic composition of gorgonin (δD_{gorg}) using vapor equilibration, and compare results from five *Primnoa* colonies collected from the northwestern North Atlantic, the Labrador Sea, and from the Strait of Georgia (British Columbia). The goals of this work are to determine the practicality and reliability of δD_{gorg} within the confines of sample mass limitations, to identify the approximate range of values to be expected, to determine whether δD_{gorg} is linked to provenance, and to identify the primary variables driving the δD_{gorg} signal.

1.1.1 Oceanographic context: North Atlantic

The Labrador Sea is a branch of the North Atlantic Ocean, located between the Labrador Peninsula and western Greenland. Circulation in the basin is cyclonic, bound to the west by the Labrador Current and by the West Greenland Current to the east. The Labrador Current is formed at the convergence of the Baffin Current and the West Greenland Current on the northern Labrador Shelf, from where it is advected along a southward trajectory towards the Hudson Strait where it is introduced to Hudson Bay Water via intense tidal mixing to form Labrador Shelf Water (Dunbar, 1951; Kollmeyer et al., 1967). Newly formed Labrador Shelf Water, which is notably colder and fresher than the primary flow of the Labrador Current, emerges from the Hudson Strait and continues along the continental shelf, along with the remainder of the Labrador Sea Water which has not been recirculated into the subpolar gyre. The Scotian Shelf, located between the western boundary currents of the subpolar gyre and the subtropical gyre, is fed by a mixture of Labrador Shelf Water, runoff from the St. Lawrence river, and by deeper and saltier slope waters. Mixing is induced by a variety of mechanisms including tidal mixing (Garrett and Loder, 1981), convective overturning (Mountain and Jessen, 1987), and by cross-shelf exchanges though the Laurentian and Northeast channels (Galbraith, 2006; Mountain and Manning, 1994) and through smaller channels in the Scotian Shelf (Drinkwater and Gilbert, 2004). Average seasonal salinities at the coral sampling sites are detailed in Table 2.

1.1.2 Oceanographic context: Strait of Georgia

The Strait of Georgia is a narrow, partially enclosed coastal basin with an area of 6,900 km2, located between the Coast Range of British Columbia and the southern half of Vancouver Island, connected to the Pacific Ocean via the Juan de Fuca Strait in the south and through the Johnstone and Queen Charlotte straits in the north. Circulation in the Strait is counter-clockwise, driven by semi-diurnal tides from from the Johnstone Strait and by southeast winds, which typically reach a maximum in December and January (Tully and Bodimead, 1957). Conditions vary dramatically with the seasonal cycle, being characterized by a warm and salty intrusion in the autumn, a gradual freshening during the winter, an abrupt cooling in the spring from meltwater discharged by the Fraser River, which accounts for ~80% of total land runoff entering the Strait, and deep-water renewal during the summer which brings in fresh Pacific Ocean water (Davenne and Masson, 2001). Since the latter half of the 20th century temperatures in southwestern British Columbia have risen by 1.4 °C, resulting in the transition of the Fraser River Basin from snow-fed regime to a rain-fed regime (Masson and Cummins 2004). These hydroclimatic changes have caused a flattening of hydrologic seasonality in the Strait of Georgia, as winter sea surface salinities (SSS) have become lower while summer SSS have risen. Seasonal surface conditions are detailed in Table 2.

1.2 Methodology

1.2.1 Sample Recovery

Colonies were live-collected using remotely operated vehicles and were frozen upon collection. Colonies 2464-A and 2464-B were collected in 2007 on the Scotian Slope near the Laurentian Channel at 1332 m during CCGS Hudson dive 1063; colony 2448 was collected in 2007 on the Scotian Shelf near the Laurentian Channel at 329 m during CCGS Hudson dive 1064; colony A51-010 was collected in 2016 in the Labrador Sea, off Hudson Strait, aboard the CCGS Amundsen during dive 51 at 632 m; colony R1513-SR-0022 was collected in the Sabine Channel of the Strait of Georgia in 2011, at at a depth of 269 m (Table 1; Figure 1). Specimens are henceforth referred to by their respective field identification codes. Water samples from ArcticNet Dive 51 were collected at standard sampling intervals (0 m, 5 m, 10 m, 20 m...80 m, 100 m, 125 m...200 m, 300 m, etc.) via CTD-rosette and collected into 30 cm^3 high-density polyethylene bottles. The bottles were subsequently sealed with parafilm and kept sealed until analysis.

1.2.2 Sample preparation

Thick sections were cut from the bottommost part of frozen colonies using a Dremel™ equipped with a circular, diamond-coated blade, and polished on a lapidary wheel. The samples were subsequently placed in Milli-Q™ water to rehydrate the gorgonin, then sonicated to remove air bubbles between the growth rings. Photographs of the thick sections were then taken under a microscope at low magnification for documentation purposes. Individual gorgonin growth rings were isolated by first decalcifying the thick sections in 5% HCl for up to 2 weeks (Sherwood et al., 2005). Once decalcified, thick sections were triple rinsed in Milli-Q™ water and submerged in Milli-Q™ water overnight to remove any residual acid. The thick sections were subsequently transferred to a Petri dish filled with Milli-Q™ water where the individual gorgonin rings were separated using forceps and a scalpel under a binocular microscope. Photographs of the sections taken before dissolution were used to guide sampling. Individual rings were triple rinsed in Milli-Q™ water and freeze-dried for 72 hours before being homogenized in clean glass vials with a stainless steel rod.

1.2.3 Vapor equilibration

The determination of the δD of organic materials is a useful and often used environmental proxy (e.g., see a review in Sessions, 2016). However, interpretation of δD may be hindered by hydrogen lability in organic compounds, wherein a portion of the total hydrogen pool is exchangeable with the ambient environment. The rate and extent of hydrogen lability is dependent upon the energy state of the material in question and upon the pH and steric accessibility (e.g., Schimmelmann et al., 1999). Hydrogen bound to aliphatic carbon structures is bound strongly enough to typically be considered non-exchangeable under normal atmospheric conditions, thus reflecting the isotopic composition of tissue at the time of hydrogen biofixation (Epstein and Yapp, 1976), whereas hydrogen bound to oxygen, nitrogen, and sulphur is exchanged on a time scale of minutes to days (Feng et al., 1993). Exchangeable hydrogen must therefore be considered when using hydrogen isotopes as a tool to infer information concerning natural systems. The issue of exchangeable hydrogen may be addressed in two ways: (1) by specific derivatization procedures wherein the exchangeable hydrogen is removed from the total hydrogen pool (e.g., nitration, wherein molecular groups containing exchangeable hydrogen are replaced with inert nitrate groups); or (2) by controlling the isotopic composition of the exchangeable hydrogen through the equilibration of the substrate of interest with water of a known hydrogen isotopic composition. Methods using either liquid water or water vapor as the exchange medium have been demonstrated to be effective (Schimmelmann, 1991; Feng et al., 1993; Chamberlain et al., 1996; Sauer et al., 2009).

In the case of gorgonin, an equilibration method is preferred to specific derivatization. Although derivatization techniques have been used for decades to address the issue of exchangeable hydrogen in plant cellulose, such an approach is inadequate for removing exchangeable hydrogen from complex animal proteins, which contain functional groups (hydroxyl, amino, etc.) that may be unaffected by specific derivatization (DeNiro and Schimmelmann, 1986). Thus, specific derivatization should not be used to account for exchangeable hydrogen in gorgonin. For the purposes of this study we define exchangeable hydrogen as hydrogen which may freely exchange with atmospheric hydrogen below <150°C.

To address the issue of exchangeable hydrogen present in the gorgonin samples we follow a modified version of the methodology suggested by Sauer et al. (2009), taking the following protocol:

> i) Duplicate 1.25 mg aliquots of each sample were weighed into silver (Ag) capsules (Costech™ 3.5 x 5.5 mm), which were left open. Elemental analysis of discrete samples find gorgonin to be 5% hydrogen by weight. Thus, 1.25 mg of dry gorgonin was used for each measurement based upon an instrumental requirement 50 μg of hydrogen per sample.
>
> ii) The open capsules were then loaded into a milled aluminum alloy (ASTM B 221) sample tray and placed into their respective vapor equilibration chambers, which were then sealed and made airtight (Figure 2). The vapor equilibration chambers were heated to an internal temperature of 150°C while simultaneously being purged with nitrogen gas. Once the chambers had been purged and heated, 1.25 cm^3 of water was injected through a silicon septa built into the side of each chamber. Chamber 'A' was injected with isotopically enriched water

(δD=+75.9‰) and chamber 'B' was injected with isotopically depleted water (δD=-99.9‰).

iii) After 8 hours the chambers were allowed to cool while being continuously purged with nitrogen (Sauer et al. 2009). The chambers were subsequently transferred to a nitrogen-purged glove box, opened, and the silver capsules were folded shut. The sealed capsules were then kept in a nitrogen-purged environment prior to being transferred to the helium-purged autosampler carousel of a Thermal Conversion Elemental Analyzer (TC/EA).

1.2.4 Analysis

Measurements of the hydrogen isotopic composition of gorgonin growth rings (δD_{gorg}) were performed using a ThermoFisher Scientific TC/EA operated at 1400°C coupled via a ConFlow IV to a ThermoFisher Scientific MAT253 isotope mass spectrometer at the Center for Marine Environmental Sciences (MARUM), in Bremen, Germany. Isotope ratios are reported in conventional delta notation (equation 1; equation 2). Certified reference materials used were IAEA-CH-7 (-100.3 ± 2‰), USGS77 (-75.9 ± 0.6‰), and USGS62 (-156.1 ± 2.1‰). $\delta^{15}N$ and $\delta^{13}C$ of gorgonin growth rings and δD of water samples were measured at Geotop-UQAM in Montreal, Canada. Nitrogen and carbon isotope ratios are reported relative to AIR and VPDB, respectively. The raw data are corrected using a calibration line constructed using 2 reference materials: $\delta^{13}C$=-42.16‰ & -11.85‰; $\delta^{15}N$=-0.22‰ & +14.36‰. The internal reference materials are normalized on the NBS19-LSVEC scale for $\delta^{13}C$ and IAEA-N1, N-2 & N-3 for $\delta^{15}N$. For each of the isotopes a third internal reference material is used to ensure the accuracy of the calibration ($\delta^{13}C$ = -28.75‰ & $\delta^{15}N$ = -0.06‰). Water samples are reported relative to the VSMOW-SLAP scale (Coplen, 1996). Reference waters of δD = -51, -99.9, -155.4‰ vs VSMOW were used.

The isotopic composition of the total hydrogen isotope pool for a given sample (δD_{sample}) is equal to the percent-weighted sum of the exchangeable hydrogen pool (δD_{ex}) and the non-exchangeable hydrogen pool (δD_{non}) (equation 3). δD_{sample} is directly measurable via TC/EA-IRMS, and the value of δD_{ex} is equal to that of the respective water vapors in equilibrating chambers A and B (δD_{water}). Therefore, δD_{non} may be determined by first solving for the percent of exchangeable hydrogen (f_{ex}) present in a sample (equation 4), then solving for δD_{non} (equation 5).

1.3 Results

1.3.1 Coral deuterium content

δD_{gorg} values are summarized in Figure 3. δD_{gorg} values differ significantly between the five *Primnoa* colonies examined in this study, ranging from a δD_{gorg} minimum of -126.2‰ in colony R1513-SR-0022 from the Strait of Georgia to a maximum enrichment of -83.6‰ in colony A51-010 from the Labrador Sea. δD_{gorg} from the northwestern North Atlantic colonies occur within an intermediate range between -105 to -95‰. On average, 11% of the total hydrogen pool in the gorgonin samples was found to be exchangeable, with an average standard of deviation between replicates of 1.8‰. The similar range of δD_{gorg} values observed amongst the northwestern North Atlantic colonies compared to the values seen in the Labrador Sea and in the Strait of Georgia indicates δD_{gorg} is strongly linked to provenance. The five colonies in this study were live-collected within 10 years of one another and at different life stages; a comparison of the time series produced from these data are presented in Figure 4, with the assumption that each separable growth band represents 1 year of growth (Sherwood et al., 2005). For a complete table of deuterium results, see Annex A.

The 40 most recent growth rings of colony R1513-SR-0022 were sufficiently massive for measurement. Collected in 2011 at 269 m in the Strait of Georgia at Dixon Entrance, located at the southwestern tip of Texada Island, the δD_{gorg} of R1513-SR-0022 ranges from -126.2 to -105.2‰ vs VSMOW, with a mean value of -115.4‰. Over the course of 40 growth periods, the colony exhibits a nearly-linear deuterium enrichment trend (Figure 4).

The seven most recent growth rings of colony A51-010 from the Labrador Sea were sufficiently massive to yield material for analysis. Collected in 2016, the δD_{gorg} values of A51-010 are the most enriched of the five coral colonies in this study, ranging from -86 to -83.6‰ vs VSMOW, making A51-010, on average, ~18‰ more enriched in deuterium relative to the northwestern North Atlantic corals.
The 8 most recent growth rings from each of the Scotian Shelf *P. resedaeformis* colonies (2464-A, 2464-B, and 2448) yielded sufficient material for analysis. The three colonies were live-collected, so it may be assumed that the growth ring sequences overlap. The δD_{gorg} of colonies 2464-A and 2464-B, which were both collected during ROPOS dive 1063 in 2006 at a depth of 1332 m, are similar and exhibit similar values over the course of 8 growth rings. Colony 2448 was collected during the subsequent ROPOS Dive 1064 at an adjacent site, but at the much shallower depth of 329 meters. 2448 is marginally more enriched in deuterium relative to 2464-A and 2464-B, but its δD_{gorg} values are nonetheless very similar to the δD_{gorg} values observed in 2464-A and 2464-B. The lack of a common trend between 2448 and the two deeper colonies, coupled with the marginally more enriched values of 2448, indicate a small but quantifiable difference between conditions on the Scotian Shelf and Scotian Slope.

1.3.2 Seawater deuterium content

The δD of the water column at the site of ArcticNet Dive 51 (61.44°N, -60.66°W) was determined from samples collected at intervals from 0 to 632 m (Figure 5). The values range from -8‰ in the surface water layer, to +0.9‰ deeper in the water column. The deuterium-depleted values in the upper water column of this site are associated with the buoyant layer of cold, low-salinity water originating from melting ice. The enriched values approaching ~0‰ are approximately representative of mean ocean water at depth. Seawater deuterium values are listed in Annex A.

1.3.3 Carbon and nitrogen isotopes

$\delta^{15}N$ and $\delta^{13}C$ values were collected to assist in differentiating the sources of food being eaten by individual colonies in order to assist with the interpretation of of δD_{gorg} values. Sufficient material was available for carbon and nitrogen isotopic analyses in colonies 2464-A, 2448, and R1513-SR-0022. $\delta^{15}N$ values range from 13.75 to 12.11‰ in colony R1513-SR-0022; from 12.71 to 11.84‰ in colony 2464-A; and from 13.01 to 12.22‰ in colony 2448. $\delta^{13}C$ ranges from -16.15 to -17.48‰ in colony R1513-SR-0022; from -18.75 to -19.18‰ in colony 2464-A; and from -18.28 to -19.98‰ in colony 2448 (Figure 6). Although carbon and nitrogen isotope data from 2464-A and 2448 are similar, there is a consistent offset between the two colonies, indicating these corals fed on different sources organic matter.

1.4 Discussion

1.4.1 Interpretation of δD_{gorg}

The deuterium content (δD) of animal tissue has been demonstrated to be an indicator of provenance and diet (Hobson and Wassenaar, 2008). Unlike carbon and nitrogen isotopic content, which are derived exclusively from food, the δD of animal tissue is also mediated by the δD of environmental waters. Unsurprisingly, it is not always possible to disentangle the relative contributions of deuterium imparted to animal tissue from both food and water sources, particularly in animals which are migratory or otherwise have large territories. Interpretation of δD may also be confounded in organisms with photosynthetic symbiotes due to kinetic fractionation during photosynthesis. By nature, deep-sea corals are not subject to these complicating factors because they are sessile, azooxanthellate, and live in deep marine environments where the δD of ambient seawater is consistently near 0‰ vs VSMOW. In consideration of the notable discrepancy between the normal range of δD in seawater below the mixed layer and the measured δD_{gorg} of corals in this study, it is evident that the dominant variable controlling δD_{gorg} is the deuterium content of dietary organic matter, which, in the case of *Primnoa,* consists predominantly of exported and resuspended phytodetrital material. The δD of total organic H in phytoplankton is controlled primarily by kinetic fractionation of the environmental water pool during photosynthesis. Natural phytoplankton communities are observed to fractionate H in environmental water by approximately -100‰, with variations in fractionation owing to differences in growth conditions affecting biosynthetic reactions as well as community assemblage (Epstein and Hoering, 1980). By extension, the deuterium content of gorgonin growth rings in *Primnoa*, and presumably other genera of azooxanthellate corals, may be interpreted as a proxy for annually-resolved sea surface deuterium content. The five *Primnoa* colonies from the Labrador Sea, northwestern North Atlantic, and Strait of Georgia exhibit distinct δD_{gorg} ranges specific to their location, which showcase a relationship between provenance dietary deuterium content. Although δD_{gorg} may provide valuable information about the local historical isotopic composition of the surface ocean, we caution against directly comparing distal colonies due to confounding dietary and environmental variables which may not be readily accounted for, as evidenced by the apparent dietary differences indicated by the carbon and nitrogen isotopic compositions of colonies 2464-A, 2448, and R1513-SR-0022 (Figure 6).

1.4.2 Strait of Georgia site

Gorgonin growth rings extracted from coral colony R1513-SR-0022 collectively represent 40 years of growth, spanning from approximately 1971 to 2011. Isotopic analysis of these rings reveal a near-linear deuterium enriching trend corresponding to δD_{gorg} values between -126.2 and -105.4‰ , which closely reflect environmental δD measured in and around the Strait of Georgia (Nissenbaum 1974). Using daily SSS data collected at Departure Bay (Nanaimo, BC) between 1971 and 2011 (Fisheries and Oceans Canada, 2018), we find a statistically significant relationship between interannual δD_{gorg} variability and summer (June-August) SSS (R^2=0.45, p-value=0.0013) (Figure 7), as well as with the strength of SSS seasonality (R^2=0.57, p-value <0.001) (Figure 1.7), which is defined here as the difference between summer and winter SSS. A linear model of interannual δD_{gorg} and summer SSS yields a relationship of ~3.43‰ PSU^{-1}, which is in good agreement with previous, globally-derived models, which estimate of the relationship between $\delta D_{seawater}$ and SSS at ~4.09‰ PSU^{-1} for extratropical regions (Xu et al. 2012). In consideration of this data, we propose that the deuterium content of gorgonin growth rings in *Primnoa* is sensitive to the same hydroclimatic processes governing SSS, thus allowing δD_{gorg} to be used, cautiously, as a predictive variable for the historical reconstruction of SSS.

The SSS and δD_{gorg} trends observed in the Strait of Georgia during the lifetime of coral colony R1513-SR-0022 are attributable to significant climatic changes in southwestern British Columbia, which have affected the annual timing of key hydrologic events in the Strait. Since the mid-20th century mean annual air temperatures in the Fraser River Basin have risen by ~1.4 °C, resulting in a greater proportion of annual precipitation falling as rain (Masson and Cummins 2004) and a 19% decrease in headwater snowmelt (Voss et al., 2014). The δD of precipitation approaching the Fraser River Basin from the Pacific Ocean, monitored at Victoria, B.C., is approximately -71±9‰ (IAEA/WMO, 2006; Voss et al., 2014), becoming progressively more depleted inland (δD values of the Fraser River to range from ~-95‰ at the mouth to ~-150‰ at the headwaters). The transition of the Fraser River Basin from a predominantly snow-fed to rain-fed system has resulted in a flattening of the Fraser River hydrograph, as a single dominant freshet beginning in spring end ending in early summer has given way to multiple discharge peaks throughout the year. These changes are manifested in the Strait of Georgia as a flattening seasonal salinity patterns, where summer SSS has increased and winter SSS has decreased. Similarly, the weakened pulse of low δD snowmelt entering the Strait of Georgia each spring and summer is anticipated to have lead to an overall sea surface deuterium enrichment during summer.

1.4.3 Labrador Sea and North Atlantic sites

Despite the shortness of the records produced by the northwestern North Atlantic and Labrador Sea corals, these δD_{gorg} data provide further insight into the potential range of δD_{gorg} in different marine environments. Notably, the δD_{gorg} of concurrent growth rings in neighboring colonies 2464-A and 2464-B are in good agreement with one another, providing evidence that δD_{gorg} is reproducible within a local environment and therefore linked to environmental conditions. The mean δD_{gorg} of colony 2448 is marginally enriched relative to the deeper colonies, 2464-A and 2464-B, which may be attributed to colony 2448 receiving greater contributions of organic matter from the distinct hydrologic regime of the Laurentian Channel, and relatively less advected material from isotopically distinct slope waters of the Scotian Shelf (Muzuka and Hillaire-Marcel, 1999). Despite differences in carbon, nitrogen, and hydrogen isotopic differences between the three northwestern North Atlantic *Primnoa* colonies, these corals exhibit only minor inter-annual δD_{gorg} variability, indicating the hydroclimatic processes governing the deuterium content of surface waters off the coast of Nova Scotia did not change significantly between 1999-2006. Similarly, results from A51-010 indicate that between 2010-2016 there was little inter-annual change in deuterium content in the surface waters of the western Labrador Sea.

The δD_{gorg} records of 2464-A, 2464-B, and 2448 are neither contemporaneous with that of A51-010, nor complimented by carbon and nitrogen isotopic measurements due to insufficient material from A51-010 remaining after δD measurements. Accordingly, it is inappropriate to directly compare the results of these colonies. Nonetheless, the difference between the mean δD_{gorg} value of the northwestern North Atlantic corals and and the Labrador Sea (ΔD_{gorg} ~15‰) remains a point of interest. If the δD_{gorg} of these corals is correlated with salinity as it is in the Strait of Georgia, and if the δD_{gorg} and SSS relationship of ~3.43‰ PSU^{-1} holds true for these sites, then we may expect a salinity difference of ~4.3 PSU between the waters off the southern coast of Nova Scotia and the waters of the central-western Labrador Sea. The waters off the southern coast of Nova Scotia are predominantly sourced from the Gulf of Saint Lawrence via the Cabot Strait and from the easterly flow of Labrador Shelf Water, the salinities of which range annually from 28.5 to 32.5 PSU (Petrie et al., 1996) and ~31-33 PSU (Zweng et al., 2013), respectively. The site of A51-010 in the central-western Labrador Sea is too far North to be heavily impacted by Hudson Strait Water and too far offshore to be dominated by Baffin Island Current Water, leaving the influence of the westward branch of the West Greenland Current System (WGCS), which transports a core of warm, salty (~34.9 PSU) (Zweng et al., 2013) water from the relatively productive Irminger Sea. The particularly enriched δD_{gorg} values of A51-010 suggest the bulk of organic matter consumed by this colony originated in neither Baffin Bay nor the Canadian Island Archipelago, which are noted for fresh, deuterium-depleted waters, but rather from the westerly branch of the West Greenland-Irminger Current. Depending upon the dominant source of origin and upon the time of year, the organic matter being consumed by corals off Nova Scotia may be reasonably expected to originate from seawater between ~2 to ~6 PSU fresher than organic matter consumed by corals in the central-western Labrador Sea.

1.5 Conclusions

The deuterium content of annual gorgonin growth rings (δD_{gorg}) in the deep-sea coral genus *Primnoa* reflects the deuterium content of their diet. Exported phytodetrital material is a primary food source of deep-sea corals, linking δD_{gorg} to hydroclimatic processes which govern the deuterium content of the surface ocean, with a probable bias towards periods of high primary productivity. Sea surface salinity and sea surface deuterium content are affected by many of the same physical mechanisms, thus making δD_{gorg} a potential proxy for sea surface salinity in the Strait of Georgia. In our work we propose a relationship of ~3.43‰ PSU^{-1} between δD_{gorg} and SSS. Deep-sea corals are ideal recorders of sea surface deuterium content in the marine food web because they feed opportunistically and generally live in environments with stable temperature and salinity conditions throughout the year in waters with δD values near 0‰. We see δD_{gorg} as an exciting tool for understanding the relationships between hydroclimatic variability and marine food webs at high geographic and temporal resolutions, particularly when coupled with carbon and nitrogen isotopic measurements. This study employs both *P. pacifica* and *P. resedaeformis* colonies, which are Pacific and Atlantic representatives of the genus *Primnoa*. In all respects the ecology and behavior of these two species is alike, and we conclude any potential metabolic hydrogen fractionation effects, if present, are likely to be overprinted by the environmental variables to which H fractionation is susceptible.

Controlled equilibration of the exchangeable hydrogen pool is applicable to a large variety of materials, and is the only approach for compounds that do not permit a chemical replacement of all their exchangeable-hydrogen-bearing groups by nitrate. Isotopic equilibration is an efficient, inexpensive, and user-friendly approach for reconciling exchangeable hydrogen in complex organic materials, and we deem a vapor equilibration method to be an effective approach for addressing exchangeable hydrogen in gorgonin. The smaller gorgonin growth rings found in juvenile corals and near the central growth axis of mature corals may not be sufficiently massive to allow for hydrogen isotopic measurement, and in these cases it may be beneficial to combine samples. Future work will benefit from individual site characterizations, including determination of sediment δD and plankton δD, and from further exploration of the deuterium content of other deep-sea coral species and genera.

1.6 Acknowledgements

The authors would like to thank Professor Yves Gelinas, Professor Michael Kucera, Dr. Jean-Francois Helie, the crew of the CCGS Amundsen, Fisheries and Oceans Canada (DFO), the Canadian Scientific Submersible Facility (CSSF), VITALS, ArcticNet, and ArcTrain, all supported by NSERC-Canada.

1.7 References

Andrews A. H., Cordes E. E., Mahoney M. M., Munk K., Coale K. H., Cailliet G. M., and Heifetz J. (2002). Age, growth and radiometric age validation of a deep-sea, habitat-forming gorgonian (Primnoa resedaeformis) from the Gulf of Alaska. *Hydrobiologia*, 471(1-3), 101-110.

Baker D. M., Webster K. L., and Kim K. (2010). Caribbean octocorals record changing carbon and nitrogen sources from 1862 to 2005. *Global Change Biology*, 16(10), 2701-2710.

Bond Z. A., Cohen A. L., Smith S. R. and Jenkins W. J. (2005) Growth and composition of high-Mg calcite in the skeleton of a Bermudian gorgonian (Plexaurella dichotoma): potential for paleothermometry. *Geochem. Geophys. Geosyst.* 6(8), 10.

Cairns S. D. and Bayer F. M. (2005). A review of the genus Primnoa (Octocorallia: Gorgonacea: Primnoidae), with the description of two new species. *Bulletin of Marine Science*, 77(2), 225-256.

Chamberlain C. P., Blum J. D., Holmes R. T., Feng X., Sherry T. W., and Graves G. R. (1996). The use of isotope tracers for identifying populations of migratory birds. *Oecologia*, 109(1), 132-141.

Chapman D. C., anmd Beardsley R. C. (1989). On the origin of shelf water in the Middle Atlantic Bight. *Journal of Physical Oceanography*, 19(3), 384-391.

Davenne E. and Masson D. (2001). Water properties in the Straits of Georgia and Juan de Fuca. *Fisheries and Oceans Canada*. Retrieved from www.sci.pac.dfo-mpo.gc.ca/osap/projects/straitofgeorgia/JdFG_e.pdf.

Drinkwater K. and Taylor G. (1982). Monthly means of the temperature, salinity and density along the Halifax Section. *Can. Tech. Rep. Fish. Aquat. Sci*, 1093: 1-67.

Drinkwater K. F. and Gilbert D. (2004). Hydrographic variability in the waters of the Gulf of St. Lawrence, the Scotian Shelf and the eastern Gulf of Maine (NAFO Subarea 4) during 1991–2000. *Journal of Northwest Atlantic Fishery Science*, 34, 83–99.

Dunbar M. J., (1951). Eastern Arctic Waters, Canada. *Fisheries Research Board Bulletin*, 88, 1-131.

Epstein S., Yapp C. J., and Hall, J. H. (1976). The determination of the d/h ratio of non exchangeable hydrogen in cellulose extracted from aquatic and land plants. *Earth and Planetary Science Letters*, 30(2), 241–251.

Epstein S., Thompson P., and Yapp C.J. (1977). Oxygen and hydrogen isotopic ratios in plant cellulose. *Science*, 198, 1209-1215

Estep M. F. and Dabrowski H. (1980). Tracing food webs with stable hydrogen isotopes. *Science*, 209(4464), 1537–1538.

Estep M. F. and Hoering T. C. (1981). Stable hydrogen isotope fractionations during autotrophic and mixotrophic growth of microalgae. *Plant Physiology*, 67(3), 474-477.

Feng X, Krishnamurthy R. V., and Epstein S. (1993) Determination of D/H ratios of nonexchangeable hydrogen in cellulose: A method based on the cellulose-water exchange reaction. *Geochimica et Cosmochimica Acta*, 57, 4249–56.

Fisheries and Oceans Canada (2018). Daily sea surface temperature and salinity. Retrieved from http://www.pac.dfo-mpo.gc.ca/science/oceans/data-donnees/lightstations-phares/data/DepartureDailySalTemp.txt.

Fratantoni P. S. and Pickart R. S. (2007). The western North Atlantic shelfbreak current system in summer. *Journal of Physical Oceanography*, 37(10), 2509-2533.

Fry B. and Sherr E. (1984). δ13C measurements as indicators of carbon flow in marine and freshwater ecosystems. *Contributions to Marine Science*, 27, 13–47.

Garrett C. J. R., and Loder J. W. (1981). Dynamical aspects of shallow sea fronts. Phil. Trans. R. Soc. Lond. A, 302(1472), 563-581.

Gili J. M., and Coma R. (1998). Benthic suspension feeders: their paramount role in littoral marine food webs. *Trends in Ecology & Evolution*, 13(8), 316-321.

Harrison P. J., Fulton J. D., Taylor F. J. R., and Parsons T. R. (1983). Review of the biological oceanography of the Strait of Georgia: pelagic environment. *Canadian Journal of Fisheries and Aquatic Sciences*, 40(7), 1064-1094.

Heikoop J. M., Hickmott D. D., Risk M. J., Shearer C. K., and Atudorei V. (2002). Potential climate signals from the deep-sea gorgonian coral Primnoa resedaeformis. *Hydrobiologia*, 471, 117–124.

Johannessen S. C., Macdonald, R.W., and Paton D. W. (2003). A sediment and organic carbon budget for the greater Strait of Georgia. *Estuarine, Coastal and Shelf Science*, 56(3-4), 845-860.

Johannessen S. C., O'Brien M. C., Denman K. L., and Macdonald R. W. (2005). Seasonal and spatial variations in the source and transport of sinking particles in the Strait of Georgia, British Columbia, Canada. *Marine Geology*, 216(1-2), 59-77.

Kiriakoulakis K., Fisher E. L., Wolff G. A., Freiwald A., Grehan A., Roberts J. M., Grehand A., and Roberts J. M. (2005). Lipids and nitrogen isotopes of two deep-water corals from the North-East Atlantic: initial results and implications for their nutrition. *Cold-water Corals and Ecosystems*, 715–729.

Kollmeyer R. C., McGill D.A., and Corwin N. (1967). Oceanography of the Labrador Sea in the vicinity of Hudson Strait in 1965. U.S. Coast Guard Oceanographic Rep. No. CG373-12, Washington, D.C, 92.

LeBlond P. H. (1983). The Strait of Georgia: functional anatomy of a coastal sea. *Canadian Journal of Fisheries and Aquatic Sciences*, 40(7), 1033-1063.

Loder J. W., Boicourt W. C., and Simpson J. H. (1998). Western ocean boundary shelves (W). *The Sea*, 11, 3-28.

Masson D. and Cummins P. F. (2004). Observations and modeling of seasonal variability in the Straits of Georgia and Juan de Fuca. *Journal of Marine Research*, 62(4), 491-516.

Morrison J., Quick M. C., and Foreman M. G. (2002). Climate change in the Fraser River watershed: flow and temperature projections. *Journal of Hydrology*, 263(1-4), 230-244.

Mortensen P. B. and Buhl-Mortensen L. (2005). Morphology and growth of the deep-water gorgonians Primnoa resedaeformis and Paragorgia arborea. *Marine Biology*, 147(3), 775-788.

Mountain D. G. and Jessen P. F. (1987). Bottom waters of the Gulf of Maine, 1978-1983. *Journal of Marine Research*, 45(2), 319-345.

Muzuka A. N. and Hillaire-Marcel C. (1999). Burial rates of organic matter along the eastern Canadian margin and stable isotope constraints on its origin and diagenetic evolution. *Marine Geology*, 160(3-4), 251270.

Nissenbaum, A. (1974) The organic geochemistry of marine and terrestrial humic substances: implications of carbon and hydrogen isotope studies. *Advances in Organic Geochemistry*, 1973, 39-52.

Petrie B. (2007). Does the North Atlantic Oscillation affect hydrographic properties on the Canadian Atlantic continental shelf? *Atmosphere-Ocean*, 45(3), 141-151.

Petrie B. and Drinkwater K. (1993). Temperature and salinity variability on the Scotian Shelf and in the Gulf of Maine 1945–1990. *Journal of Geophysical Research: Oceans*, 98(C11), 20079-20089.

Riche O., Johannessen S., and Macdonald R. (2014). Why timing matters in a coastal sea: Trends, variability and tipping points in the strait of georgia, canada. *Journal of Marine Systems*, 131, 36–53.

Risk M. J., Heikoop J. M., Snow M. G., and Beukens R. (2002). Lifespans and growth patterns of two deep-sea corals: Primnoa resedaeformis and Desmophyllum cristagalli. *Hydrobiologia*, 471(1-3), 125-131.

Risk M. J., Lapointe B. E., Sherwood O. A., and Bedford B. J. (2009). The use of δ15N in assessing sewage stress on coral reefs. *Marine Pollution Bulletin*, 58(6), 793–802.

Sauer P. E., Schimmelmann A., Sessions A. L., and Topalov K. (2009). Simplified batch equilibration for d/h determination of non-exchangeable hydrogen in solid organic material. *Rapid Communications in Mass Spectrometry,* 23(7), 949–956.

Schimmelmann A. and DeNiro M. J. (1986). Stable isotopic studies on chitin. III. The D/H and 18O/16O ratios in arthropod chitin. *Geochimica et Cosmochimica Acta*, 50(7), 1485-1496.

Schimmelmann A., Lewan M. D., and Wintsch R. P. (1999). D/H isotope ratios of kerogen, bitumen, oil, and water in hydrous pyrolysis of source rocks containing kerogen types i, ii, iis, and iii. *Geochimica et Cosmochimica Acta*, 63(22), 3751–3766.

Session A.L. (2016). Factors controlling the deuterium contents of sedimentary hydrocarbons. *Organic Geochemistry*, 96, 43–64.

Shearman R. K. and Lentz S. J. (2010). Long-term sea surface temperature variability along the US East Coast. *Journal of Physical Oceanography*, 40(5), 1004-1017.

Sherwood O. A., Guilderson T. P., Batista F. C., Schiff J. T., and McCarthy M. D. (2014). Increasing subtropical north pacific ocean nitrogen fixation since the little ice age. *Nature*, 505(7481), 78–81.

Sherwood O. A., Heikoop J. M., Scott D. B., Risk M. J., Guilderson T. P., and McKinney R.A. (2005). Stable isotopic composition of deep-sea gorgonian corals Primnoa spp.: A new archive of surface processes. *Marine Ecology Progress Series*, 301, 135–148.

Sherwood O. A., Heikoop J. M., Sinclair D. J., Scott D. B., Risk M. J., Shearer C., and Azetsu-scott K. (2005). Skeletal Mg / Ca in Primnoa resedaeformis: relationship to temperature? *Cold-water Corals and Ecosystems*. 1061–1079.

Sherwood O. A., Lehmann M. F., Schubert C. J., Scott D. B., and McCarthy M. D. (2011). Nutrient regime shift in the western north atlantic indicated by compound-specific δ15N of deep-sea gorgonian corals. *Proceedings of the National Academy of Sciences*, 108(3), 1011–1015.

Sherwood O. A., Scott D. B., and Risk M. J. (2006). Late holocene radiocarbon and aspartic acid racemization dating of deep-sea octocorals. *Geochimica et Cosmochimica Acta*, 70(11), 2806–2814.

Sinclair D. J., Sherwood O. A., Risk M. J., Hillaire-Marcel C., Tubrett M., Sylvester P., McCulloch M., and Kinsley L. (2005). Testing the reproducibility of mg/ca profiles in the deep-water coral primnoa resedaeformis: putting the proxy through its paces. *Cold-water corals and Ecosystems*, 1039–1060.

Smith J. E., Schwarcz H. P., Risk M. J., McConnaughey T. A., and Keller N. (2000). Paleotemperatures from Deep-Sea Corals: Overcoming 'Vital Effects'. *Palaios*, 15(1), 25.

Voss B. M., Peucker-Ehrenbrink B., Eglinton T. I., Fiske G., Wang Z. A., Hoering K. A., and Gillies, S. L. (2014). Tracing river chemistry in space and time: Dissolved inorganic constituents of the Fraser River, Canada. *Geochimica et Cosmochimica Acta*, 124, 283-308.

Waldichuk, M. (1957). Physical oceanography of the Strait of Georgia, British Columbia. *Journal of the Fisheries Board of Canada*, 14(3), 321-486.

Wilkinson G. M., Cole J. J., and Pace M. L. (2015). Deuterium as a food source tracer: Sensitivity to environmental water, lipid content, and hydrogen exchange. *Limnology and Oceanography: Methods*, 13(5), 213–223.

Williams B. and Grottoli A. G. (2011). Solution and laser ablation inductively coupled plasma-mass spectrometry measurements of Br, I, Pb, Mn, Cd, Zn, and B in the organic skeleton of soft corals and black corals. *Geochemistry, Geophysics, Geosystems*, 12(3), 1–16.

Williams B., Risk M. J., Ross S. W., and Sulak K. J. (2006). Deep-water antipatharians: proxies of environmental change. *Geology*, 34(9), 773–776.

Williams B., Thibodeau B., Chikaraishi Y., Ohkouchi N., Walnum A., Grottoli A. G., and Colin P. L. (2017). Consistency in coral skeletal amino acid composition offshore of palau in the western pacific warm pool indicates no impact of decadal variability in nitricline depth on primary productivity. *Limnology and Oceanography*, 62(2), 399–407.

Xu X., Werner M., Butzin M., and Lohmann G. (2012). Water isotope variations in the global ocean model MPI-OM. *Geoscientific Model Development*, 5(3), 809-818.

Zweng M. M, Reagan J. R, Antonov J. I., Locarnini R. A., Mishonov A. V., Boyer T. P., Garcia H.E., Baranova O. K., Johnson D. R., Seidov D., and Biddle M.M., 2013. *World Ocean Atlas 2013, Volume 2: Salinity*. S. Levitus, Ed., A. Mishonov Technical Ed.; *NOAA Atlas NESDIS,* 74, 39 pp.

1.8 Tables

Table 1.1 Sample recovery

Colony ID	Species	Dive	Year	Depth (m)	Location
A51-010	P. resedaeformis	ArcticNet 51	2016	632	61.440°N, 60.664°W
R1513-SR-0022	P. pacifica	ROPOS 1513	2011	269	49.517°N, 124.207°W
2448	P. resedaeformis	ROPOS 1064	2006	329	44.473°N, 57.175°W
2464-A	P. resedaeformis	ROPOS 1063	2006	1332	44.420°N, 57.170°W
2464-B	P. resedaeformis	ROPOS 1063	2006	1332	44.420°N, 57.170°W

Table 1.2 Seawater salinities

Site	SSS (Jun - Aug)	SSS (Dec - Feb)
R1513-SR-0022	23.97	25.67
A51-010	33.4	33.67
2464-A, -B	31.59	32.12
2448	31.43	31.96

Sea surface salinity (SSS) conditions near coral collection dive sites. Values for Atlantic coral sites are reported are based on the World Ocean Atlas 1955-2013, 0.25° grid dataset (Zweng et al., 2013). Values for the Strait of Georgia site are based on daily measurements at Departure Bay (Fisheries and Oceans Canada, 2018) from 1971-2011.

1.9 Figures

Figure 1.1 Summary of coral sampling sites.

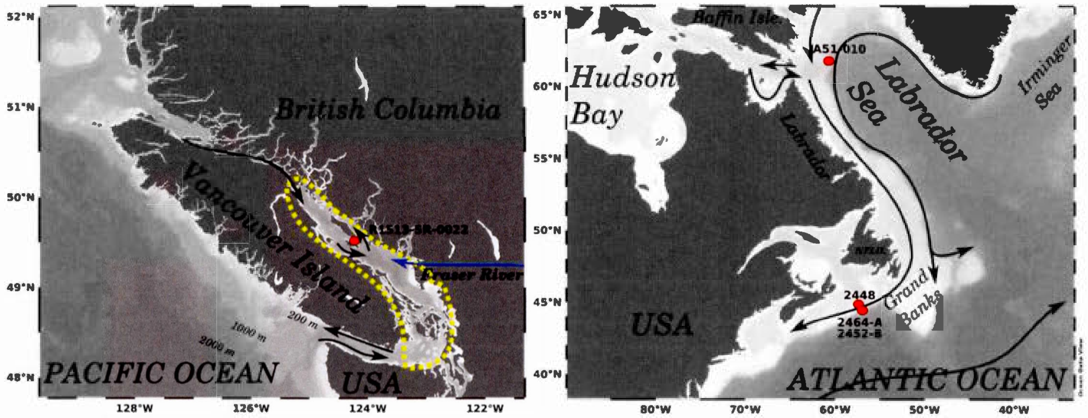

Strait of Georgia colony R1513-SR-0022 (left);. Labrador Sea colony A51-010 and northwestern North Atlantic colonies 2464-A, 2464-B, and 2448 (right).

Figure 1.2 Vapor equilibration chambers

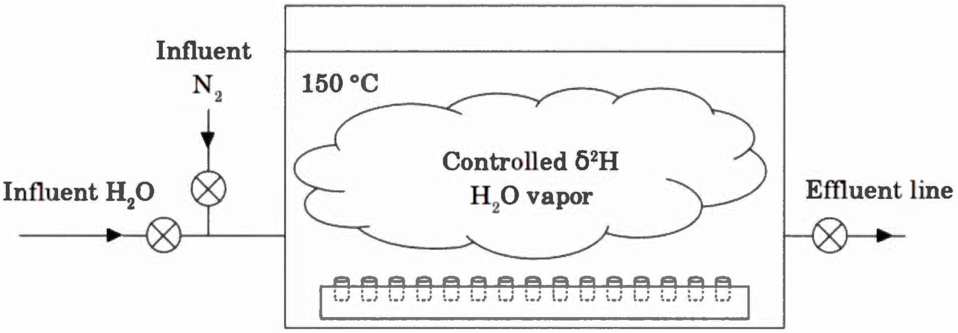

Schematic design of vapor equilibration chambers A and B. Samples were loaded into chambers, which were subsequently heated to an internal temperature of 150°C, while simultaneously purged with nitrogen. 1.25 mL H_2O with a known δD was injected into each chamber. Samples were then allowed to equilibrate with the isotopically-controlled atmosphere for 8 hours.

Figure 1.3 Summary of non-exchangeable deuterium content

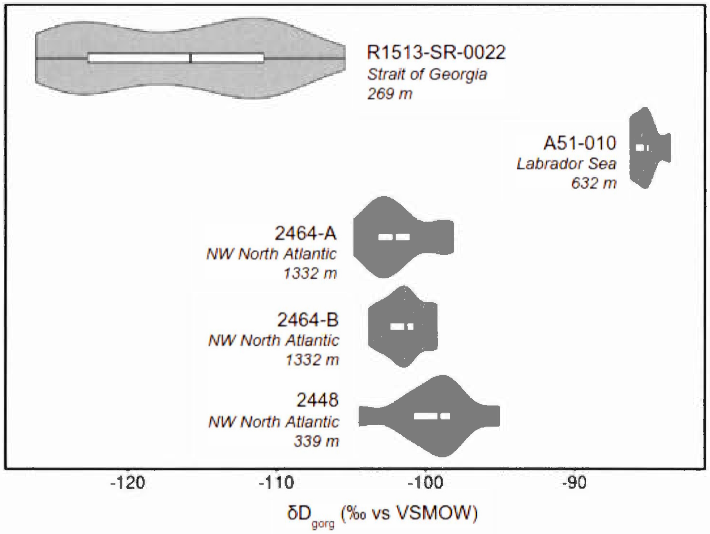

δD_{gorg} results summary showing the probability density (gray shaded), and the upper quartile, lower quartile, median, minima, and maxima (white box and whisker plots) of δD_{gorg} values measured in each of the five *Primnoa* colonies.

Figure 1.4 Deuterium time series

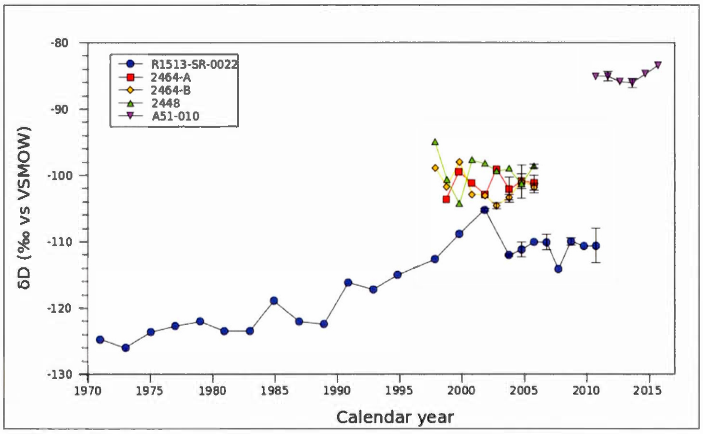

δD_{gorg} of the five *Primnoa* colonies plotted against estimated growth years.

Figure 1.5 Deuterium water column profile

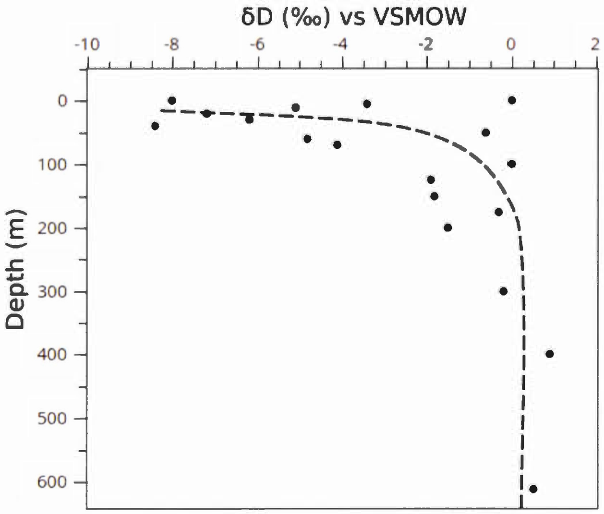

Water column profile from the site of ArcticNet Dive 51. July, 2016.

Figure 1.6 Nitrogen and carbon isotope comparison

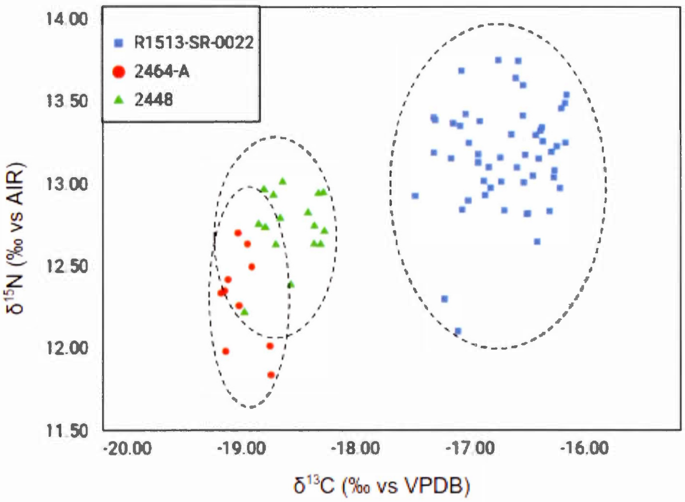

δ^{15}N and δ^{13}C reveal a large offset between Strait of Georgia colony R1513-SR-0022 and northwestern North Atlantic colonies 2464-A and 2448, which suggests these corals fed upon different sources of organic carbon.

Figure 1.7 Deuterium – salinity relationship in the Strait of Georgia

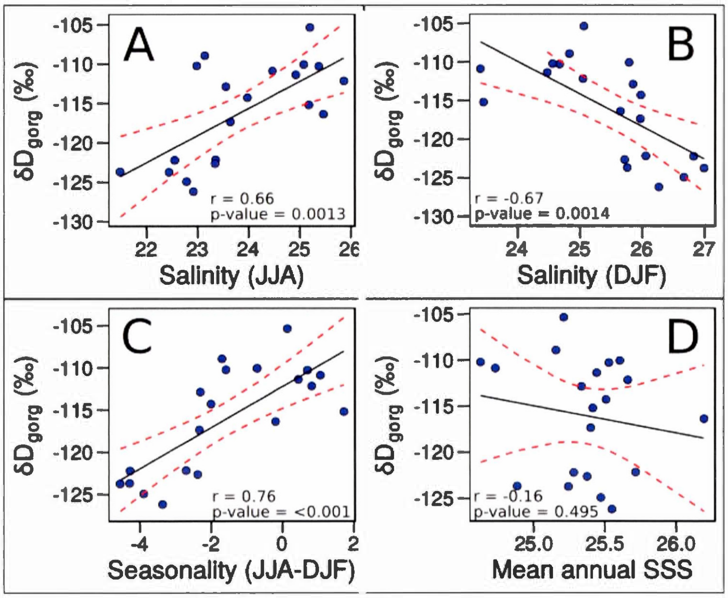

δDgorg measured in the annual growth rings of coral colony R1513-SR-0022 shares a statistically significant relationship with winter sea surface salinity, summer sea surface salinity, and with the summer-winter seasonal SSS difference over the past four decades, suggesting a link between hydroclimatic processes and the average annual deuterium content of gorginin. No meaningful relationship is found between annual average sea surface salinity and the deuterium content of gorgonin.

1.10 Equations

$$R = \frac{^{2}H}{^{1}H} \tag{1.1}$$

$$\delta D = \left[\left(\frac{R_{sample}}{R_{standard}}\right) - 1\right] \times 1000] \tag{1.2}$$

$$\delta D_{sample} = (1 - f_{ex}) \times \delta D_{non} + (f_{ex} \times \delta D_{ex}) \tag{1.3}$$

$$f_{ex} = \left(\frac{\delta D^{A}_{sample} - \delta D^{B}_{sample}}{\delta D^{A}_{water} - \delta D^{B}_{water}}\right) \tag{1.4}$$

$$\delta D_{non} = \left[\left(\frac{-f_{ex} \times \delta D_{water}}{1 - f_{ex}}\right) + \left(\frac{\delta D_{sample}}{1 - f_{ex}}\right)\right] \tag{1.5}$$

CHAPTER II

LABRADOR CURRENT CHANGES IN RESPONSE TO THE RECENT NAO MODAL SHIFT AS RECORDED BY DEEP-WATER CORALS OFF NEWFOUNDLAND

Samuel Davin[1], Claude Hillaire-Marcel[1], Evan Edinger[2]

[1]Geotop – Université du Québec à Montréal, Montreal, Canada

[2]Departments of Biology, Geography, and Earth Sciences, Memorial University of Newfoundland, St. John's, Newfoundland, Canada

Submitted to *Geophysical Research Letters*

Key points

i. The multi-decadal $\delta^{15}N$ enriching trend observed in the organic growthe rings of North Atlantic bamboo corals provides evidence for strengthening influence of the Labrador Current over the Newfoundland Shelf and Slope during the last century.

ii. A statistically significant relationship between organic skeletal $\delta^{13}C$ and mineralized skeletal Ba/Ca (Colony 2442: $r=0.71$, p-value <0.001; Colony 2452: $r=0.56$, p-value <0.001) lends support for the use of barium content as a paleo-productivity proxy and provides evidence of coherency between the mineralized and and proteinaceous components of deep-water coral skeletons.

iii. Pb/Ca in the skeletons of North Atlantic bamboo corals suggest the environmental residence time of anthropogenic lead on the North Atlantic slope is approximately 20 years.

Abstract

We present the Ba/Ca, Pb/Ca, $\delta^{15}N$, and $\delta^{13}C$ data from two ~80 yr-old colonies of deep-water bamboo corals (*Keratoisis grayi*) collected from the southwestern Newfoundland Slope which document 20th and 21st century trends in primary productivity and anthropogenic contamination. A steady increase in nodal $\delta^{15}N$ and $\delta^{13}C$ mark the pre-1960 years before $\delta^{13}C$ began to decline in response to the post-World War II increase in fossil carbon burning. The $\delta^{15}N$ records lend support for a simultaneous strengthening of Labrador Current influence over the Labrador and northeastern Newfoundland slopes as cold slope water is forced northwards by positive phase North Atlantic Oscillation. A significant relationship between Ba/Ca and $\delta^{13}C$ lends support for the use of Ba/Ca as a paleo-productivity indicator (Colony 2442: R=0.71, p-value <0.001; Colony 2452: R=0.56, p-value <0.001). The Pb/Ca records indicate a ~20-year residence time of anthropogenic lead on the North Atlantic slope following peak production of leaded paint and gasoline.

Plain language summary

Since the 19th-century the North Atlantic has undergone a series of rapid changes resulting from natural variations in ocean-atmosphere circulation patterns as well human activities. These changes have affected the availability of key nutrients which support the base of the marine food web as well as the distribution of contaminants, implicating the environmental health and economic security of northeastern communities. Until recently, the study of modern oceanographic variability has been limited by the limited geographic distribution and and brevity of instrumental records. Here, geoscientists have exploited natural records of environmental change by using the isotopic and elemental composition of natural materials as forensic evidence of past conditions. Deep-water corals, which are often long-lived and may be characterized by incremental growth rings, have emerged as excellent candidates for such studies.

In this study we have endeavored to identify and characterize ~80 years of oceanographic change recorded in the skeletons of two deep-water bamboo coral colonies collected from off the Grand Banks of Newfoundland. To do so, we have measured the nitrogen and carbon isotopic compositions of proteinaceous skeletal growth rings, as well as the relative amount of barium and lead present in the corresponding carbonate portions of the skeletons. Common trends amongst these variables are preserved in both skeletons, indicating that the two corals responded similarly to external environmental forcings while they were alive. From the resulting time-resolved data, we arrive at several key conclusions: (1) The carbon isotope records demonstrate a progressive increase in the uptake of CO_2 from the combustion of fossil fuels into the North Atlantic since post-World War II. (2) The nitrogen isotope data suggest waters arriving at the Newfoundland Slope have become increasingly nutrient-poor since at least the 1920s. This trend is thought to be associated with the slow intensification of atmospheric pressure over the North Atlantic since the mid-19th century, which has driven warm slope waters associate with the Gulf Stream further north while simultaneously constricting and intensifying the Labrador Current north of Newfoundland. (3) The lead content of the corals is tightly-linked to lead production in North America (e.g., leaded gasoline and leaded paint) with a time lag of ~20 years between peak production and the peak signal, suggesting anthropogenic lead in the North Atlantic has an environmental residence time of approximately two decades before it is sequestered. These findings also suggest the time required for the exchange between the atmosphere and the North Atlantic Ocean (to a depth of 700 m) occurs on decadal timescales. (4) The barium content and carbon isotopic composition of the corals shares a significant statistical relationship (Colony 2442: $R=0.71$, p-value <0.001; Colony 2452: $R=0.56$, p-value <0.001). Carbon isotopes are well-established as a proxy for primary productivity; the positive link between barium content and carbon isotopes suggests that barium content can be used as a proxy for primary productivity as well. This finding is meaningful for future studies because the barium content of corals can be measured more much more rapidly and with significantly less material than is required to measure carbon isotopes.

2.1 Introduction

2.1.1 Deep-water corals

Deep-water corals have gained attention in the marine and climate science communities for their potential as biological archives of (paleo)oceanographic variability. They are particularly attractive in instances where instrumental records are unavailable or sparse, and the temporal resolution of other archives is insufficient. Living at depth, such corals are azooxanthellate and are thus devoid of the potentially confounding direct biochemical signatures of photosynthesis. Similarly, these corals are insulated from seasonal extremes and abrupt hydrographic fluctuations by virtue of living at depth. Some genera (e.g., *Primnoa, Keratoisis)* live on centennial timescales, form incremental growth rings, and have hybrid mineralized-proteinaceous skeletons, which harbor distinct records of oceanographic processes: while the trace element composition of the mineralized skeletal components may reflect that of environmental water at depth [*Lea et al.*, 1989], the isotopic composition of proteinaceous tissues, as with all animals, reflect diet and trophic level [*DeNiro et al*., 1981; *Fry and Sherr*, 1989]. Deep-water corals are passive, opportunistic feeders thought to primarily feed on particulate organic matter (POM) exported from the ocean surface [*Gili & Coma*, 1998; *Sherwood et al.*, 2005; *Sherwood et al.*, 2008; *Williams and Grottoli* 2010; *Salvo et al.*, 2018]. Thus, by measuring the isotopic composition of proteinaceous skeletal tissue it is possible to infer historical changes in the composition of POM, and by extension gain insight into surficial ocean processes.

Progresses have been made in the past two decades in developing coral-based proxy studies of oceanographic variability. However, to this point studies have typically focused upon either proteinaceous portion of coral skeletons [e.g. *Heikoop et al.*, 2002; *Kiriakoulakis et al.*, 2005; *Sherwood et al.*, 2005; *Williams et al.*, 2006; *Sherwood et al.*, 2006; *Risk et al.*, 2009; *Baker et al.*, 2010; *Sherwood et al.,* 2011; *Sherwood et al.*, 2014; *Williams et al.*, 2017] or upon the mineralized component [e.g. *Smith et al.*, 2000; *Heikoop et al.*, 2002; *Bond et al.*, 2005; *Sinclair et al.*, 2005; *Sherwood et al.*, 2005b; *Grottoli and Williams et al.*, 2011). Here we present an exploratory study which seeks coherency between the trace element composition of the mineralized skeleton and the

C and N isotopic composition of proteinaceous growth nodes in two bamboo corals belonging to the species *Keratoisis grayi* collected from the southwestern Grand Banks of Newfoundland. *K. grayi* is an arborescent "bamboo" octocoral belonging to the family *Isididae,* known to inhabit shelf and slope environments in the North Atlantic, including off Nova Scotia, Newfoundland, and Labrador [*Buhl-Mortensen et al.*, 2015; *Neves et al.*, 2015; *Cordeiro et al.*, 2018]. *Keratoisis* skeletons are arborescent and feature proteinaceous growth nodes connected to massive internodal calcitic growth via a hollow central growth axis (see SI figure 1). The rationale for confronting records from two distinct colonies was to ascertain that they were indeed reproducible when linked to abiotic/external processes of interest for proxy-based paleoceanographic reconstructions.

2.1.2 Oceanographic context

Circulation on the shelf and slope of Newfound is characterized by the southeastern advection of the Labrador Current and its associated slope and shelf flows [*Smith et al.*, 1937]. The Labrador Current is produced by the merging of the Baffin Island Current with the West Greenland Current on the northern Labrador Slope. There, Labrador Shelf Water is formed by the modification of Labrador Sea Water in the Hudson Strait where it is mixed with waters of the Hudson Strait and Foxe Basin via intense intertidal mixing [*Drinkwater*, 1986]. The circulation of the Labrador Current on the southeastern Canadian Margin is impacted by modal fluctuations of the North Atlantic Oscillation (NAO) [*Petrie*, 2007]. During positive NAO modal shifts deep convection is enhanced in the Labrador Sea due to increased atmospheric cooling at the sea surface [*Häkkinen and Rhines*, 2004; *Han et al.*, 2010], driving an intensification of the subpolar gyre and, by extension, an intensification of Labrador Sea circulation. This results in the Labrador-Newfoundland Slope being dominated by relatively cold, fresh, nutrient-poor water associated with the Labrador Current. Positive NAO conditions also result in the northward advance of the Gulf Stream [*Drinkwater et al.*, 1994; *Han*, 2007], which introduces relatively warm, saline, and nutrient-rich Warm Slope Water (WSW) onto the continental slope from Georges Bank to Nova Scotia [*Petrie*, 2007]. During negative NAO modal shifts the opposite conditions are observed [*Petrie*, 2007]. In short, conditions on the Labrador-Newfoundland Slope are out of phase with conditions east of the Gulf of Saint Lawrence [*Han et al.*, 2014].

2.2 Methods

2.2.1 Sample recovery and preparation

Colonies 2442 and 2452 of *K. grayi* were live-collected in 2007 aboard the CCGS Hudson from the Newfoundland Slope at depths of 676 and 601 m (Figure 2), using a remotely operated vehicle, and subsequently frozen aboard.

Organic growth rings slated for δ^{15}N and δ^{13}C analyses were procured and prepared in the following manner: proteinaceous nodes were cut from the frozen colonies using a Dremel™ fitted with a circular, diamond-coated blade. Individual organic growth rings were isolated by first decalcifying the proteinaceous nodes in 5% HCl for up to 2 weeks (Sherwood et al., 2005). Once decalcified, proteinaceous nodes were triple rinsed in Milli-Q™ water and submerged in Milli-Q™ water overnight to remove any residual acid. The nodes were subsequently transferred to a Petri dish filled with Milli-Q™ water where individual organic growth rings were separated, under a binocular microscope, using forceps and a scalpel. Photographs of the sections taken before dissolution were used to guide sampling. Individual samples were triple rinsed in Milli-Q™ water and freeze-dried for 72 hours before being homogenized in clean glass vials with a stainless-steel rod. Calcitic cross-sectional skeletal thick sections slated for LA-ICP-MS analysis were cut from directly beneath the harvested proteinaceous nodes with the same Dremel™ tool (Figure 1). The thick sections were set in epoxy resin and subsequently polished on a lapidary wheel. Photographs of the polished thick sections were taken under binocular microscope to provide reference during laser ablation.

2.2.2 Stable isotope analysis and data handling

$\delta^{15}N$ and $\delta^{13}C$ of gorgonin growth rings were measured at Geotop-UQAM in Montreal, Canada via EA-IRMS. Nitrogen and carbon isotope ratios are reported relative to AIR and VPDB, respectively. The raw data are corrected using a calibration line constructed from 2 reference materials: $\delta^{13}C$ = -42.16‰ and -11.85‰; $\delta^{15}N$ = -0.22‰ and + 14.36‰. The internal reference materials are normalized on the NBS19-LSVEC scale for $\delta^{13}C$ and IAEA-N1, N-2 and N-3 for $\delta^{15}N$. For each of the isotopes a third internal reference material is used to ensure the accuracy of the calibration ($\delta^{13}C$ = -28.75‰ and $\delta^{15}N$ = -0.06‰). To assist with the statistical comparison of individual isotope time series with LA-ICP-MS elemental profiles a conservative numeric model was built using R to interpolate between individual isotope measurements at a 1-year timestep [*R Core Team*, 2013].

2.2.3 Trace element analysis

Trace elements were measured across the radius of each skeletal thick section from the central growth axis of the coral to the outer edge via LA-ICP-MS at Geotop-UQAM (Montreal, Canada). Thick sections were mounted into ablation cells with a motorized stage and scanned under a Photon-Machines G2 193 nm laser system with a 4 ns pulse duration, fitted with a Helix double-volume ablation cell. Each track was pre-ablated by pulsing an 80 μm laser spot at 50 Hz while continuously scanning at a rate of 100 μm/s. Analytical passes were completed with a 60 μm laser spot pulsing at 10 Hz while scanning at 10 μm/s. Ablated material was carried to a NuAttom High Resolution Inductively Coupled Plasma Mass Spectrometer (HR-ICP-MS) with an enhanced sensitivity interface by a continuous stream of He gas at a rate of 1.5 mL/min, with Ar make-up gas added before the torch. Three radial transects were performed on each thick section as a quality assurance measure. The raw data are corrected based on a calibration line constructed using two reference glasses, NIST 610 and NIST 612, which were measured before and after each radial transect. Trace element concentrations are reported relative to the isotope ^{43}Ca. Time resolved data were processed using Iolite software [*Paton et al.*, 2011] and R [*R Core Team*, 2013].

2.2.4 Age model

A bomb 14C-based chronology has been established in one of the *K. grayi* colonies (#2452) by *Sherwood and Edinger* [2009]. These data constrain the radial growth rate to 74 ± 6 μm·year-1 along the primary growth axis and the age of the colony to 94 ± 7 years. Specimen 2442 was live collected during the same expedition. Its chronology was determined by aligning ^{208}Pb/^{43}Ca time series profiles measured via LA-ICP-MS along the primary growth axis of each specimen (Figure 3). Pb/Ca was chosen for age model validation because of the widespread dissemination of anthropogenic Pb production in the 20th century, which manifests in each coral as two peaks centered around calendar years 1945 and 1980. These Pb peaks are associated with the production of leaded paint in the early 20th century and the sharp rise in production of gasoline containing tetraethyl lead post World War II [*Filippelli et al.*, 2005; *Nriagu*, 1990]. By this method we determined the age of specimen 2442 to be approximately 82 years, and its annual mean growth rate to average 71 μm·year-1, which is in good agreement with the measured growth rate of other North Atlantic *K. grayi* colonies [*Sherwood and Edinger*, 2009]. Pb/Ca is reported graphically as a 3-year running average superimposed upon aggregated annual mean values.

2.3 Results

2.3.1 Isotopic composition of proteinaceous nodes

$\delta^{15}N$ and $\delta^{13}C$ measurements of the proteinaceous node growth rings extracted from each *K. grayi* specimen are illustrated Figure 4. The innermost layers of nodal growth, representing the initial years of growth, were of insufficient mass for isotopic analysis. $\delta^{15}N$ values range from 12.25 to 14.01‰ in specimen 2442 and from 12.72 to 15.02‰ in specimen 2452; $\delta^{13}C$ values range from -18.14 to -17.22‰ in specimen 2442 and from -18.13 to -16.52‰ in specimen 2452. Mean standard deviation for $\delta^{15}N$ and $\delta^{13}C$ are ±0.23‰ and ±0.18‰ in colony 2442 and ±0.20‰ and ±0.14‰ in colony 2452. Time series produced from the two specimens overlap for a period of approximately 82 years from ~1925 to 2007. Based upon the ages established for each coral specimen and the number of growth rings successfully separated from the proteinaceous node, we estimate each sample to represent approximately 1 to 3 years of growth. Isotope results are reported in Annex B.

Both *K. grayi* specimens exhibit overall ^{15}N enrichment and ^{13}C depletion in incremental soft tissue samples collected from the central growth axis to the outer edge. Superimposed upon these long-term trends are multi-decadal and pluri-annual trends. From the early 20th century until the mid-1930, $\delta^{13}C$ and $\delta^{15}N$ trends are decoupled as the isotopic composition of carbon depletes and nitrogen enriches. From the mid 1930s until approximately 1970, both isotope systems enter an enriching phase, before ultimately decoupling again for the remainder of both records. The timings of these dual isotopic shifts are synchronous with broad modal shifts in the North Atlantic Oscillation (NAO) in which the positive mode is associated with a decoupling of carbon and nitrogen isotopes and the negative mode is associated with a coupling of the isotopes (Figure 4). On a multiannual basis the $\delta^{13}C$ records of the two corals are significantly correlated (R^2=0.65, p-value=0.002) and the $\delta^{15}N$ records each exhibit a distinct life-long enriching trend, despite having been collected at separate sites (Figure 4). These data suggest that the isotope signal is not driven by physiological or ontogenetic variability between corals but by the isotopic composition of their food sources.

The ^{13}C-depletion trend observed in the $\delta^{13}C$ values of both corals starting around 1970 may be explained by increasing CO_2 emissions from the combustion of fossil fuels, the effects of which are noted most sharply in the North Atlantic starting around 1960 [*Swart et al.*, 2010] (but recorded with a ~20 year-lag in the corals) (Figure 4), resulting in a $\delta^{13}C$ decrease of surface ocean dissolved inorganic carbon (DIC) of about 0.018‰ per year [*Bacastow et al.*, 1996]. Dead and sinking phytoplankton exported from the ocean surface represent a primary food source of azooxanthellate corals [e.g., *Sherwood et al.*, 2005], thus imparting a surface ocean isotopic signature to opportunistic consumers (e.g., cold-water corals). We conclude that the decoupling of $\delta^{13}C$ and $\delta^{15}N$ at ~1970 is largely due to the delay of penetration of the light isotopic signature of anthropogenic CO_2 into the North Atlantic. The delay of ~20 years in the onset of the ^{13}C-Suess Effect in these corals corresponds to the approximately 20-year lag in the skeletal Pb/Ca concentrations associated with emissions from the combustion of gasoline containing tetraethyl lead.

2.3.2 Internodal ^{137}Ba/^{43}Ca

Internodal ^{137}Ba/^{43}Ca (henceforth referred to as Ba/Ca) measurements of both specimens are illustrated Figure 4. Skeletal Ba/Ca in each of the cross-sectional thick sections was measured along three separate laser transects from the central growth axis to the outer edge. Data collected along the three transects were aggregated to create composite elemental profiles of both thick sections, each of which were subsequently reduced to mean annual values. From these data we find barium concentrations in each specimen relative to calcium to be between 2 and 5 parts per thousand. A comparison of the two Ba/Ca profiles after applying a 3-year running mean to denoise the data yields a highly significant relationship between the Ba content of each coral (R=0.46, p-value <0.001, n=77). These findings suggest that while the Ba content of the two corals share a statistically significant relationship, there are other factors influencing the Ba content of the two corals which are not accounted for. Ba/Ca values can be found in Annex B.

2.3.3 Skeletal $^{208}Pb/^{43}Ca$

Composite $^{208}Pb/^{43}Ca$ profiles for each of the corals (henceforth referred to as Pb/Ca) were created in the same way as the composite Ba/Ca profiles. This methodology is described in the previous subsection.While differences are noted in the Pb/Ca profiles of the two corals, they are highly correlated (Figure 3) (R=0.69, p-value <0.001). In addition to providing age control, the timing of the lead enrichment peaks give insight into the rate at which environmental contaminants have historically entered the marine system. Each coral exhibits two distinct Pb/Ca peaks, centered around 1945 and 1985. The first Pb/Ca peak corresponds to leaded paint production Production of leaded paint peaked during the early 1920s, at which time >150,000 tons of lead were produced per year in the United States alone [*Filippelli et al.*, 2005]. The second and larger Pb/Ca peak originates from the use of tetraethyl lead as a gasoline additive. Introduced in 1923, leaded gasoline production rose rapidly from the mid 1930s, plateaued briefly in the 1950s, and finally reached peak production in the Western World in 1971 when the annual consumption of lead for gasoline additives reached 377,000 metric tonnes [*Nriagu*, 1990]. Mounting public health concerns resulted in the eventual discontinuation of leaded gasoline, with production falling steeply from 1978. Based on the preexisting bomb-^{14}C chronology of specimen 2452 and the observed signature of the rise and fall of leaded gasoline in both specimens, there is an apparent lag of ~14-22 years between source contamination and the appearance of lead enrichment in the corals, broadly matching the DIC-^{13}C recording of recent changes in the isotopic composition of atmospheric CO_2. Based on the timing of the two lead peaks in each of the corals, which are determined by applying a constant-growth rate model, it appears the two corals grew at similar rates until the mid-20th century, at which point the growth rate of colony 2452 slowed relative to colony 2442. Pb/Ca values can be found in Annex B.

2.4 Discussion

2.4.1 Carbon and nitrogen isotopes in *Keratoisis grayi*

As a general rule for animals living in an open ocean food web, each successive increase in trophic level is accompanied by the enrichment of $\delta^{13}C$ and $\delta^{15}N$ by ~1.1‰ and ~3.4‰, respectively [*DeNiro and Epstein*, 1981]. However, C and N isotopic variability in suspension feeders likely reflect changes in the composition of their primary food source, POM, of which dead and dying phytoplankton constitute the bulk. The $\delta^{15}N$ of proteinaceous coral growth rings has been found to be a reliable proxy for the $\delta^{15}N$ of fixed nitrogen utilized by phytoplankton, which in turn is closely linked to ocean circulation and the mixing of water masses [*Sherwood et al.*, 2011]. $\delta^{13}C$ is sensitive to carbon export (including the relative flux of carbon from atmospheric and deep marine sources) and to the assemblage and lipid content of phytoplankton communities. Furthermore, the sinking rate of POM varies widely depending on size and density, and may take up to several weeks and travel hundreds of kilometers before sinking to a depth of 600 m [*Jeffrey et al.*, 1983; *Druffel et al.*, 2003]. Thus, the C and N isotopic composition of deep-water corals are sensitive to processes affecting phytoplankton communities, and may record changes occuring far afied of the corals themselves.

High baseline $\delta^{15}N$ values and long-term ^{15}N-enrichment trends are observed in both *K. grayi* specimens. Deep-water corals feed primary upon sinking POM [*Roark et al.*, 2005, 2006; *Sherwood et al.*, 2005b, *Williams et al.*, 2007a], thus we suggest that the high baseline $\delta^{15}N$ values result from the corals feeding on POM featuring high $\delta^{15}N$ phytodetrital material exported from the nutrient-poor surface waters of the Labrador Current [*Townsend et al.*, 2006]. While bacterial modification of sinking POM could feasibly explain the enriched $\delta^{15}N$ values observed in the corals, sinking POM on the eastern Canadian Margin is not thought to undergo significant modification [*Muzuka and Hillaire-Marcel*, 1999]. In explanation of the long-term $\delta^{15}N$ enriching trend observed in both corals, we suggest an increase in the $\delta^{15}N$ of POM driven by the isotopic composition of fixed N .

2.4.2 Nodal $\delta^{15}N$ link to strengthening of the Labrador Current over the slope with positive NAO

Beginning ~160 years ago, and particularly since 1970, the North Atlantic Oscillation (NAO) has shifted from a 1600-year predominantly negative mode [*Kegwin et al.*, 2003) to a positive/warm mode [*Hurrell*, 1995]. Positive modal shifts in the NAO drive the relatively cold, fresh, and nitrate poor Labrador Slope Water (>16–17 μM) on the Scotian Shelf and Grand Banks of Newfoundland further north, displacing it with the relatively warm, saline, nitrate-rich (>23 μM) Warm Slope Water (WSW) associated with the Gulf Stream [*Townsend et al.*, 2006; *Townsend and Ellis*, 2010]. Nitrate present in the WSW originates from nutrient-rich waters below the Gulf Stream [*Csanady and Hamilton*, 1988; *Townsend et al.*, 2010] and has an isotopic composition of 5.02 ± 0.27‰ whereas nitrate in the Labrador Slope Water originates in the low-nutrient Labrador Sea Water and has a mean $\delta^{15}N$ value of 6.00 ± 0.028‰. Thus, displacement of Labrador Slope Water with WSW results in 1‰ $\delta^{15}N$ decrease of the available nitrate pool. Primary production in the northeastern North Atlantic is nitrogen limited, and as such the trend towards lower $\delta^{15}N$-values nitrate in the presence of WSW is preserved in phytoplankton and resulting POM due to complete utilization of the fixed nitrogen pool. Long-term ^{15}N-depletion trends spanning the 20th and early 21st century are observed in deep-water gorgonians on the Scotian Shelf, in response to the increasing presence of WSW off Nova Scotia [*Sherwood et al.*, 2011].

Two *K. grayi* specimens presented herein, which were collected approximately 700 km northeast of the *P. resedaeformis* colonies studied by *Sherwood et al.* [2011], exhibit a progressive ^{15}N-enrichment rather than a depletion. The δ^{15}N trend observed in these corals contests the influence of WSW on the ^{15}N content of POM over the southwestern Newfoundland Slope. In consideration of this data we suggest (1) that POM consumed on the Newfoundland Slope originates from the Labrador-Newfoundland Slopes, and (2) that the influence of the Labrador Current has incrementally intensified over the Labrador-Newfoundland slope during the 20th and early 21st century in response to the concurrent long-term positive modal shift of the NAO. To test whether a northern source of POM could potentially reach the *K. grayi* colonies on the southwestern Newfoundland Shelf, we consider the following: POM settling velocities in marine shelf environments have been estimated to range from approximately 1 m/day-1 for large aggregates (4-5 mm) to 36 m/day-1 (1-2.5 mm) [*Asper*, 1987]. The dominant water masses on the Grand Banks and Newfoundland Slope are Labrador Slope Water and Labrador Shelf Water, the mean velocities of which are each 0.3-0.5 m/s [*Greenberg and Petrie*, 1985; *Lazier and Wright*, 1991]. Assuming a rapid sinking velocity of 30 m/day, a conservative estimate of the time for POM advected with Labrador Shelf Water and sinking to a depth of 700 m is ~23 days. Assuming a mean current velocity of 0.4 m/s, a rough calculation of the minimum distance POM may have travelled before reaching the *K. grayi* colonies is >800 km, with greater distances for POM settling more slowly. As such, we suggest that the consumption of POM advected from the Labrador-Newfoundland Slope is the reason why the *K. grayi* colonies do not exhibit the same δ^{15}N depleting trend observed in Scotian Shelf gorgonians in *Sherwood et al.* 2011. We also suggest the observed δ^{15}N enriching trend in both corals is due to the long-term shift of the NAO from a predominantly negative mode prior to 1860 to a predominantly positive mode after 1860 [*Kegwin et al.*, 2003].

Our findings lend support to Petrie (2007) and Han et al. (2014), in which the influence of the Labrador Current is found to be positively correlated with the winter NAO index over the Labrador and northeastern Newfound slopes and negatively over the Scotian Slope. Due to the length of the δ^{15}N records, these findings also suggest hydrographic conditions east and west of the Gulf of Saint Lawrence have become increasingly decoupled since the early 20th century.

2.4.3 Covariation of nodal δ^{13}C and internodal Ba/Ca

Barium has generated interest as a proxy of biological productivity because of the correlation between the distribution of barium bound to POM and POM concentrations in sediments [*Bishop*, 1998, *Calvert et al.*, 2007, *Sternberg et al.*, 2007]. Coral skeletal Ba concentration islinked to the barium content of ambient seawater [*LaVigne et al.*, 2016; *Serrato-Marks et al.*, 2017] This relationship has previously been exploited to identify the cycling and export of nutrients on inter-annual timescales [*Lea et al., 1989*; *Serrato-Marks et al.*, 2017). Due to its association with export production the behavior of barium in the marine system may be described as "nutrient like", with concentrations of Ba in seawater typically found to be depleted in surface waters and enriched at abyssal depths [*Dehairs et al.*, 1980]. δ^{13}C of sediments and sinking POM is sensitive to carbon export and may be interpreted as a proxy for marine productivity, in which higher ^{13}C values correspond to periods of enhanced productivity and lower ^{13}C values represent periods of decreased productivity. Prior to 1970, we observe a significant correlation between nodal δ^{13}C and internodal Ba/Ca in both colony 2452 ($R^2=0.31$, p-value <0.001) and colony 2442($R^2=0.51$; p-value <0.001). After 1970 the δ^{13}C records are compromised by the ^{13}C-Suess effect. Although the magnitude of discrete Ba/Ca excursions differ between the two corals, this is also the case between individual transects within the same coral. Based on these observations we speculate that while the general Ba/Ca trend is linked to the concentration of barium in ambient seawater, the rate of barium uptake into the skeletal internode may be sensitive to the growth rate of the calcite internodes. From these data we infer that positive Ba/Ca excursions recorded in *K. grayi* are linked to periods of decreased biological utilization of Ba in seawater, which is in agreement with the findings of *Chan et al.* [2017] who present similar findings in crustose coralline algae.

2.5 Conclusions

We present the first example of covariation between trace elements and C and N isotopes in deep-water coral skeletons. From nodal $\delta^{15}N$ data we infer an intensification of the Labrador Current over the Labrador and Newfoundland slopes during positive modal shifts of the NAO. The long-term $\delta^{15}N$ enriching trend observed in both colonies suggests a long-term shift in the nutrient regime of the Labrador-Newfoundland Slope from at least the early 20th century until the early 21st century. The good phasing of contemporaneous nodal $\delta^{13}C$ and internodal Ba/Ca in each of the corals confirms the interest of deep-water coral Ba concentrations as a proxy for productivity and carbon export. However, we note that Ba/Ca reproducibility betweenindividual laser transects is imperfect. These discrepencies raise questions about the sensitivity of skeletal Ba uptake to biological effects such as asymmetric radial growth rates. The negative shift in nodal $\delta^{13}C$ values post-World War II matches the increased concentrations of internodal Pb in response to leaded gasoline emissions, both of which support decadal-scale ventilation on the Newfoundland Slope to a depth of 600-700 m.

2.6 Acknowledgements

We extend our thanks to Geotop members Dr. Jean-Francois Helie, Prof. Andre Poirier, and Rebecca Paisley for their assistance with the acquisition of data presented herein, and to the crews of the CCGS Hudson assistance in procuring these *K. grayi* samples.

This work was supported by funding from the Natural Sciences and Engineering Research Council of Canada (NSERC), VITALS, and ArcTrain.

2.7 References

Akenhead, S. A, Petrie, B, Ross, C.K., and D.M Ware (1981), Ocean climate and the marine fisheries of Atlantic Canada: an assessment, Bedford Institute of Oceanography Report Series, BI-R-81-6, 121 p.

Bacastow, R. B., Keeling, C. D., Lueker, T. J., Wahlen, M., and W.G. Mook (1996), The ^{13}C Suess effect in the world surface oceans and its implications for oceanic uptake of CO2: Analysis of observations at Bermuda, Global Biogeochemical Cycles, 10(2), 335-346.

Baker D. M., Webster K. L., and K. Kim (2010), Caribbean octocorals record changing carbon and nitrogen sources from 1862 to 2005, Global Change Biology, 16(10), 2701-2710.

Bishop, J. B. K. (1988), The barite-opal-organic carbon association in oceanic particulate matter, Nature, 332, 341–343, doi:10.1038/332341a0.

Bond Z. A., Cohen A. L., Smith S. R. and W. J. Jenkins (2005), Growth and composition of high-Mg calcite in the skeleton of a Bermudian gorgonian (Plexaurella dichotoma): potential for paleothermometry, *Geochemistry, Geophysics, Geosystems*, 6(8), 10.

Buhl-Mortensen, L., Olafsdottir, S. H., Buhl-Mortensen, P., Burgos, J. M., and S. A. Ragnarsson (20^{15}), Distribution of nine cold-water coral species (Scleractinia and

Gorgonacea) in the cold temperate North Atlantic: effects of bathymetry and hydrography, *Hydrobiologia*, *759*(1), 39-61.

Calvert, S. E., and T. F. Pederson (2007), Elemental proxies for palaeoclimatic and palaeooceanographic variability in marine sediments: Interpretation and application, in *Proxies in the Late Cenozoic Paleoceanography*, edited by C. Hillaire-Marcel, and A. de Vernal, pp. 567–644, Elsevier, Amsterdam, doi:10.1016/S1572-5480(07)01019-6

Chan, P., Halfar, J., Adey, W., Hetzinger, S., Zack, T., Moore, G. W. K., Wortmann, U.G,, Williams, B., and A. Hou (2017), Multicentennial record of Labrador Sea primary productivity and sea-ice variability archived in coralline algal barium, *Nature communications*, 8, 15543.

Cordeiro, R., van Ofwegen, L., and G. Williams (2018), World List of Octocorallia. *Keratoisis grayi* Verrill, 1878, Accessed through: World Register of Marine Species at: http://www.marinespecies.org/aphia.phpδp=taxdetails&id=158285 on 2018-11-17

Csanady, G. T., and P. Hamilton (1988), Circulation of slopewater, *Continental Shelf Research*, 8(5-7), 565-624.

Dehairs, F., Chesselet, R., and J. Jedwab (1980), Discrete suspended particles of barite and the barium cycle in the open ocean, *Earth and Planetary Science Letters*, 49, 528–550.

DeNiro, M. J., and S. Epstein (1981), Influence of diet on the distribution of nitrogen isotopes in animals, *Geochimica et cosmochimica acta*, *45*(3), 341-351.

Drinkwater, K. F. (1986), Physical oceanography of Hudson strait and Ungava Bay, In *Elsevier oceanography series* (Vol. 44, pp. 237-264), Elsevier.

Drinkwater, K. F., Myers, R. A, Pettipas, R. G., and T. L. Wright (1994). Climatic data for the northwest Atlantic: the position of the shelf/slope front and the northern boundary of the Gulf Stream between 50W and 75W, 1973-1992. *Canadian Data Report of Fisheries and Ocean Sciences*, 125, Department of Fisheries and Oceans, Canada

Filippelli G.M., Laidlaw M., Latimer, J. C., and R. Raftis (2005), Urban lead poisoning and medical geology: An unfinished story. *GSA Today,* 15, 4–11.

Fry, B., and E. B. Sherr (1989), $\delta^{13}C$ measurements as indicators of carbon flow in marine and freshwater ecosystems, Stable isotopes in ecological research (196-229), Springer, New York, NY.

Gili J. M., and R. Coma (1998), Benthic suspension feeders: their paramount role in littoral marine food webs, Trends in Ecology & Evolution, 13(8), 316-321.

Greenberg, D. A., and B. D. Petrie (1988), The mean barotropic circulation on the Newfoundland shelf and slope, Journal of Geophysical Research: Oceans, 93(C12), 15541-15550.

Häkkinen, S. and P. B. Rhines (2004), Decline of subpolar North Atlantic circulation during the 1990s, Science, 304(5670), 555-559.

Han, G., Ohashi, K., Chen, N., Myers, P. G., Nunes, N., and J. Fischer (2010), Decline and partial rebound of the Labrador Current 1993–2004: Monitoring ocean currents from altimetric and conductivity-temperature-depth data, Journal of Geophysical Research: Oceans, 115(C12).

Han, G., Chen, N., and Z. Ma (2014), Is there a north-south phase shift in the surface Labrador Current transport on the interannual-to-decadal scaleδ, Journal of Geophysical Research: Oceans, 119(1), 276-287.

Hetzinger, S., Halfar, J., Zack, T., Mecking, J. V., Kunz, B. E., Jacob, D. E., and W. H. Adey (20^{13}), Coralline algal Barium as indicator for 20th century northwestern North Atlantic surface ocean freshwater variability, Scientific Reports, 3, 1761.

Heikoop J. M., Hickmott D. D., Risk M. J., Shearer C. K., and V. Atudorei (2002), Potential climate signals from the deep-sea gorgonian coral *Primnoa resedaeformis*, Hydrobiologia, 471, 117–124.

Hurrell, J. W. (1995), Decadal trends in the North Atlantic Oscillation: regional temperatures and precipitation, Science, 269(5224), 676-679.

Keigwin, L. D., Sachs, J. P., and Y. Rosenthal (2003), A 1600-year history of the Labrador Current off Nova Scotia, Climate Dynamics, 21(1), 53-62.

Kiriakoulakis, K., Fisher, E., Wolff, G. A., Freiwald, A., Grehan, A., and J. M. Roberts (2005), Lipids and nitrogen isotopes of two deep-water corals from the North-East Atlantic: initial results and implications for their nutrition, Cold-water corals and ecosystems (pp. 715-729), Springer, Berlin, Heidelberg.

LaVigne, M., Grottoli, A. G., Palardy, J. E., and R. M. Sherrell (2016), Multi-colony calibrations of coral Ba/Ca with a contemporaneous in situ seawater barium record, Geochimica et Cosmochimica Acta, 179, 203-216.

Lazar, B., Enmar, R., Schossberger, M., Bar-Matthews, M., Halicz, L., and M. Stein (2004), Diagenetic effects on the distribution of uranium in live and Holocene corals from the Gulf of Aqaba, Geochimica et Cosmochimica Acta, 68(22), 4583-4593.

Lea, D. and E Boyle (1989a), Barium content of benthic foraminifera controlled by bottom-water composition, Nature, 338, 751–753.

Lea, D., Shen, G. T., and E. A. Boyle (1989b), Coralline barium records temporal variability in equatorial Pacific upwelling. Nature, 340, 373–376.

Muzuka, A. N. and C. Hillaire-Marcel, (1999), Burial rates of organic matter along the eastern Canadian margin and stable isotope constraints on its origin and diagenetic evolution. Marine Geology, *160*(3-4), 251-270.

Neves, B., Edinger, E., Hillaire-Marcel, C., Saucier, E. H., France, S. C., Treble, M. A., and V. E. Wareham (2015), Deep-water bamboo coral forests in a muddy Arctic environment, *Marine Biodiversity*, *45*(4), 867-871.

Nriagu, J. O. (1990), The rise and fall of leaded gasoline, Science of the Total Environment, 92, 13-28.

Paton, C., Hellstrom, J., Paul, B., Woodhead, J., and J. Hergt (2011), Iolite: Freeware for the visualisation and processing of mass spectrometric data, Journal of Analytical Atomic Spectrometry, 26(12), 2508-2518.

Petrie, B. (2007), Does the North Atlantic Oscillation affect hydrographic properties on the Canadian Atlantic continental shelfδ, *Atmosphere-Ocean*, 45(3), 141-151.

Petrie, B., and A. Isenor (1985), The near-surface circulation and exchange in the Newfoundland Grand Banks region, *Atmosphere-Ocean*, 23(3), 209-227

R Core Team (2013), R: A language and environment for statistical computing, R Foundation for Statistical Computing, Vienna, Austria, URL http://www.R-project.org/

Risk M. J., Lapointe B. E., Sherwood O. A., and B. J. Bedford (2009), The use of δ^{15}N in assessing sewage stress on coral reefs, Marine Pollution Bulletin, 58(6), 793–802.

Salvo, F., Hamoutene, D., Hayes, V. E. W., Edinger, E. N., and C. C. Parrish (2018), Investigation of trophic ecology in Newfoundland cold-water deep-sea corals using lipid class and fatty acid analyses, Coral Reefs, 37(1), 157-171.

Serrato Marks G, LaVigne M, Hill TM, Sauthoff W, Guilderson TP, Roark EB, Dunbar RB, and T. J. Horner (2017), Reproducibility of Ba/Ca variations recorded by northeast Pacific bamboo corals, Paleoceanography, 32(9), 966-979.

Sherwood O. A., Heikoop J. M., Scott D. B., Risk M. J., Guilderson T. P., and R. A. McKinney (2005a), Stable isotopic composition of deep-sea gorgonian corals *Primnoa* spp.: A new archive of surface processes, Marine Ecology Progress Series, 301, 135–148.

Sherwood, O. A., Heikoop, J. M., Sinclair, D. J., Scott, D. B., Risk, M. J., Shearer, C., and K. Azetsu-Scott (2005b), Skeletal Mg/Ca in Primnoa resedaeformis: relationship to temperatureδ, Cold-water corals and ecosystems (pp. 1061-1079). Springer, Berlin, Heidelberg.

Sherwood O. A., Scott D. B., and M. J. Risk (2006). Late holocene radiocarbon and aspartic acid racemization dating of deep-sea octocorals, Geochimica et Cosmochimica Acta, 70(11), 2806–2814.

Sherwood, O. A., Jamieson, R. E., Edinger, E. N., and V. E. Wareham (2008), Stable C and N isotopic composition of cold-water corals from the Newfoundland and Labrador continental slope: Examination of trophic, depth and spatial effects, Deep Sea Research Part I: Oceanographic Research Papers, 55(10), 1392-1402.

Sherwood, O. A., and E. N. Edinger, E. N (2009), Ages and growth rates of some deep-sea gorgonian and antipatharian corals of Newfoundland and Labrador, Canadian Journal of Fisheries and Aquatic Sciences, 66(1), 142-152.

Sherwood O. A., Lehmann M. F., Schubert C. J., Scott D. B., and M. D. McCarthy (2011), Nutrient regime shift in the western north atlantic indicated by compound-specific δ^{15}N of deep-sea gorgonian corals, *Proceedings of the National Academy of Sciences*, 108(3), 1011–10^{15}.

Sherwood O. A., Guilderson T. P., Batista F. C., Schiff J. T., and M. D. McCarthy (2014), Increasing subtropical North Pacific Ocean nitrogen fixation since the little ice age, Nature, 505(7481), 78–81.

Sinclair, D. J., Sherwood, O. A., Risk, M. J., Hillaire-Marcel, C., Tubrett M., Sylvester, P., McCulloch, M., and L. Kinsley (2005), Testing the reproducibility of Mg/Ca profiles in the deep-water coral Primnoa resedaeformis: putting the proxy through its paces, In *Cold-water corals and ecosystems* (pp. 1039-1060), Springer, Berlin, Heidelberg.

Smith J. E., Schwarcz H. P., Risk M. J., McConnaughey T. A., and N. Keller (2000), Paleotemperatures from Deep-Sea Corals: Overcoming 'Vital Effects', *Palaios*, 15(1), 25.

Smith, E. H., Soule, F. M., and O. Mosby (1937), The Marion and General Greene Expeditions to Davis Strait and Labrador Sea, Under Direction of the United States Coast Guard: 1928-1931-1933-1934-1935: Scientific Results, Part 2: Physical Oceanography, US Government Printing Office.

Sternberg, E., C. Jeandel, J.-C. Miquel, B. Gasser, M. Souhaut, R. Arraes-Mescoff, and R. Francois (2007), Particulate barium fluxes and export production in the northwestern Mediterranean, *Marine Chemistry*, 105, 281–295.

Swart, P. K., Greer, L., Rosenheim, B. E., Moses, C. S., Waite, A. J., Winter, A., Dodge R. E., K. Helmle (2010), The ^{13}C Suess effect in scleractinian corals mirror changes in the anthropogenic CO2 inventory of the surface oceans, Geophysical Research Letters, 37(5).

Townsend, D. W., Thomas, A. C., Mayer, L. M., Thomas, M. A., and J. A. Quinlan (2006), Oceanography of the northwest Atlantic continental shelf (1, W), The sea: the global coastal ocean: interdisciplinary regional studies and syntheses, 14, 119-168.

Townsend, D. W., Rebuck, N. D., Thomas, M. A., Karp-Boss, L., and R. M. Gettings (2010), A changing nutrient regime in the Gulf of Maine, Continental Shelf Research, 30(7), 820-832.

Williams B., Risk M. J., Ross S. W., and K. J. Sulak (2006), Deep-water antipatharians: proxies of environmental change, Geology, 34(9), 773–776.

Williams, B. and A. G. Grottoli (2010), Recent shoaling of the nutricline and thermocline in the western tropical Pacific, Geophysical Research Letters, 37(22).

Williams B., Thibodeau B., Chikaraishi Y., Ohkouchi N., Walnum A., Grottoli A. G., and P. L. Colin (2017), Consistency in coral skeletal amino acid composition offshore of Palau in the western Pacific warm pool indicates no impact of decadal variability in nitricline depth on primary productivity, Limnology and Oceanography, 62(2), 399–407.

2.8 Figures

Figure 2.1 Diagram of a *Keratoisis* skeleton

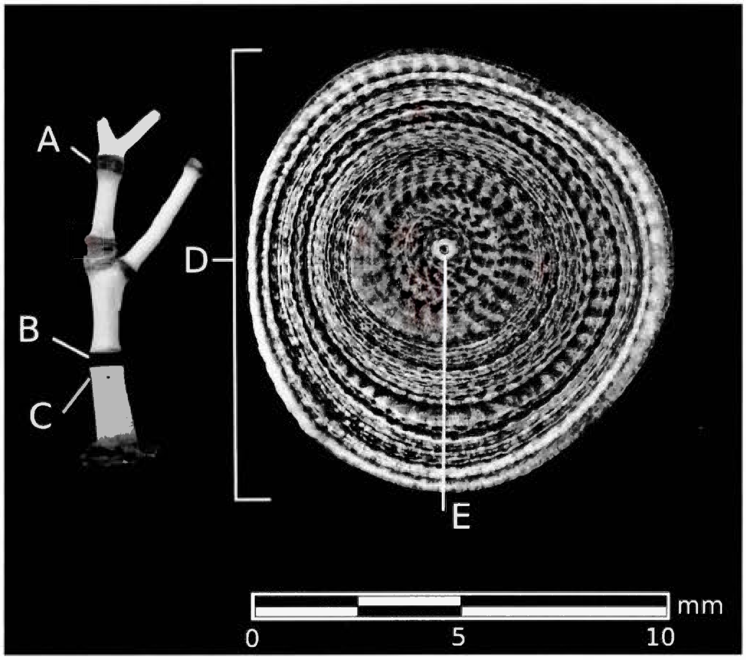

Laboratory specimen of K. grayi (2454) cleaned of coenosarc and polyps. (A) Proteinaceous growth node; (B) Proteinaceous growth node removed for analysis; (C) Location where calcite thick section was cut from; (D) Enhanced contrast image of a thick section of skeletal calcite internode featuring incremental growth banding. Light and dark regions reflect zones of higher density growth. (E) Transect of dominant growth direction from central axis (approximate). The partial skeleton on left is approximately 11 cm in height; the diameter of the thick section on right is approximately 1 cm.

Figure 2.2 Map of the Grand Banks

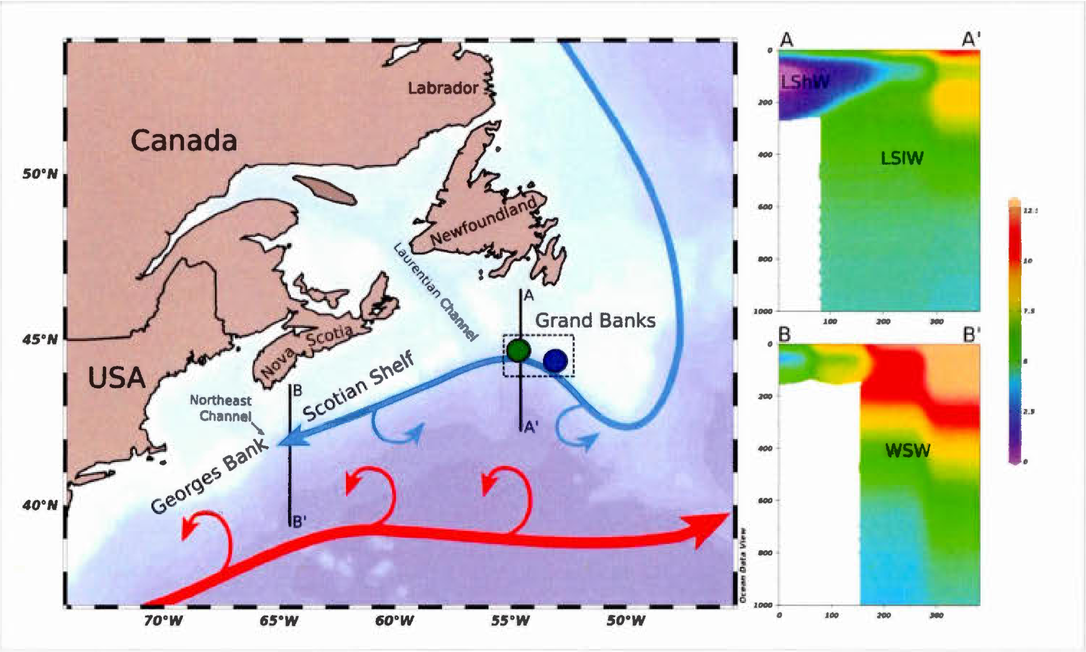

K. grayi colonies 2442 (green circle) and 2452 (blue circle), were collected in by remotely operated vehicle in 2007 on the Grand Banks of Newfoundland at 676 and 601 m, respectively. General circulation of the shelf and slope of Newfoundland is characterized by the associated shelf and slope waters of the Labrador Current (blue lines), which run counter to the Gulf Stream (red lines).26 Northward encroachment of the Gulf Stream associated with positive NAO modal shifts results in the displacement of the relatively cold, fresh, and nutrient poor Labrador Shelf and Slope Waters present from the southwestern Grand Banks to Georges Bank with warmer, more saline, and nutrient replete Warm Slope Water (WSW) associated with the Gulf Stream. Two

depth transects (A to A', B to B') illustrate the stronger influence of Labrador Shelf Water on the Grand Banks relative
to on the Scotian Shelf.

Figure 2.3 Coral lead content versus anthropogenic lead production

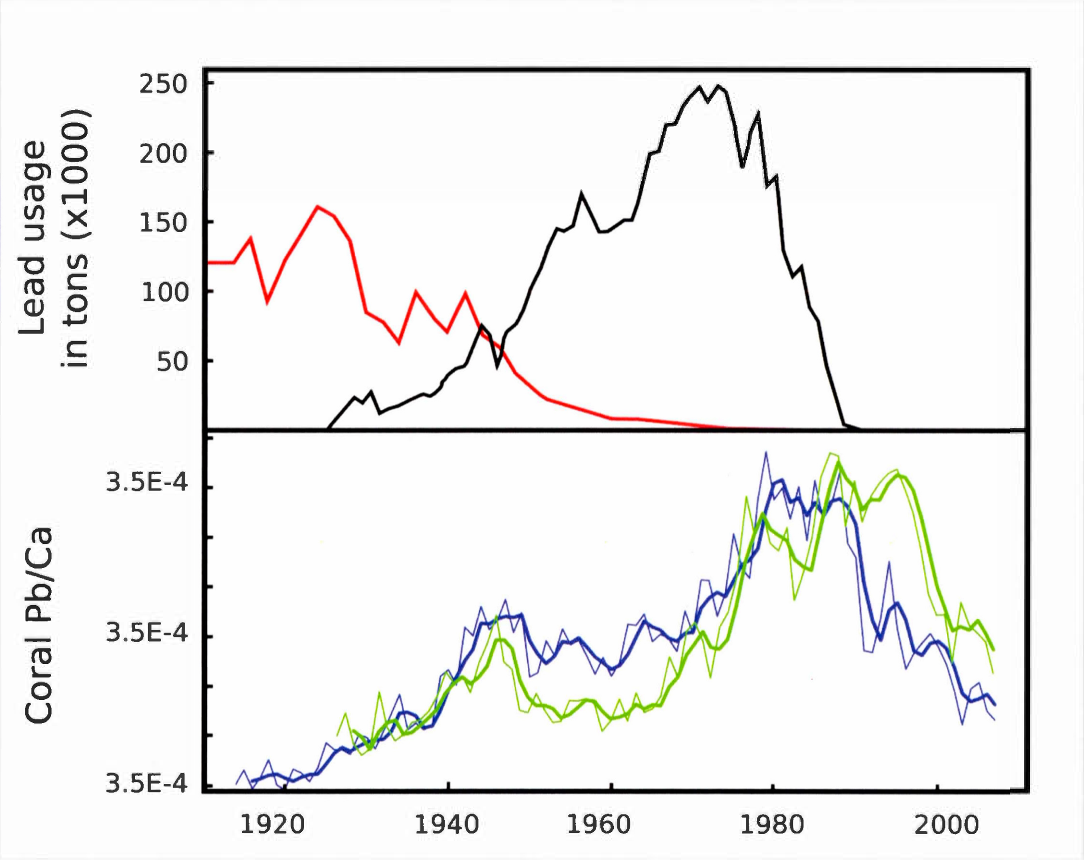

20th century North American lead use (upper panel) versus the ^{208}Pb/^{43}Ca profiles of *K. grayi* colonies 2452 (blue), 2442 (green) (15-point moving average superimposed on full resolution data). A chronology for 2452 has been previously established by bomb-^{14}C (Sherwood and Edinger, 2009). The ages and growth rates of colony 2442 is determined by aligning ^{208}Pb/^{43}Ca time series profiles measured along the primary growth axis of each specimen via LA-ICP-MS with that of 2452.

Figure 2.4 Summary of Ba/Ca, $\delta^{15}N$, $\delta^{13}C$, and NAO index

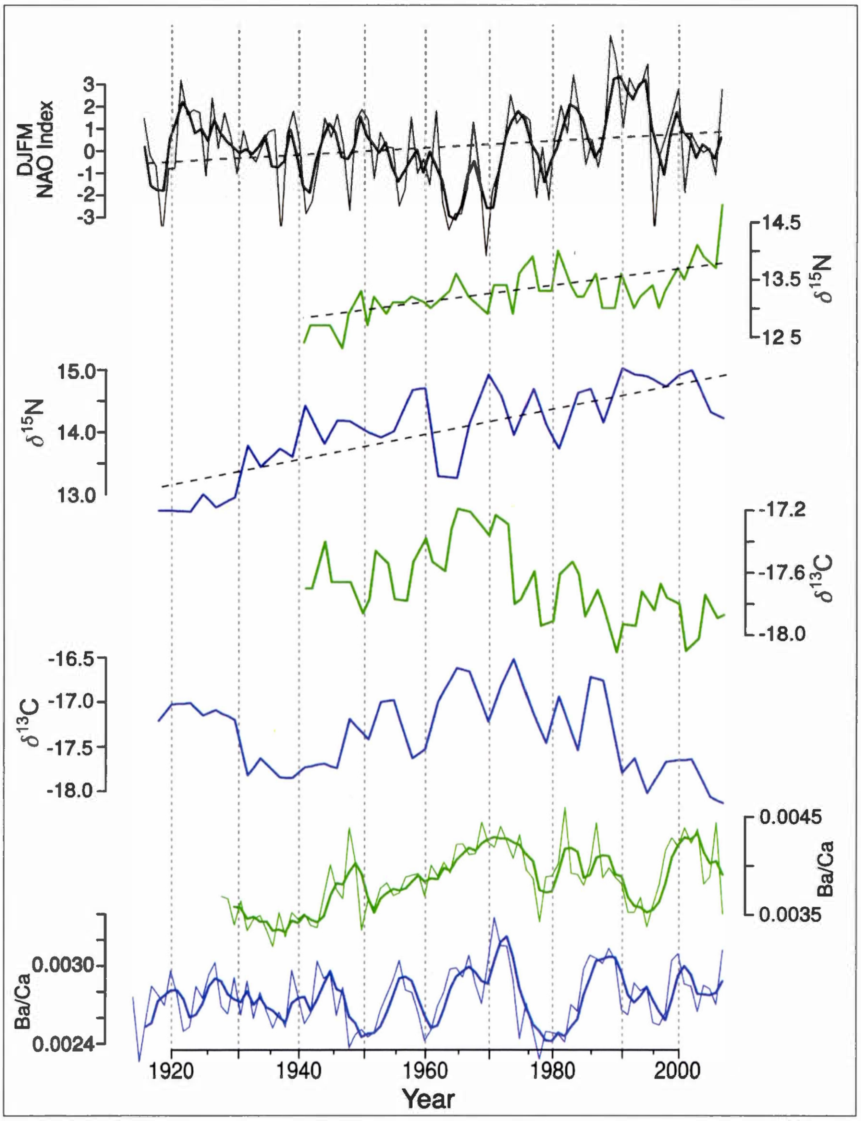

Summary of Ba/Ca, $\delta^{15}N$ and $\delta^{13}C$ data from *K. grayi* colonies 2442 (green), and 2452 (blue) plotted as a time series. Calendar year estimates are based on growth rates derived from bomb-$_{14}C$ measurements. Individual carbon and nitrogen isotope data points represent 1-3 years of growth and Ba/Ca data is plotted as a 3-year running mean. Isotope data does not match the full length of Ba/Ca transects due to sample mass limitations of nodal growth rings towards approaching the central growth axis

CHAPTER III

^{15}N AND ^{18}O MONITORING OF NITRATE CYCLING ALONG THE LABRADOR SEA CORRIDOR UNDER OPEN WATER CONDITIONS

Samuel Davin[1], Owen A. Sherwood[2], Carolyn Buchwald[2], Claude Hillaire-Marcel[1]

[1]GEOTOP – Université du Québec à Montréal, Montreal, Canada

[2]Department of Earth Science, Dalhousie University, Halifax, Nova Scotia, Canada

Pre-submission to *Biogeochemistry*

Abstract

A basin-wide sampling program of nitrate isotopes ($\delta^{15}N_{NO3}$, $\delta^{18}O_{NO3}$) in the Labrador Sea and Davis Strait, with emphasis on the Labrador Slope and Labrador Shelf, is presented. This isotope dataset is used to investigate nitrate cycling in the Labrador Sea corridor, and is supplemented by nitrate, phosphate, and silicate concentration data. We observe the following: Nitrate advected by the westward branch of the West Greenland Current is consumed en route to the Labrador Slope in the Central Labrador Sea. Nutrient renewal in central Labrador Sea and along the Labrador Slope is hindered by summer stratification, leaving nutrients at depth and hindering primary productivity. As a result, the upper 30m of the western Slope is limited by both silicate and nitrate. We infer remineralization to be the primary mechanism of nitrate renewal on the Labrador Slope. Here, nitrate is immediately assimilated and remineralized before being returned to the euphotic zone, resulting in only minor net isotopic fractionation and thus yielding isotope values close to the deep-ocean mean ($\delta^{15}N_{NO3}$=~5.5‰; $\delta^{18}O_{NO3}$=~2.5‰). Labrador Sea Water entering the Hudson Strait is modified by intertidal mixing with Hudson and Foxe Basin waters, emerging as well-mixed Labrador Shelf Water bearing isotopically light nitrate ($\delta^{15}N_{NO3}$=~2.5‰). As Labrador Shelf Water is advected southwards along the Labrador Peninsula the isotopic composition of nitrate becomes more enriched with distance from the Hudson Strait due to changing rates of nitrate renewal and loss. The distinctive dual isotopic signatures of the Labrador Slope and Labrador Shelf indicate that they are separate nutrient regimes, though evidence of shelf-slope mixing is observed at one site. We find the Baffin Shelf experiences a net loss of nitrate, that the Labrador Slope and southern Shelf are dependent upon nitrate recycling.

3.1 Introduction

The Labrador Sea is of ecological and economic importance to Canada, serving as a strategic gateway to the Arctic and as host to valuable fisheries and extractable resources. From a climatological standpoint the basin is a key component of the global thermohaline circulation, the site of North Atlantic deep-water formation, and one of the few regions where the deep ocean exchanges gases with the atmosphere (Clarke and Coote, 1988; Azetsu-Scott et al., 2003; DeGrandpre et al., 2006). In recent decades resource extraction industries have progressively moved further offshore, threatening ocean productivity and, by extension, marine ecosystem health. Similar threats are imposed by multinational interests in shipping via the Northwest Passages (Johnston 2002) and by the recent uptick in northern tourism (Maher 2007). Furthermore, uptake of anthropogenic CO_2 during deep winter convection (DeGrandpre et al. 2006) is expected to exacerbate ocean acidification along the eastern Canadian margin. Despite the importance of the Labrador Sea corridor and in spite of the impacts of human activity on the global ocean at large, surprisingly little is known about the current and pre-anthropogenic state of nutrient cycling in the Labrador Sea. Here, we attempt to shed light on the biogeochemical cycling of the key, biolimiting nutrient, nitrate (NO_3^-) based on water column profiles at 11 sites in the Labrador Sea and Davis Strait.

Nitrogen constitutes 78% of Earth's atmosphere as the gaseous species dinitrogen (N_2) and is critical for a number of reactions necessary to life, yet it is inert and must be made bioavailable ("fixed") by diazotrophs before it can be assimilated by plants. Marine phytoplankton cannot fix N_2 and must assimilate biologically available species of nitrogen such as nitrate (NO_3^-), nitrite (NO_2^-), and ammonium (NH_4^+) present in the environment. Nitrate (NO_3^-) is the predominant form of fixed nitrogen present in the ocean, arguably making it both the most important form of fixed nitrogen to the marine trophic ecosystem as well as the the most readily studied. The nitrogen and oxygen isotopic composition of NO_3^- may be used as a tool to disentangle the processes of nitrogen utilization in marine environments, making it possible to identify zones of nitrogen fixation as well as the relative rates of renewal and loss (e.g., Sigman et al., 2001; Casciotti et al. 2002; Granger et al. 2004). Utilizing the N ($^{15}N/^{14}N$) and O ($^{18}O/^{16}O$) isotopic compositions of nitrate and the concentrations of nutrients measured in seawater samples collected during the summer and early autumn of 2016, we aim to assess the relative rates of N_2 fixation and denitrification in the Labrador Sea and Davis Strait, identifying where nitrate is gained, where it is lost, where the rates are approximately equal, and where the supply of nitrate exceeds biological demand.

Qualifying the relative rates of N_2 fixation and denitrification is made possible by the combination of isotopic data coupled with the nitrate-to-phosphate ratio at each site. Deviations in the nitrate-to-phosphate relationship from the global "Redfield" ratio (Redfield 1963) are driven by N inputs (N_2 fixation) and outputs (denitrification), and by variations in the stoichiometry of nitrate assimilation and remineralization. The semi-conservative tracer, "N*", defined as [nitrate] - 16 x [phosphate] + 2.9 (in µmol/l) (Deutsch et al. 2001; Gruber and Sarmiento 1997), quantifies excesses and deficits of NO_3^- relative to the global "Redfield" nitrate-to-phosphate ratio, which in turn may be related to fixation and denitrification, respectively. Due to the isotopic fractionation effects of nitrification and denitrification on NO_3^- $^{15}N/^{14}N$, complementary $\delta^{15}NO_3$- measurements provide a way to discern whether N* is driven by the relative rates of fixation and denitrification, or whether it is driven by stoichiometric variability (Sigman et al., 2005).

3.1.1 Oceanographic context

Circulation within the Labrador Sea is cyclonic to a depth of 1200 m (Swallow and Worthington, 1969), bound at the peripheries by the West Greenland Current system, the Labrador Current system, and the Atlantic Current. The West Greenland Current system (WGC) flows northwestwards from its origin at Cape Farewell as a continuation of the East Greenland Current, along the western shelf of Greenland to form the western boundary current of the subpolar gyre. At ~61°N the West Greenland Current splits, with one branch continuing on a northern trajectory into the eastern Davis Strait and Baffin Bay, while the majority continues westward to join the Labrador Current along the northern Shelf of the Labrador Sea. The West Greenland Current is composed of cold, low-salinity Arctic water atop a core of relatively warm and saline Irminger Sea Water (Smith, Soule, and Mosby, 1937). Much of the Irminger Sea water is lost to the subpolar gyre and circulated into the Labrador Sea, however, some continues along the western slope of Greenland below the more buoyant Arctic water and into the Davis Strait and Baffin Bay via the West Greenland Current (Bourke et al., 1989). At ~78°N the remainder of the West Greenland Current takes a westward trajectory, contributing to the cyclonic circulation of Baffin Bay (Tang et al. 2004), and joins the cold and fresh Baffin Island Current (BIC), which sits atop the Polar Water comprising the integrated outflow of the Canadian Island Archipelago. The BIC and underlying Polar Water is advected southward along the eastern coast of Baffin Island and through the western Davis Strait where it is further modified by water from the western branch of the West Greenland Current on the northern shelf of the Labrador Sea to form Labrador Sea Water (LSW), marking the origin of the Labrador Current. From the northern shelf the Labrador Current continues southward, following the cyclonic circulation path of the basin. A portion of the freshly formed LSW enters the mouth of the Hudson Strait and is modified via intense mixing with Hudson Bay and Hudson Strait Water, forming Labrador Shelf Water (LShW), which subsequently flows south along the shallow shelf of the Labrador Peninsula. LShW bears strong similarities to Polar Water, being colder and fresher than LSW, which receives greater contributions of WG-IW. Labrador Slope Water (LSlW) is the mixed intermediary between the relatively warm and salty LSW and the cold, fresh LShW along the continental slope of the Labrador Peninsula from approximately 100m depth.

3.2 Materials and methods

3.2.1 Sample recovery

Hydrographic data from the ArcticNet expedition in July and September 2016 were collected using a Sea-Bird SBE 911 CTD profiles equipped with sensors for dissolved oxygen, fluorescence and turbidity. Seawater samples were collected using a rosette of 24 x 12 L Niskin bottles. Seawater samples from the ArcticNet expedition in July and September 2016 were collected at standard sampling intervals via hydrocast (5 m, 10 m, 20 m...80 m, 100 m, 125 m...200 m, 300 m...etc.) into 30 mL HDPE bottles and stored frozen at -20°C for later isotopic analyses at the University of Basel. Nutrients (nitrate, nitrite, phosphate, silicate) were measured on board the CCGS Amundsen according to colorimetric methods (Grasshoff, 1969) using a Bran+Luebbe AutoAnalyzer 3.

3.2.2 Sample preparation

Samples were prepared for measurement following the denitrifier method (Sigman et al., 2001; Casciotti et al., 2002) and are reported relative to AIR and VSMOW, respectively. In short, the denitrifer method converts nitrate present in the water samples to nitrous oxide (N_2O) by introducing bacteria (*Pseudomonas aureofaciens*) that lack N_2O reductase activity. Isotopic analyses of the resulting N_2O gas is then performed by IRMS. Reported measurements are of nitrate and nitrite, but because nitrite is preferentially consumed by primary producers over nitrate (and is thus rapidly removed), and also owing to the almost total absence of nitrite in our samples, we refer to the analyses simply as "nitrate" or "NO_3^-".

3.2.3 $^{15}N/^{14}N$ and $^{18}O/^{16}O$ analysis

All samples were analyzed at Universität Basel for nitrate N and O isotopes in May/June 2017 using a ThermoFisher Delta V Plus isotope ratio mass spectrometer (IRMS) (Bremen, Germany) with a CTC Analytics GC PAL autosampler (Zwingen, Switzerland) fitted with a user-made, special autosampler needle and vial tray, coupled with a customized purge and trap system (modified after McIlvin & Casciotti, 2010, 2011) based on a ThermoFisher Gasbench II (Bremen, Germany), using helium 5.0 (purity of 99.999%) as both a purge and carrier gas. Gas chromatographic separation of N_2O from any remaining (after passing the H_2O and CO_2 traps earlier in the system), interfering gases (e.g. CO_2, NO_2) are facilitated by an RT-Q-BOND GC-column (30 m x 0.32 mm; Restek) at an isothermal temperature of 23°C. As in the system described by McIlvin & Casciotti (2010), this gas chromatographic column was split into two equal halves (15 m + 15 m), which were connected to each other by an 8-port, 2-way Valco valve (VICI, Schenkon, Switzerland) to facilitate backflushing between samples.

3.3 Results

3.3.1 Identification of hydrographic regimes

The 11 stations are categorized into four separate hydrologic regimes (Table 1) on the basis of temperature, salinity, and empirically derived seawater density (Figures and 3). Temperature and salinity measurements were conducted concurrently with seawater sampling. The four regimes are: (1) Labrador Shelf, (2) Labrador Slope, (3) Baffin Shelf, and (4) Disko Fan. A degree of water column stratification is present at all 11 sites, reflecting typical summer conditions in the Labrador Sea Corridor. Stratification is greatest within the Disko Fan and Labrador Slope regimes, and least along Labrador Shelf despite the strong contribution of Polar Water to LShW. The upper 30 meters of the Baffin Shelf sites are sharply stratified by the buoyant surface waters of the Baffin Island Current overlying a more homogeneous core of Polar Water.

Water column concentrations of nitrate, phosphate, and silicate data for all stations are summarized in Figure 4. In summary, the euphotic zone is nitrate limited at all sites except those on the Labrador Shelf. Euphotic phosphate is in excess of utilization at all sites except those on the Labrador Slope, where it is drawn down almost completely. Euphotic silicate concentrations are most depleted on the Labrador Slope and most enriched at Disko Fan. Isotope values ($\delta^{15}N_{NO3}$, $\delta^{18}O_{NO3}$, Δ15-18) are summarized in Figure 5. Δ15-18, the difference between the $\delta^{15}N_{NO3}$ and $\delta^{18}O_{NO3}$, is used here to identify decoupling of the nitrogen and oxygen isotope systems. Among the 11 depth profiles the average $\delta^{15}N_{NO3}$ is 5.5‰, ranging from a minimum of 1.4‰ at Station-640 (100 m), located immediately below the Hudson Strait outflow, to a maximum of 9.6‰ at Station-177 (150 m), located off the southeastern coast of Baffin Island. The average $\delta^{18}O_{NO3}$ is 3.3‰, ranging from a minimum of 1.2‰ at Station-179 (125 m) to a maximum of 10‰ at Station-177 (70 m). Physical, nutrient, and isotope values are found in Annex C.

3.3.2 Disko Fan area

Disko Fan site ROV-7 is situated in the northeastern Davis Strait (**Figure 1**). The profile of this site is complex because it contains contributions from both WG-IW and PW, resulting in significant density stratification of the upper water column (**Figure 2**). The site is characterized by a shallow mixed layer (<10 m) of cold (~0.6°C), fresh (~30.5 PSU) water atop a well-defined dicothermal layer of Baffin Water (~-1.5°C, ~33.5 PSU) extending to ~100 m, a core of warmer (~2°C) and saltier (34.5 PSU) West Greenland - Irminger Water from 100-500 m, which ultimately transitions into Polar Water from 500 m to bottom (902 m) (~1.1°C, ~34.5 PSU).

The nutricline, as defined by the depth at which the NO_3^- concentration first becomes >1 μmol, begins at 30 m. NO_3^- concentrations rise steadily until the reaching a maximum of 18.1 μmol at 902 m. An abundance of phosphate and silicate in the upper water column implies ROV-7 bears a closer relationship to the waters of Baffin Bay than to those of the Labrador Sea. Although the concentration of nitrate is lower relative to silicate, nitrate is not *completely* depleted in the biological productive zone. Between 0 to 20 m depth the average nitrate concentration is 0.58 μM, abruptly rising to 4 μM at 30 m depth. Within the nutricline $\delta^{15}N_{NO3}$ reaches a maximum of 7.5‰. Below the nutricline $\delta^{15}N_{NO3}$ varies little and has a mean value of of 5.3‰ from 30 meters to bottom (902 m). $\delta^{18}O_{NO3}$ ranges between 3-5‰ until a depth of 70 m. Below 70 m $\delta^{18}O_{NO3}$ values vary between 1-2‰.

3.3.3 Baffin Shelf

To the southwest of Disko Fan lay Sites-177 and -179, which are located on the southeastern shelf of Baffin Island (Figure 1) and sit squarely within the circulation path of the Baffin Island Current (BIC). Station 177 is also under the influence of coastal runoff/effects as it is located only 3 km from shore, near three major outflow glaciers of the 6,000 km² Penny Ice Cap (Auyuittuq National Park). These two sites are marked by the cold (-1 to 2 °C), fresh (29 to 31 PSU) and relatively buoyant water of the Baffin Island Current and underlying cold (-1 to -1.6 °C), saline (32-34 PSU) Polar Water of the integrated Canadian Island Archipelago outflow. It is noted that surface of Station-177 is warmer and fresher than that of Station-179. Excepting the particularly cold and fresh conditions which characterize the upper tens of meters at each site, Stations 177 and 179 are more homogenous than Disko Fan and Labrador Slope sites due to the less complex mixture of waters on the Baffin Shelf.

Similarly as at ROV-7, phosphate is not depleted at any depth at either Station-177 or -179, though silicate and nitrate are depleted within the upper 20 m of the water column both sites. The $\delta^{15}N_{NO3}$ and $\delta^{18}O_{NO3}$ profiles of Station-177 and Station-179 are enriched and variable, particularly the $\delta^{18}O_{NO3}$ profile of Station-177, which may be the product of near-shore effects. N* is strongly negative, suggesting that the rate of denitrification is greater than the rate of N_2 fixation on the Baffin Shelf.

3.3.4 Labrador Slope

Labrador Slope sites are characterized by a warm (4 to 6°C) and relatively saline (33.5 to 34 PSU) mixed layer between 10 and 30 m thick, sitting atop a pronounced dicothermal layer (0.5°C, 34.2 PSU) extending to 250 m, below which temperature and salinity are more-or-less homogenous (3-4°C, ~35 PSU) . The cold, fresh dicothermal layer is the product of mixing between of Polar Water exported from Baffin Bay and the West Greenland current on the northern shelf of the Labrador Sea. Below the dicothermal layer is relatively warm, dense West Greenland-Irminger Water.

Generally, the nutrient ratio of Labrador Slope Sites is approximately at equilibrium with the global 15:1 ratio N:P ratio, standing in stark contrast with the Shelf Sites, which, at their deepest points, do not exceed 11:1 (Figure 6). Regardless, surface [NO_3-] at Labrador Slope sites was below detection limits, and the uppermost depths with measurable concentrations reveal $\delta^{15}NO_3^-$ enrichment (7‰). Below the nutricline, $\delta^{15}N_{NO3}$ is generally ~5.5‰ and $\delta^{18}O_{NO3}$ is generally ~2.5‰ for all Slope Water sites for all sites (Δ(15-18) = ~3).

3.3.5 Labrador Shelf

The mixed layer at Labrador Shelf sites ranges from 10 m at the southernmost shelf site Station-650 to 30 m at the northernmost shelf site, Station-640. The mixed layer of the Labrador Shelf is much colder than the mixed layer of the Labrador Slope (2 to

2.5°C), and markedly fresher (32 to 33 PSU). The Labrador Shelf is inherently shallow and neither a well-defined halocline nor thermocline is observed at Station-640, Station-645, or Station-650 due to intense mixing. The conditions observed at depth at Station-650 are the coldest and freshest of the sites below the Arctic Circle in this study. $\delta^{15}N_{NO3}$ at Station-640, located nearest the mouth of the Hudson Strait, is 2.5‰ at the surface, with a minimum of 1.8‰ at 60 m and maximum of 4.5‰ at 50 m. Labrador Shelf Water at Station-645, which is located off of the middle of the Labrador Peninsula, sees upper water column concentrations reduced by half to ~1.5 μM. Within the mixed layer nitrate concentrations were below instrumental limitations for isotopic measurement. At Station 650, located near the southern terminus of the Labrador Peninsula, nitrate concentrations are extremely low in the upper water column, and $\delta^{15}N_{NO3}$ is substantially enriched. The NP: ratios of the Labrador Shelf sites (11:1) are akin to the Baffin Shelf sites-177 and -179, indicating that below the upper water column the nutrient concentration of Shelf Waters are strongly influenced by Polar Water.

3.4 Discussion

Seawater in the Labrador Sea and Davis Strait is by-and-large a mixture of BIC, PW, WG-IW water accompanied by smaller contributions from Hudson Bay, Foxe Basin, continental runoff, and meteorologic water. The physical and chemical attributes of the water column at each of the 11 sites presented in this study reflect iterative modifications upon source waters prior to arriving at the respective locations and times of sampling. So too is the isotopic composition of nitrate at each site the product of all previous biogeochemical transformations associated with marine nitrogen cycling up to the moment of sampling.

3.4.1 Nitrate renewal in the Hudson Strait

Newly formed Labrador Sea Water modified in the Hudson Strait emerges onto the Labrador Shelf with an abundance phosphate relative to nitrate, and with measurable concentrations of both nitrate and silicate within the upper water column. While the relative abundance of nutrients in the euphotic zone can be explained solely by vertical mixing induced by intertidal mixing in the Hudson Strait, the $\delta^{15}N_{NO3}$ emerging from the Hudson Strait is isotopically light (~2.5‰), which is indicative of N_2 fixation. However, the N:P ratios and N* values suggest net nitrate loss rather than renewal. We suggest that these seemingly contrasting data may be explained by considering the the precursor water masses which make up Labrador Shelf Water. Labrador Shelf Water is more strongly influenced by the Baffin Island Current than by Labrador Slope Water, which can be observed in the temperature and salinity profiles of our study sites. In this study BIC waters are noted for net denitrification, negative N* values, low N:P ratios, and density stratification. Intense vertical mixing of Labrador Sea Water containing a significant BIC component in the Hudson Strait can therefore explain these "BIC-like" characteristics. This is supported by Sutcliffe et al. (1983), who find >40% of Labrador Shelf Water in summer to originate from BIC waters. The low $\delta^{15}N_{NO3}$ values in Shelf Water, however, cannot be explained by vertical mixing because no other sites exhibit comparably low $\delta^{15}N_{NO3}$ values. Thus, the origins of "fresh" nitrate in northern Labrador Shelf Water is constrained either to net fixation near the mouth of the Hudson Strait and/or to riverine sources. Further south along the Labrador Peninsula, at Stations 645 and -650 $\delta^{15}N_{NO3}$ is more indicative of a regime dependent upon nitrate recycling than upon fixation or upwelling of “fresh” nitrate.

While the large difference between $\delta^{15}N_{NO3}$ and $\delta^{18}O_{NO3}$ (Δ(15-18)) (Figure 5), which is most negative at Station-640, may feasibly be the product of nitrate-nitrite redox cycling, it is unlikely the prerequisite sub-oxic conditions are met in the well-mixed waters of the Hudson Strait. Rather, it is more likely the Δ(15-18) difference at Station-640 originates from N_2 fixation in the Hudson Strait in the presence of meltwater enriched in ^{18}O, followed by complete assimilation of the nitrate pool, sinking, and remineralization back to nitrate, effectively enriching $\delta^{18}O_{NO3}$ relative to $\delta^{15}N_{NO3}$ prior to arriving at Station 640. Further south along the Labrador Peninsula $\delta^{15}N_{NO3}$ becomes more enriched in response to nitrate drawdown as the rate of nitrate renewal via both vertical mixing and N_2 fixation wanes with distance from the Hudson Strait. The simultaneous depletion of $\delta^{18}O_{NO3}$ further south along the Peninsula (e.g. Station 645 and Station 650) is thus likely driven by remineralization occurring in more southerly shelf waters less enriched in ^{18}O. Although the N* values of Labrador Shelf sites Station-640, Station 645, and Station 650 are low (N*=~-2.5) (Figure 6), they do not necessarily indicate net denitrification. Excess phosphate originating from the Integrated Arctic Outflow (Yamamoto-Kawai et al., 2008) is advected southwards by the BIC, the influence of which is stronger in the Davis Strait and on the Labrador Shelf than it is on the Labrador Slope (Figure 4). In consideration of these data, we conclude that the Hudson Strait and possibly the northern Labrador Peninsula are areas of nitrate renewal (via the processes of vertical mixing and N_2 fixation), while the rates of nitrate renewal and loss along the middle and southern portions of the Labrador Shelf are approximately equal.

3.4.2 Evidence of nitrate recycling and possible net N_2 fixation on the Labrador Slope

The presence of WG-IW water is most clearly observed in Labrador Sea Water along the western Labrador Slope at sites ROV-1, ROV-2, ROV-3, ROV-5, and ROV-6, which are warmer, more saline, and denser relative to all other sampling locations. These sites are nitrate and silicate limited, stratified, with a warm and salty upper water column. Nitrate and silicate advected by the westward branch of the WGC, if initially present in the biological productive zone, is evidently consumed en route to the Labrador Slope in the Central Labrador Basin. Nutrient renewal via vertical mixing in the Central Labrador Basin and along the northern and western Labrador Slope is presumably hindered by summer stratification. As a result, nutrients at depth remain largely inaccessible and productivity in the upper 30 m of the Western Slope is limited by both silicate and nitrate.

The nitrogen and oxygen isotopic compositions of nitrate at the Labrador Slope sites are approximately equal to mean deep-ocean nitrate isotope values (4.5-5‰ and 2.5‰, respectively) (Liu and Kaplan, 1989; Sigman 2000, 2009; Casciotti et al. 2002), and, with the exception of site ROV-2 which represents a mixed Shelf-Slope regime, only exhibit minor $\delta^{15}N_{NO3}$ enrichment in the upper water column where detectable concentrations of nitrate exist. The nutrient depletion observed in the upper 30 m of the Labrador Slope sites coupled with relatively stable and light $\delta^{15}N_{NO3}$ and $\delta^{18}O_{NO3}$ values suggests the primary mechanism of nitrogen cycling on the Labrador Slope is recycling of organic matter, which proceeds as a cycle of complete assimilation of available nitrate by phytoplankton followed by sinking, remineralization, and rapid assimilation.

The lack of a southward isotope enriching trend following the cyclonic circulation of the basin indicates that the total flux of "fresh" nitrate introduced into the biological productive zone is approximately equal to the rate of denitrification across much of the western Labrador Slope, which is further supported by the nitrate-to-phosphate ratio of these sites. The water column of the Labrador Sea is generally well-oxygenated, and as such we infer denitrification to occur in sediments. Although "fresh" nitrate may in this instance be introduced via N_2 fixation and/or vertical mixing, summer stratification in the Labrador Sea precludes significant upwelling, leading us to conclude that the origin of fresh nitrate at these sites originates at least in part from N_2 fixation. While no sites in this study exhibit extreme N* values (Figure 6), there is a clear distinction between those characterized by positive N* (Labrador Slope sites) and those by negative N* (Labrador Shelf, Baffin Shelf, and Disko Fan sites). Furthermore, $\delta^{15}N_{NO3}$ from the Labrador Slope is observed to be somewhat lighter than on the Baffin Shelf and the Disko Fan area. These findings suggest that while net N_2 fixation and denitrification appear to be closely balanced in much of the Labrador Sea Corridor, the rate of N_2 fixation on the Labrador Slope may be marginally greater than the rate of denitrification. Conversely, the rate of denitrification is greater than the rate of fixation in the Davis Strait.

3.4.3 Shelf-slope exchange

While the physical and nutrient properties of the upper water column at Slope Site ROV-2 resemble those of other Labrador Slope sites, below 100 m the waters are an intermediate product of Shelf and Slope waters. This is evidenced by the semi-conservative tracers of temperature, salinity, and nutrient content. N*, which may be used to identify zones of nutrient depletion and enrichment relative to the globally-derived Redfield Ratio, at Site ROV-2 gives evidence of mixing between Slope and Shelf Waters, as opposed to Stations ROV-1, ROV-5, and ROV-6 which represent a more “pure” Slope Water system. It is noted that sites ROV-5, -1, and -2 are silicate and nitrate limited, which may be attributed to either a different phytoplankton assemblage present at the Slope-Shelf boundary, or to a weaker presence of BIC water on the Slope relative to on the Shelf. While the isotopic composition of nitrate at ROV-2 is similar to other Slope sites, the N:P ratio is lower, owing in part to a relative abundance of phosphate in the upper water column. In this regard, ROV-2 similar to sites on the Labrador Shelf and in the Davis Strait. In multiple respects, Disko Fan site ROV-7 is similar to Labrador Slope Site ROV-2. ROV-7 contains core of modified WG-IW water, which is warmer, saltier, and more nutrient-rich than surrounding Polar Water present in the subsurface of the Davis Strait. Below 100 m both sites represent an intermediate product of WG-IW water and Polar Water, with ROV-2 being more strongly influenced by WG-IW water and ROV-7 being more strongly influenced by Polar Water.

3.5 Conclusions

We find the Baffin Shelf to be a zone of net denitrification, the Labrador Slope and southern Shelf to be dependent upon nitrate recycling, and the Hudson Strait (and possibly the shelf waters of the northern Labrador Peninsula) to be a key area of nitrate renewal. Evidence of shelf-slope exchange is found in this study (notably from the isotopic composition of nitrate at site ROV-2), but the geographic coverage of our study sites make it unclear whether nitrate from the Hudson Strait is introduced to the Slope in significant quantities. Due to the somewhat similar seawater densities of Labrador Shelf Water and Labrador Seawater, we do not dismiss the potential importance of nitrate in Labrador Shelf Water to productivity on the Labrador Slope. Beyond Station-640, there is not evidence for significant net N_2 fixation along the Labrador Peninsula, which further highlights the ecological importance of the Hudson Strait and possibly of newly-formed Labrador Shelf Water. Although the highest euphotic nutrient concentrations observed along the Labrador Shelf are near the Hudson Strait (e.g. Station 640) where intertidal mixing is strongest, the chemical and physical structure of the water columns at Station-645 and Station-640 suggest that vertical mixing may also play a role in making nutrients available along the middle and southern Labrador Peninsula.

Although we observe the Hudson Strait to be an important source of nitrate renewal for the Labrador Sea, the existence of a "conveyor belt" food chain produced by the nutrient-rich Hudson Strait Outflow/Labrador Shelf Water (Sutcliffe et al., 1983; Drinkwater and Harding, 2001) is neither proven nor disproven by our data. Despite the productivity of the Labrador Shelf, renewal of the nitrate pool is dependant upon nitrate recycling along the middle and southern Labrador Peninsula. These findings suggest this system is potentially susceptible to change and may be negatively impacted by a significant loss of biomass with implications for downstream fisheries, highlighting the continued need for responsible resource management in the Labrador Sea.

The Labrador Sea Corridor, with exception to the well-mixed waters of the Labrador Shelf near the Hudson Strait, functions on a limited nitrate budget. The Labrador Slope features a high degree of nutrient recycling coupled with approximately balanced rates of nitrate renewal and and denitrification. The $\delta^{15}N_{NO3}$, $\delta^{18}O_{NO3}$, and N* at the Baffin Shelf sites are indicative of net denitrification (Figures 5 and 6). The opposite is true within the Disko Fan area off western Greenland. This suggests the northern branch of the West Greenland Current and waters from Disko Bay form a unique nutrient regime. Supplementation of our dataset with isotope and nutrient data from sites situated in the primary arm of the West Greenland Current could provide further insight into the status of WG-IW prior to biological modification in the Central Labrador Basin, allowing us to better understand the role of nitrate cycling on the Labrador Slope. Future integration of this data with $\delta^{15}N$ measurements of high resolution marine archives (e.g., deep-water corals) collected north and south of the Hudson Strait could potentially provide valuable insight into the pre-anthropogenic state of the western Labrador Sea nutrient regime.

3.6 Acknowledgements

We extend our thanks to Moritz Lehmann and Thomas Kuhn at the University of Basel for their assistance with the isotopic measurements presented herein, to Jean-Eric Tremblay for making available nutrient concentration data presented here, and to the captain and crew of the C.C.G.S. Amundsen for their assistance in collecting the data presented in the study. Funding provided by ArcticNet, ArcTrain, and VITALS – all supported by NSERC Canada.

3.7 References

Azetsu-Scott, K., Jones, E. P., Yashayaev, I., & Gershey, R. M. (2003). Time series study of CFC concentrations in the Labrador Sea during deep and shallow convection regimes (1991–2000). *Journal of Geophysical Research: Oceans, 108*(C11).

Bourke, R. H., Addison, V. G., & Paquette, R. G. (1989). Oceanography of Nares Strait and northern Baffin Bay in 1986 with emphasis on deep and bottom water formation. *Journal of Geophysical Research: Oceans*, 94(C6), 8289-8302.

Casciotti, K. L., Sigman, D. M., Hastings, M. G., Böhlke, J. K., & Hilkert, A. (2002). Measurement of the oxygen isotopic composition of nitrate in seawater and freshwater using the denitrifier method. *Analytical Chemistry, 74*(19), 4905-4912.

Clarke, R. A., & Coote, A. R. (1988). The formation of Labrador Sea Water. Part III: The evolution of oxygen and nutrient concentration. *Journal of Physical Oceanography, 18*(3), 469-480.

DeGrandpre, M. D., Körtzinger, A., Send, U., Wallace, D. W., & Bellerby, R. G. J. (2006). Uptake and sequestration of atmospheric CO2 in the Labrador Sea deep convection region. *Geophysical Research Letters, 33*(21).

Deutsch, C., N. Gruber, R. M. Key, J. L. Sarmiento, & A. Ganachaud (2001), Denitrification and N2 fixation in the Pacific Ocean, *Global Biogeochemical Cycles*, 15(2), 483–506, doi: 10.1029/2000GB001291.

Drinkwater, K. F., & Harding, G. C. (2001). Effects of the Hudson Strait outflow on the biology of the Labrador Shelf. *Canadian Journal of Fisheries and Aquatic Sciences, 58*(1), 171-184.

Granger, J., Sigman, D. M., Needoba, J. A., & Harrison, P. J. (2004). Coupled nitrogen and oxygen isotope fractionation of nitrate during assimilation by cultures of marine phytoplankton. *Limnology and Oceanography*, *49*(5), 1763-1773.

Grasshoff, K. (1969). A simultaneous multiple channel system for nutrient analysis in seawater with analog and digital data record. Contribution 2338, Woods Hole Oceanographic Institution.

Gruber, N., & J. L. Sarmiento (1997), Global patterns of marine nitrogen fixation and denitrification, *Global Biogeochem. Cycles*, 11(2), 235–266, doi: 10.1029/97GB00077.

Johnston, D. M. (2002). The Northwest Passage Revisited. *Ocean Development & International Law*, *33*(2), 145-164.

Liu, K. K., & Kaplan, I. R. (1989). The eastern tropical Pacific as a source of 15N-enriched nitrate in seawater off southern California. *Limnology and Oceanography*, *34*(5), 820-830.

Maher, P. T. (2007). Arctic tourism: a complex system of visitors, communities, and environments. *Polar Geography*, *30*(1-2), 1-5.

Redfield, A. C. (1963). The influence of organisms on the composition of seawater. *The sea*, *2*, 26-77.

Sigman, D. M., Altabet, M. A., McCorkle, D. C., Francois, R., & Fischer, G. (2000). The δ15N of nitrate in the Southern Ocean: Nitrogen cycling and circulation in the ocean interior. *Journal of Geophysical Research: Oceans*, *105*(C8), 19599-19614.

Sigman, D. M., Casciotti, K. L., Andreani, M., Barford, C., Galanter, M. B. J. K., & Böhlke, J. K. (2001). A bacterial method for the nitrogen isotopic analysis of nitrate in seawater and freshwater. *Analytical chemistry*, *73*(17), 4145-4153.

Sigman, D. M., Granger, J., DiFiore, P. J., Lehmann, M. M., Ho, R., Cane, G., & van Geen, A. (2005). Coupled nitrogen and oxygen isotope measurements of nitrate along the eastern North Pacific margin. *Global Biogeochemical Cycles*, *19*(4).

Smith, E. H., Soule, F. M., & Mosby, O. (1937). The Marion and General Greene Expeditions to Davis Strait and Labrador Sea, Under Direction of the United States Coast Guard: 1928-1931-1933-1934-1935: Scientific Results, Part 2: Physical Oceanography. US Government Printing Office.

Sutcliffe Jr, W. H., Loucks, R. H., Drinkwater, K. F., & Coote, A. R. (1983). Nutrient Flux onto the Labrador Shelf from Hudson Strait and its Biological Consequences. *Canadian Journal of Fisheries and Aquatic Sciences*, *40*(10), 1692-1701.

Swallow, J. C., & Worthington, L. V. (1969, February). Deep currents in the Labrador Sea. In *Deep Sea Research and Oceanographic Abstracts* (Vol. 16, No. 1, pp. 77-84). Elsevier.

Tang, C. C., Ross, C. K., Yao, T., Petrie, B., DeTracey, B. M., & Dunlap, E. (2004). The circulation, water masses and sea-ice of Baffin Bay. *Progress in Oceanography*, *63*(4), 183-228.

Yamamoto-Kawai, M., Carmack, E., & McLaughlin, F. (2006). Nitrogen balance and Arctic throughflow. *Nature*, *443*(7107), 43.

3.8 Tables

Table 3.1 Sampling stations

Regime	Site	Depth (m)	Latitude	Longitude
Disko Fan	ROV-7	901.7	67.979	-59.522
Baffin Island	Stn-177	360.1	67.474	-63.797
	Stn-179	177.3	67.503	-61.53
Labrador Slope	ROV-6	453.8	63.001	-60.642
	ROV-5	567.4	61.444	-60.679
	ROV-1	545.5	61.341	-61.159
	ROV-3	430	60.469	-61.28
	ROV-2	280	60.325	-62.191
Labrador Shelf	Stn-640	129.1	58.932	-62.154
	Stn-645	104.6	56.699	-59.696
	Stn-650	196.4	53.799	-55.436

3.9 Figures

Figure 3.1 Water sampling stations

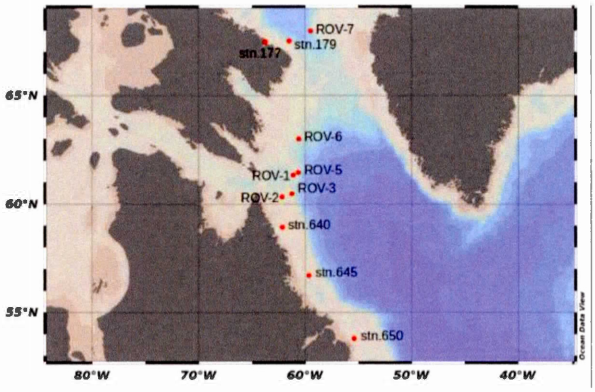

Locations of the 11 stations sampled in the Labrador Sea - Baffin Bay Corridor during aboard the C.C.G.S. Amundsen from July to September of 2016.

Figure 3.2 Temperature – salinity plot

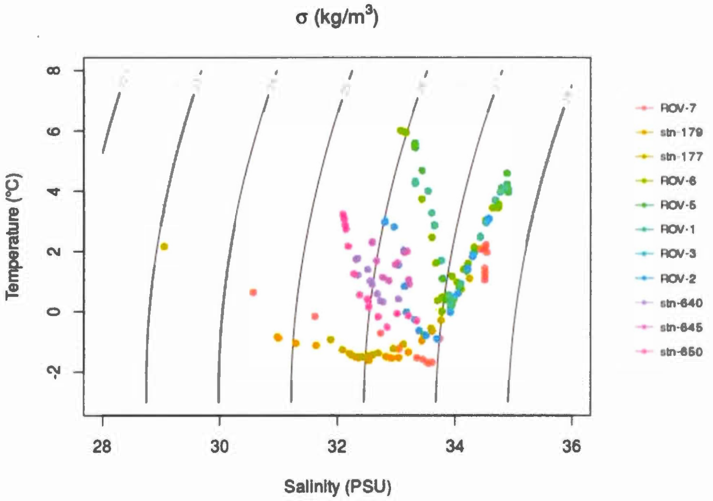

Seawater densities of the 11 stations plotted along isopycnals, where σ = ρ(S,T) - 1000 kg m−3 at standard atmospheric pressure (101325 Pa). Four distinct hydrographic regimes are identified: Baffin Shelf (Stations 177 and 179), Labrador Shelf (Stations 640, 645, and 650), Labrador Slope (ROV-1, -2, -3, -5, -6), and Disko

Fan (ROV-7). These regimes are the product of mixing between West Greenland-Irminger Water (WG-IW), Baffin Water (BIC), Polar Water (PW), and freshwater.

Figure 3.3 Temperature and salinity profiles

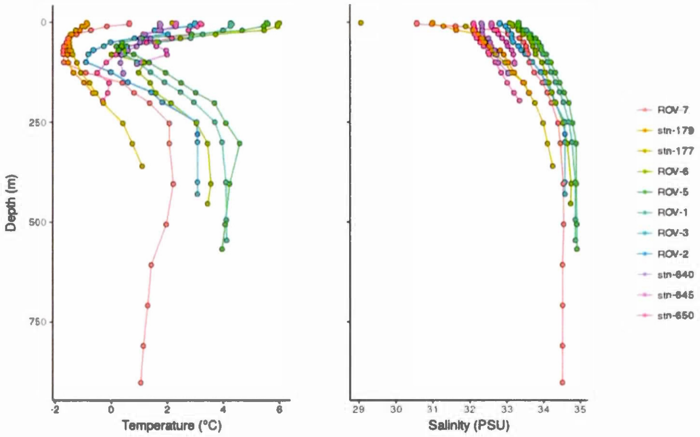

Temperature (left) and salinity (right) profiles of the sampling stations.

Figure 3.4 Nutrient profiles

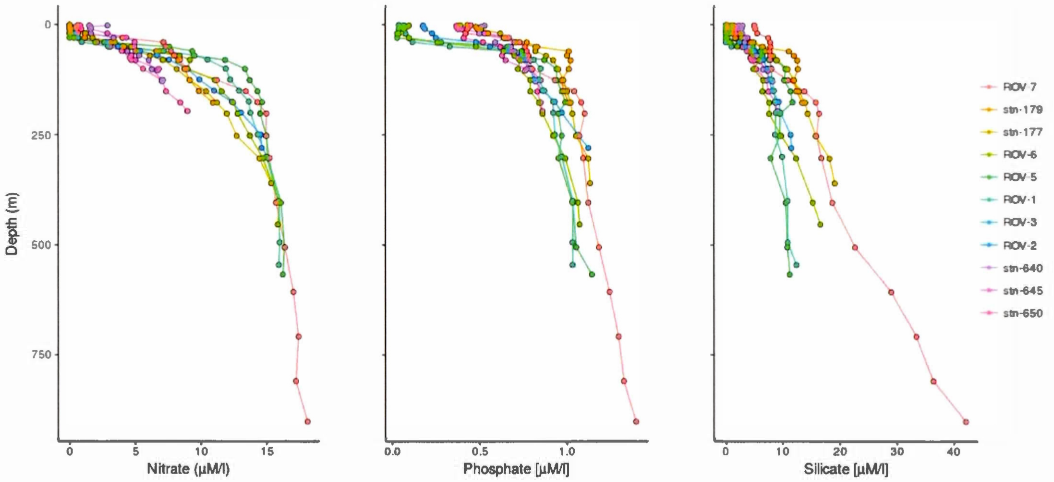

Nitrate (left), phosphate (middle), and silicate (right) concentrations determined from samples collected concurrently with samples slated for isotopic analysis.

Figure 3.5 Oxygen and nitrogen isotope profiles

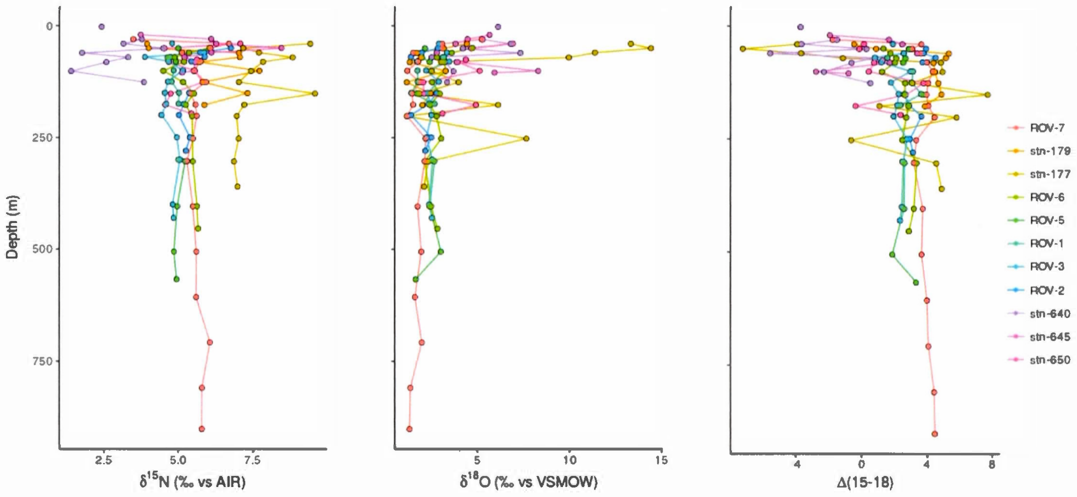

N (left) and O (middle) isotopic compositions of nitrate. Δ(15-18) (right) is used to describe discrepancies between nitrogen and oxygen isotope fractionation, indicating instances where processes affecting only one of the isotope systems is predominant.

Figure 3.6 N :P and N* profiles

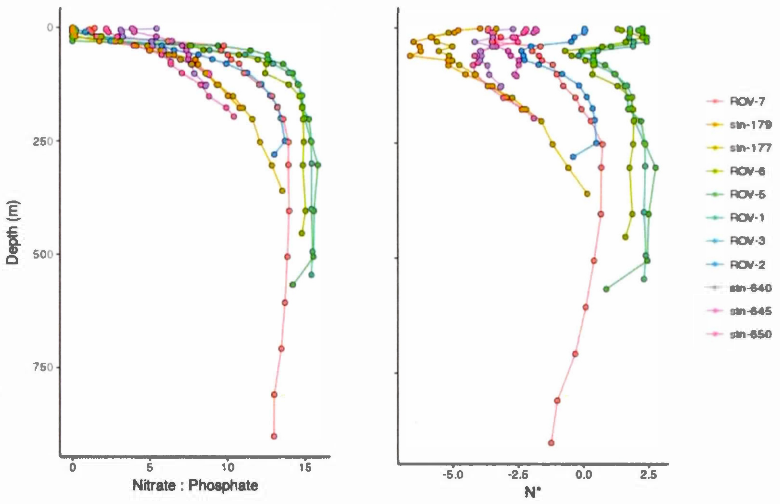

The ratio of nitrate-to-phosphate at standard sampling depths; (right) "N*", defined as: ([nitrate] - 16 x [phosphate] + 2.9) (in µmol/l) (Gruber and Sarmiento 1997), quantifies excesses and deficits of NO_3- relative to the global "Redfield" nitrate-to-phosphate ratio, which in turn may be related to fixation and denitrification, respectively.

CONCLUSION

The face of proxy-based paleoceanography is changing. While there are as of yet many contributions to be made regarding paleoceanography on geologic timescales, the focus of the field is increasingly on shorter (hundreds of years), high-resolution archives collected from strategic locations (e.g., transitional hydrographic boundaries). Such proxy-based records of oceanographic variability serve to extend and supplement both temporal and geographic gaps in instrumental records, as well as to support (or contest) mathematical ocean models. Indeed, a major advantage of high-resolution archives which partially overlap with instrumental records is that they may be directly calibrated to historical hydrographic and atmospheric conditions, something which is not possible with traditional low-resolution marine archives (e.g., sediment cores). However, many high-resolution marine archives are of biological origin (e.g., the skeletons and shells of long-lived calcifying organisms) and carry inherent uncertainty. Interpretation of proxy data from biological archives may be beset with difficulties related to metabolic, ontogenetic, or other complicating factors which fall under the broad umbrella of *biological effects*. Here, there is much work to be done on life habits and biochemistry of select marine organisms which will improve oceanographic interpretations drawn from biological archives. Such work will have implications not only for future studies, but also for the interpretations and conclusions drawn from previously published works.

From a method development standpoint, many questions remain unanswered in field of proxy-based paleoceanography. Despite the suite of interpretative conclusions presently drawn from marine biological archives, there is still much to be learned from the isotopic, elemental, and molecular makeup of biological materials of marine origin. This work will require further extrapolation upon existing techniques as well as the development of entirely new proxies. At present, the most exciting area of ongoing development is perhaps the study of the relationships between multiple proxies, particularly those which can be used to document the interplay between physical and biological systems. I believe this line of questioning will drive the most notable proxy-based discoveries of the coming decade.

The work presented herein reflect my efforts to confront some of the issues and outstanding questions in the field of paleoceanography. From these studies, which focus on proxy records extracted from the skeletons of deep-water corals and on marine trophic ecology, I have drawn conclusionspertinent to our understanding of oceanographic conditions on the Canadian margins during the 20th and 21st centuries.

In Chapter I, I presented the first measurements of deuterium in a deep-water coral and discuss a methodology for doing so. From these data it is concluded that the deuterium content of the deep-water coral genus *Primnoa* is linked to diet, which is dominated by sinking and resuspended particulate carbon exported from the epipelagic zone, and to coral provenance. In *Primnoa* collected from the Strait of Georgia, we note a significant correlation between coral deuterium content and instrumental records of annual mean sea surface salinity, which appears to be driven by a regional shift from a snow-driven regime to a rain-driven regime in coastal British Columbia. In light of these findings, we conclude that the deuterium content of proteinaceous growth rings in *Primnoa* reflect changes in sea surface deuterium content, which in turn is dominated by hydroclimatic variability. Future work on this subject will benefit from a wide assessment of deuterium in the marine system, including the deuterium content of settling particulate organic matter, of varying plankton size fractions, of sediments, and of seawater. Of additional interest would be the development of laboratory subsampling techniques which do not involve decalcification of the coral skeleton, thus eliminating the possibility of isotopic fractionation effects during acidification. Black coral skeletons offer such an opportunity, but, as they do not inhabit northern waters, were not a viable option for those studies presented in this thesis. Furthermore, sepration of black coral growth rings requires the liberal application of chemical agents which may also potentially alter the isotopic composition of growth rings. Thus, I suggest that future work work deep-water genera (e.g.,*Primnoa* and *Keratoisis)* may consider extractive processes such as microdrilling as an alternative to skeletal decalcification.

Chapter II seeks coherence between elemental and isotopic measurements of the calcite and proteinaceous skeletal components of two *Keratoisis ornata* colonies live-collected from the Newfoundland Slope. It shows that the time-resolved signals of $\delta^{13}C$, $\delta^{15}N$, Pb/Ca, and to a lesser extent, Ba/Ca, are quite reproducible between distinct colonies, confirming the utility of *Keratoisis* as a reliable archive of paleoceanographic proxy data. Based on the time-resolved Pb/Ca ratios of both colonies and historical records of anthropogenic Pb utilization, we find a lag time of ~20 years between Pb production and Pb bioaccumulation; from this we infer the residence time of Pb on the northwestern North Atlantic Slope to be approximately two decades. From the $\delta^{15}N$ observed in both colonies, we infer an intensification of the subpolar gyre since at least the early 20th century. This is thought to be in response to the long-term shift towards positive North Atlantic Oscillation conditions, resulting in the decreased influence of Warm Slope Water associated with the Gulf Stream, on the Newfoundland Slope. From the statistically significant relationship observed between $\delta^{13}C$ and Ba/Ca, we confirm the interest of deep-water coral Ba concentrations as a proxy for productivity and carbon export. This chapter highlights the interplay between the proteinaceous and mineralized portions of deep-water coral skeletons and demonstrates the advantage of utilizing multiple proxies from a single archive. While the findings of this study are intriguing, broader insight into North Atlantic oceanographic processes could be gained by studying additional deep-water coral colonies from the Scotian, Newfoundland, and Labrador Slopes. In particular, a companion study examining bulk δ^{15}N in corals collected from locations southwest and northeast of those presented here might be used to determine the historical limits of Warm Slope Water and Labrador Slope Water on the southeastern Canadian margin.

Chapter III provided insight into nitrogen cycling in the Labrador Sea corridor based on the dual isotope (δ^{15}N and δ^{18}O) composition of the key biolimiting nutrient, nitrate. The data gleaned from this study permits several broad conclusions: The Hudson Strait plays a critical role in supplying "fresh" nitrate to the Labrador Sea, particularly the Labrador Shelf. There does not appear to be a downstream continuation of nitrate renewal along the Labrador Peninsula, which further highlights the importance of the Hudson Strait to productivity along the Labrador Peninsula and northeastern Newfoundland. Furthermore, there is apparently only a small degree of mixing between the Labrador Shelf and Labrador Slope. This data, in conjunction with supporting bulk coral δ^{15}N, could be used to determine the historical trophic health of the Labrador Slope and Shelf system relative to modern conditions. Of additional value would be nitrate isotope data from Baffin Bay and the Canadian Island Archipelago, as well as from the western slope of Greenland.

The role of the modern paleoceanographer is increasingly to contextualize ocean processes on human timescales. In the face of anthropogenic climate change there has been a rush to characterize the recent past in an effort to understand the present and to gain foresight into what the future may hold. While true, such motivation is perhaps too much a textbook model. As in all branches of science, paleoceanography serves to advance human understanding of the natural world. Progress is incremental, and findings often lead to peripheral discoveries which may explain phenomena outside the original aim and scope of the study. In this regard, biological archives continue to yield information not only about the physical processes which dominate the Earth System, but also the ecology of marine organisms which serve important roles in regulating the biological health of our planet. In this work, I have described my efforts to contribute to our understanding of the natural world. These records describe a dynamic, living ocean driven by complex interactions between chemical, biological, and geological process.

ANNEX A

DEUTERIUM CONTENT OF SEAWATER AND *PRIMNOA*

Table A.1 Coral deuterium values

Specimen ID	**Calendar year (estimate)**	**δD (‰ VSMOW)**	**δD -sigma (‰)**
R1513-SR-0022	2011	-124.9	2.5526555
R1513-SR-0022	2009	-126.16	
R1513-SR-0022	2007	-123.71	0.4525483
R1513-SR-0022	2005	-122.89	
R1513-SR-0022	2003	-122.15	1.1808683
R1513-SR-0022	2001	-123.66	
R1513-SR-0022	1999	-123.65	1.1313709
R1513-SR-0022	1997	-119.14	0.0636396
R1513-SR-0022	1995	-122.19	0.212132
R1513-SR-0022	1993	-122.62	
R1513-SR-0022	1991	-116.37	
R1513-SR-0022	1989	-117.35	
R1513-SR-0022	1987	-115.2	
R1513-SR-0022	1983	-112.87	
R1513-SR-0022	1981	-108.94	
R1513-SR-0022	1980	-105.38	
R1513-SR-0022	1979	-112.165	
R1513-SR-0022	1978	-111.38	
R1513-SR-0022	1977	-110.29	
R1513-SR-0022	1976	-110.235	
R1513-SR-0022	1975	-114.28	
R1513-SR-0022	1974	-110.07	
R1513-SR-0022	1973	-110.89	
R1513-SR-0022	1972	-110.785	
2464-A	2006	-101.345	1.251579
2464-A	2005	-101.13	2.5455844

2464-A	2004	-102.205	1.7182695
2464-A	2003	-99.26	
2464-A	2002	-102.98	
2464-A	2001	-101.32	
2464-A	2000	-99.57	
2464-A	1999	-103.78	
2464-B	2006	-102.125	0.7000357
2464-B	2005	-101.01	1.1384419
2464-B	2004	-103.54	0.7848885
2464-B	2003	-104.79	0.4525483
2464-B	2002	-103.225	
2464-B	2001	-103.06	
2464-B	2000	-98.16	
2464-B	1999	-102	
2464-B	1998	-99.11	
2448	2006	-98.67	0.0424264
2448	2005	-101.345	0.0777817
2448	2004	-99.09	
2448	2003	-99.53	
2448	2002	-98.3	
2448	2001	-97.84	
2448	2000	-104.45	
2448	1999	-100.83	
2448	1998	-95.08	
A51-010	2016	-83.6	
A51-010	2015	-84.9	
A51-010	2014	-86.23	0.6505382
A51-010	2013	-86.16	
A51-010	2012	-85.225	0.7000357
A51-010	2011	-85.34	

Table A.2 Water deuterium values

Latitude	**Longitude**	**Depth**	**δD (‰ VSMOW)**
60.469	-61.2803	Surface	-8.0
60.469	-61.2803	5	-3.4
60.469	-61.2803	10	-5.1
60.469	-61.2803	20	-7.2
60.469	-61.2803	30	-6.2
60.469	-61.2803	40	-8.4

60.469	-61.2803	50		-0.6
60.469	-61.2803	60		-4.8
60.469	-61.2803	70		-4.1
60.469	-61.2803	80		
60.469	-61.2803	100		0.0
60.469	-61.2803	125		-1.9
60.469	-61.2803	150		-1.8
60.469	-61.2803	175		-0.3
60.469	-61.2803	200		-1.5
60.469	-61.2803	300		-0.2
60.469	-61.2803	400		0.9
60.469	-61.2803		Bottom (418.7)	0.5

ANNEX B

BARIUM, LEAD, AND STABLE ISOTOPES OF *KERATOISIS*

Table B.1 *Keratoisis* elemental and isotope data (annually resolved)

Est. Cal yr	**Ba/Ca 2452 (CPS)**	**PbCa 2452 (CPS)**	**δ13C 2452 (‰VPDB)**	**δ15N 2452 (‰ AIR)**	**BaCa 2442 (CPS)**	**PbCa 2442 (CPS)**	**δ13C 2442 (‰ VPDB)**	**δ15N 2442 (‰ AIR)**
1914	2.76E-03	5.19E-05	NA	NA	NA	NA	NA	NA
1915	2.26E-03	6.59E-05	NA	NA	NA	NA	NA	NA
1916	2.57E-03	4.74E-05	NA	NA	NA	NA	NA	NA
1917	2.85E-03	5.84E-05	NA	NA	NA	NA	NA	NA
1918	2.78E-03	7.64E-05	-17.21	12.74	NA	NA	NA	NA
1919	2.70E-03	5.12E-05	-17.12	12.74	NA	NA	NA	NA
1920	2.97E-03	4.65E-05	-17.03	12.74	NA	NA	NA	NA
1921	2.78E-03	6.70E-05	-17.02	12.73	NA	NA	NA	NA
1922	2.50E-03	6.32E-05	-17.02	12.73	NA	NA	NA	NA
1923	2.53E-03	5.44E-05	-17.01	12.72	NA	NA	NA	NA
1924	2.84E-03	6.82E-05	-17.08	12.86	NA	NA	NA	NA
1925	2.75E-03	9.33E-05	-17.15	13	NA	NA	NA	NA

1926	2.93E-03	8.66E-05	-17.12	12.9	NA	NA	NA	NA
1927	3.03E-03	8.63E-05	-17.09	12.79	NA	NA	NA	NA
1928	2.69E-03	8.18E-05	-17.13	12.84	3.69E-03	1.02E-04	NA	NA
1929	2.63E-03	1.02E-04	-17.16	12.9	3.67E-03	1.28E-04	NA	NA
1930	2.91E-03	9.87E-05	-17.2	12.95	3.40E-03	9.30E-05	NA	NA
1931	2.62E-03	8.73E-05	-17.51	13.37	3.64E-03	7.98E-05	NA	NA
1932	2.88E-03	1.05E-04	-17.82	13.78	3.34E-03	8.69E-05	NA	NA
1933	2.60E-03	1.23E-04	-17.73	13.61	3.46E-03	1.52E-04	NA	NA
1934	2.80E-03	1.42E-04	-17.63	13.44	3.50E-03	1.11E-04	NA	NA
1935	2.65E-03	1.06E-04	-17.7	13.54	3.35E-03	9.62E-05	NA	NA
1936	2.52E-03	1.13E-04	-17.77	13.63	3.18E-03	1.03E-04	NA	NA
1937	2.65E-03	1.06E-04	-17.84	13.73	3.53E-03	1.17E-04	NA	NA
1938	2.53E-03	1.11E-04	-17.85	13.67	3.28E-03	1.20E-04	NA	NA
1939	2.97E-03	1.60E-04	-17.85	13.6	3.53E-03	1.30E-04	NA	NA
1940	2.76E-03	1.67E-04	-17.79	14.01	3.46E-03	1.47E-04	NA	NA
1941	2.56E-03	1.51E-04	-17.73	14.42	3.51E-03	1.75E-04	-17.73	12.4
1942	2.64E-03	2.10E-04	-17.72	14.22	3.39E-03	1.62E-04	-17.73	12.7
1943	3.04E-03	2.01E-04	-17.7	14.01	3.37E-03	1.70E-04	-17.58	12.7
1944	2.91E-03	2.30E-04	-17.69	13.81	3.70E-03	1.51E-04	-17.43	12.7
1945	2.95E-03	2.07E-04	-17.72	14	4.01E-03	1.85E-04	-17.69	12.7
1946	2.62E-03	2.16E-04	-17.74	14.18	3.76E-03	2.08E-04	-17.69	12.5

1947	2.84E-03	2.38E-04	-17.47	14.18	3.66E-03	2.39E-04	-17.69	12.3
1948	2.37E-03	2.04E-04	-17.19	14.17	4.39E-03	1.86E-04	-17.69	12.9
1949	2.47E-03	2.24E-04	-17.27	14.11	4.03E-03	1.78E-04	-17.79	13.1
1950	2.51E-03	1.60E-04	-17.34	14.05	3.34E-03	1.31E-04	-17.89	13.3
1951	2.45E-03	1.64E-04	-17.42	13.99	3.65E-03	1.28E-04	-17.8	12.7
1952	2.49E-03	1.96E-04	-17.21	13.95	3.57E-03	1.50E-04	-17.49	13.2
1953	2.65E-03	1.81E-04	-17	13.91	3.77E-03	1.31E-04	-17.53	13.05
1954	2.78E-03	2.08E-04	-16.99	13.96	3.83E-03	1.17E-04	-17.57	12.9
1955	2.90E-03	1.92E-04	-16.98	14.01	3.70E-03	1.18E-04	-17.8	13.1
1956	3.04E-03	1.96E-04	-17.2	14.23	3.73E-03	1.42E-04	-17.805	13.1
1957	2.82E-03	1.80E-04	-17.41	14.45	3.89E-03	1.41E-04	-17.81	13.1
1958	2.80E-03	1.62E-04	-17.63	14.67	3.90E-03	1.44E-04	-17.56	13.2
1959	2.64E-03	1.79E-04	-17.58	14.69	3.92E-03	1.38E-04	-17.485	13.15
1960	2.43E-03	1.60E-04	-17.53	14.7	3.69E-03	1.07E-04	-17.41	13.1
1961	2.51E-03	1.74E-04	-17.27	14	4.01E-03	1.19E-04	-17.56	13
1962	2.69E-03	2.13E-04	-17	13.29	3.89E-03	1.44E-04	-17.59	13.1
1963	2.80E-03	2.11E-04	-16.87	13.28	4.04E-03	1.19E-04	-17.62	13.2
1964	2.98E-03	2.23E-04	-16.75	13.27	3.93E-03	1.51E-04	-17.35	13.3
1965	2.99E-03	1.95E-04	-16.62	13.26	4.22E-03	1.28E-04	-17.22	13.6
1966	2.91E-03	2.02E-04	-16.64	13.7	4.22E-03	1.33E-04	-17.23	13.4
1967	3.08E-03	1.99E-04	-16.66	14.14	4.11E-03	1.47E-04	-17.24	13.2

1968	2.86E-03	1.85E-04	-16.85	14.4	4.13E-03	1.92E-04	-17.29	13.1
1969	2.71E-03	2.26E-04	-17.03	14.66	4.45E-03	1.68E-04	-17.34	13
1970	3.02E-03	2.03E-04	-17.22	14.92	4.24E-03	2.21E-04	-17.39	12.9
1971	3.37E-03	2.57E-04	-17.02	14.75	4.19E-03	2.31E-04	-17.26	13.4
1972	3.16E-03	2.57E-04	-16.82	14.58	4.41E-03	2.09E-04	-17.29	13.4
1973	3.15E-03	2.21E-04	-16.67	14.27	4.24E-03	1.68E-04	-17.32	13.4
1974	2.89E-03	2.44E-04	-16.52	13.95	4.08E-03	2.25E-04	-17.83	12.9
1975	2.44E-03	3.04E-04	-16.72	14.2	4.32E-03	2.42E-04	-17.8	13.6
1976	2.71E-03	2.69E-04	-16.93	14.44	3.96E-03	2.83E-04	-17.71	13.75
1977	2.50E-03	2.59E-04	-17.13	14.69	3.87E-03	3.75E-04	-17.62	13.9
1978	2.28E-03	3.39E-04	-17.3	14.4	3.43E-03	3.33E-04	-17.97	13.3
1979	2.50E-03	3.87E-04	-17.46	14.11	3.89E-03	3.57E-04	-17.955	13.3
1980	2.49E-03	3.38E-04	-17.2	13.92	3.90E-03	3.21E-04	-17.94	13.3
1981	2.48E-03	3.50E-04	-16.94	13.73	4.03E-03	3.12E-04	-17.64	14
1982	2.41E-03	3.19E-04	-17.14	14.03	4.60E-03	3.39E-04	-17.6	13.7
1983	2.70E-03	3.51E-04	-17.34	14.33	3.92E-03	2.56E-04	-17.56	13.4
1984	2.65E-03	2.97E-04	-17.54	14.63	3.91E-03	2.88E-04	-17.64	13.2
1985	2.98E-03	3.58E-04	-17.13	14.66	3.80E-03	3.27E-04	-17.91	13.2
1986	3.08E-03	3.19E-04	-16.72	14.69	4.01E-03	3.97E-04	-17.825	13.4
1987	3.06E-03	3.34E-04	-16.74	14.42	4.44E-03	4.24E-04	-17.74	13.6
1988	3.02E-03	3.66E-04	-16.76	14.15	3.88E-03	4.20E-04	-17.86	13

1989	3.14E-03	2.94E-04	-17.1	14.44	3.98E-03	3.40E-04	-18	13
1990	3.05E-03	2.80E-04	-17.45	14.73	3.89E-03	3.93E-04	-18.14	13
1991	2.66E-03	1.86E-04	-17.79	15.02	3.82E-03	3.46E-04	-17.96	13.6
1992	2.62E-03	1.85E-04	-17.71	14.97	3.62E-03	3.75E-04	-17.965	13.3
1993	2.87E-03	2.20E-04	-17.63	14.92	3.62E-03	3.90E-04	-17.97	13
1994	2.81E-03	2.76E-04	-17.83	14.91	3.77E-03	4.01E-04	-17.75	13.2
1995	2.84E-03	2.07E-04	-18.02	14.89	3.47E-03	4.06E-04	-17.81	13.3
1996	2.57E-03	1.68E-04	-17.9	14.84	3.70E-03	3.82E-04	-17.87	13.4
1997	2.55E-03	1.84E-04	-17.79	14.78	4.01E-03	3.56E-04	-17.7	13
1998	2.64E-03	1.94E-04	-17.67	14.73	4.36E-03	3.16E-04	-17.79	13.3
1999	3.04E-03	2.03E-04	-17.66	14.82	4.49E-03	2.63E-04	-17.81	13.5
2000	3.10E-03	1.90E-04	-17.65	14.91	4.40E-03	2.40E-04	-17.83	13.7
2001	2.86E-03	1.73E-04	-17.65	14.95	4.59E-03	2.40E-04	-18.13	13.5
2002	2.85E-03	1.46E-04	-17.64	14.99	4.43E-03	1.85E-04	-18.09	13.8
2003	2.65E-03	1.12E-04	-17.78	14.77	4.58E-03	2.54E-04	-18.05	14.1
2004	2.85E-03	1.48E-04	-17.92	14.54	4.02E-03	2.28E-04	-17.77	13.9
2005	2.83E-03	1.55E-04	-18.06	14.32	4.09E-03	2.19E-04	-17.845	13.8
2006	2.70E-03	1.26E-04	-18.1	14.27	4.65E-03	2.09E-04	-17.92	13.7
2007	3.12E-03	1.17E-04	-18.13	14.22	3.60E-03	1.73E-04	-17.9	14.8

ANNEX C

LABRADOR SEA : WATER COLUMN PROFILE DATA

Table C.1 Physical, nutrient, and isotope sampling data

Station	**Depth (m)**	**Temp (C)**	**PSU**	**Nitrate [uM]**	**Silicate [uM]**	**Phosphate [uM]**	**δ15N NO_3^- (‰ AIR)**	**δ18O NO_3^- (‰ VSMOW)**
650	2.8	3.17	32.10	0.82	1.59	0.37	5.927	18.66
650	5	3.22	32.09	0.81	2.46	0.37	11.055	19.936
650	10.4	3.06	32.12	0.89	1.65	0.38	6.735	19.36
650	20.4	2.74	32.14	1.22	1.77	0.42	NA	NA
650	30.4	2.86	32.13	1.15	1.75	0.41	NA	NA
650	39.9	2.16	32.18	2.06	2.41	0.52	7.07	6.933
650	50.6	1.25	32.28	3.08	2.98	0.62	4.521	4.658
650	60.5	0.55	32.37	3.97	3.74	0.69	NA	NA
650	75.7	0.41	32.50	4.58	4.35	0.72	5.617	19.798
650	80.9	0.16	32.53	4.71	4.57	0.74	4.67	3.924
650	100.6	-0.17	32.69	5.59	5.37	0.79	5.549	5.126
650	126.2	-0.5	32.85	7.03	7.16	0.85	5.805	2.061
650	151.8	-0.07	33.01	7.31	7.53	0.83	4.736	2.109
650	176.8	-0.12	33.20	8.43	8.78	0.85	4.548	4.915
650	196.4	-0.3	33.35	8.96	9.18	0.86	5.429	3.082
645	2.4	2.31	32.59	1.5	2.32	0.39	NA	NA
645	5.5	2.3	32.59	1.55	2.14	0.39	NA	NA
645	10.1	2.29	32.59	1.59	2.16	0.4	NA	NA
645	20.2	1.68	32.66	2.87	2.87	0.53	3.737	5.659
645	29.8	1.14	32.77	4.31	3.86	0.67	6.093	4.459
645	40.2	1.03	32.87	4.96	4.65	0.7	6.26	3.814
645	50.1	1.56	32.99	4.93	4.63	0.67	8.437	12.79
645	60.2	1.61	33.02	5.03	4.89	0.67	6.1	2.772
645	70.3	1.96	33.14	4.71	4.79	0.63	5.195	8.917
645	80.9	1.99	33.18	5.02	5.01	0.65	5.554	3.87

645	100.9	1.06	33.21	6.78	7.5	0.77	5.507	8.3
645	104.6	0.91	33.22	6.7	7.42	0.76	5.13	5.932
640	2.5	1.73	32.32	2.88	2.94	0.53	2.426	6.134
640	5.2	1.76	32.33	1.59	2.75	0.51	NA	NA
640	10	1.74	32.34	1.6	2.75	0.5	NA	NA
640	20.4	1.77	32.34	1.63	2.77	0.5	NA	NA
640	30.4	1.21	32.35	3.33	3.47	0.65	3.78	5.277
640	40.3	1.4	32.51	3.05	3.36	0.59	3.162	6.822
640	50.6	1.02	32.55	4.02	4.17	0.68	4.49	4.212
640	60.8	0.9	32.58	4.39	4.52	0.7	1.779	7.334
640	70.4	0.59	32.68	5.29	5.46	0.76	3.322	2.51
640	81.4	0.36	32.73	6.06	6.12	0.79	2.586	3.205
640	101.5	0.32	32.77	6.29	6.58	0.8	1.413	3.709
640	126.2	0.42	33.04	7.07	8.21	0.82	3.855	3.338
640	129.1	0.42	33.04	7.03	8.28	0.82	NA	NA
ROV-2	2	2.98	32.81	0.02	0	0.18	NA	NA
ROV-2	5	2.96	32.80	0.04	0	0.18	NA	NA
ROV-2	10	2.8	32.96	0.16	0	0.19	NA	NA
ROV-2	20	1.55	33.03	0.42	0.61	0.23	NA	NA
ROV-2	30	2.02	33.13	0.62	0.2	0.25	NA	NA
ROV-2	40	0.83	33.14	2.77	2.4	0.48	NA	NA
ROV-2	50	-0.02	33.17	3.68	3.42	0.56	6.75	2.843
ROV-2	60	-0.26	33.32	5.36	5.12	0.66	5.732	1.984
ROV-2	70	-0.63	33.39	6.68	6.22	0.74	6.877	1.391
ROV-2	80	-0.8	33.50	7.54	6.61	0.76	5.423	1.737
ROV-2	100	-0.89	33.69	8.91	7.3	0.79	NA	NA
ROV-2	125	-0.01	33.92	9.88	7.62	0.81	NA	NA
ROV-2	150	0.59	34.04	10.98	8.19	0.86	5.355	2.764
ROV-2	175	1.43	34.21	12.33	9.35	0.93	5.183	2.36
ROV-2	200	1.82	34.30	13.05	9.67	0.97	5.022	1.405
ROV-2	250	3.04	34.57	14.55	11.44	1.06	5.375	2.491
ROV-2	280	3.07	34.58	14.61	11.56	1.12	5.246	2.173
ROV-3	2	NA	NA	NA	NA	NA	NA	NA
ROV-3	5	NA	NA	NA	NA	NA	NA	NA
ROV-3	10	NA	NA	NA	NA	NA	NA	NA
ROV-3	20	NA	NA	NA	NA	NA	NA	NA
ROV-3	30	NA	NA	NA	NA	NA	NA	NA
ROV-3	40	NA	NA	NA	NA	NA	4.786	2.905
ROV-3	50	NA	NA	NA	NA	NA	1.758	7.373
ROV-3	60	NA	NA	NA	NA	NA	5.859	3.331
ROV-3	70	NA	NA	NA	NA	NA	3.886	3.106
ROV-3	80	NA	NA	NA	NA	NA	4.656	3.471

ROV-3	100	NA	NA	NA	NA	NA	5.15	2.219
ROV-3	125	NA	NA	NA	NA	NA	4.638	2.877
ROV-3	150	NA	NA	NA	NA	NA	4.531	2.29
ROV-3	175	NA	NA	NA	NA	NA	4.583	2.427
ROV-3	200	NA	NA	NA	NA	NA	4.427	2.5
ROV-3	250	NA	NA	NA	NA	NA	4.953	2.235
ROV-3	300	NA	NA	NA	NA	NA	5.053	2.542
ROV-3	400	NA	NA	NA	NA	NA	4.804	2.374
ROV-3	430	NA	NA	NA	NA	NA	4.839	2.521
ROV-1	1.8	4.25	33.33	0	0	0.07	NA	NA
ROV-1	4.8	4.3	33.32	0	0	0.07	NA	NA
ROV-1	9.9	4.24	33.32	0	0	0.07	NA	NA
ROV-1	20	3.98	33.54	0.13	0	0.08	NA	NA
ROV-1	30	3.26	33.60	0.62	0	0.1	NA	NA
ROV-1	40	2.83	33.65	0.92	0	0.12	NA	NA
ROV-1	49.9	1.69	33.77	2.92	1.02	0.33	NA	NA
ROV-1	60.2	0.55	33.89	7.14	4.38	0.64	NA	NA
ROV-1	70	0.28	33.93	9.45	6.47	0.75	4.72	3.173
ROV-1	80	0.47	33.98	10.49	7.69	0.81	NA	NA
ROV-1	100.1	0.91	34.10	11.88	8.09	0.85	4.841	1.758
ROV-1	125.1	1.4	34.19	12.21	8.1	0.84	4.773	1.775
ROV-1	150	1.9	34.32	12.89	8.52	0.87	5.024	1.424
ROV-1	174.6	2.46	34.43	13.64	8.71	0.92	5.009	2.663
ROV-1	200.3	2.94	34.53	13.76	8.85	0.92	NA	NA
ROV-1	249.8	3.69	34.68	14.31	8.7	0.93	NA	NA
ROV-1	300	3.95	34.77	14.98	9.93	0.97	4.999	2.539
ROV-1	400.2	4.08	34.86	15.89	10.9	1.03	NA	NA
ROV-1	494.3	4.1	34.86	15.96	10.92	1.03	NA	NA
ROV-1	545.5	4.11	34.86	15.89	12.46	1.03	NA	NA
ROV-5	1	5.53	33.32	0	0	0.04	NA	NA
ROV-5	4.9	5.58	33.32	0	0	0.05	NA	NA
ROV-5	9.6	5.43	33.32	0	0	0.04	NA	NA
ROV-5	20.4	4.67	33.44	0	0	0.03	NA	NA
ROV-5	30.2	2.86	33.65	0	0	0.03	NA	NA
ROV-5	40.3	1.09	33.78	2.63	0.52	0.28	NA	NA
ROV-5	50.5	0.38	33.86	7.58	4.78	0.66	4.998	2.163
ROV-5	60.4	0.18	33.93	9.33	6.18	0.74	NA	NA
ROV-5	71.3	0.25	33.95	9.51	6.32	0.75	4.624	1.996
ROV-5	80.7	0.8	34.07	11.84	8.88	0.87	4.916	2.414
ROV-5	100.8	1.35	34.20	13.36	10.55	0.94	NA	NA
ROV-5	126.3	1.94	34.32	13.71	10.31	0.94	NA	NA
ROV-5	151.5	2.48	34.43	14.3	11.42	0.97	5.448	1.736

ROV-5	176.3	3.01	34.56	14.65	11.78	0.99	NA	NA
ROV-5	202.1	3.68	34.69	14.5	9.58	0.95	NA	NA
ROV-5	252.3	4.08	34.79	14.98	9.53	0.97	NA	NA
ROV-5	303.3	4.58	34.89	15.06	7.91	0.95	5.222	2.652
ROV-5	404.3	4.21	34.89	16.07	10.57	1.03	4.967	2.408
ROV-5	505.4	4.06	34.90	16.34	10.86	1.05	4.853	3.998
ROV-5	567.4	3.95	34.91	16.2	11.27	1.14	4.945	1.661
ROV-6	2.1	5.99	33.08	0	1.29	0.1	NA	NA
ROV-6	4.9	5.93	33.15	0	1.24	0.09	NA	NA
ROV-6	10.1	5.93	33.17	0	0.71	0.07	NA	NA
ROV-6	20.3	5.44	33.31	0	0.21	0.04	NA	NA
ROV-6	30.4	3.72	33.44	0.31	0.28	0.1	NA	NA
ROV-6	40.6	2.46	33.61	1.97	0.8	0.26	NA	NA
ROV-6	49.7	1.61	33.67	4.06	2.05	0.48	6.035	4.733
ROV-6	60.5	0.37	33.70	6.88	4.28	0.64	5.349	3.61
ROV-6	70.8	0.48	33.78	8.37	4.82	0.7	4.872	2.791
ROV-6	80.7	0.01	33.78	9.15	5.82	0.73	5.186	3.173
ROV-6	100.9	1.17	33.95	8.96	4.9	0.72	4.486	3.265
ROV-6	126	0.97	34.04	11.04	6.58	0.79	5.157	2.535
ROV-6	151.6	1.39	34.14	11.57	6.47	0.79	5.519	2.939
ROV-6	177	1.59	34.22	12.44	7.69	0.84	5.236	2.426
ROV-6	202.3	2.13	34.32	12.78	7.66	0.86	5.451	2.77
ROV-6	252.3	3.03	34.52	13.72	9.77	0.92	5.472	3.019
ROV-6	303.5	3.43	34.64	14.7	12.4	0.99	5.479	2.156
ROV-6	404	3.55	34.75	15.93	15.22	1.06	5.625	2.483
ROV-6	453.8	3.43	34.73	15.82	16.59	1.07	5.66	2.821
177	1.5	2.17	29.06	0	1.12	0.39	NA	NA
177	5	NA	NA	NA	NA	NA	NA	NA
177	10.4	-0.92	31.89	0.11	1.29	0.51	NA	NA
177	20	-1.26	32.09	1.18	2.53	0.62	NA	NA
177	30.2	-1.43	32.23	1.74	2.74	0.64	NA	NA
177	40.5	-1.49	32.36	3.45	4.95	0.71	9.406	13.307
177	50.4	-1.49	32.42	4.69	6.55	0.82	7.166	14.41
177	60.3	-1.47	32.52	5.09	6.95	0.82	7.693	11.369
177	71	-1.42	32.60	6.16	8.33	0.88	8.814	9.962
177	80.8	-1.37	32.69	7.08	9.05	0.92	7.829	3.021
177	101.2	-1.22	32.95	8.16	10.92	0.95	7.427	2.515
177	126.2	-1.08	33.12	9.14	11.99	0.98	7.023	3.986
177	151.6	-0.76	33.47	10.37	12.88	1	9.561	1.862
177	176.9	-0.55	33.59	11.22	13.93	1.02	7.205	6.135
177	202.2	-0.28	33.76	11.96	14.37	1.03	6.949	1.176
177	252.6	0.41	33.98	12.71	15.72	1.05	7.017	7.659

177	303.8	0.75	34.10	14.43	18.24	1.12	6.856	2.323
177	360.1	1.1	34.24	15.32	19.16	1.13	6.98	2.116
179	1.1	-0.86	31.00	0.02	0.27	0.43	NA	NA
179	5	-0.83	30.98	0	0.29	0.48	NA	NA
179	10.1	-1.04	31.29	0.01	0.18	0.49	NA	NA
179	20	-1.11	31.64	0.11	1.15	0.55	NA	NA
179	30.3	-1.38	32.20	1.16	1.66	0.66	NA	NA
179	40.5	-1.49	32.30	3.16	4.43	0.77	3.96	4.417
179	50.4	-1.52	32.35	4.16	6.38	0.83	4.021	3.153
179	60.7	-1.61	32.54	6.63	11.14	1.01	7.022	1.73
179	70.5	-1.48	32.82	7.94	12.02	1	7.058	1.949
179	81.3	-1.54	32.92	8.26	12.62	1.02	5.689	1.334
179	100.9	-1.52	33.04	8.75	12.72	1.01	7.709	3.264
179	126.2	-1.34	33.20	9.13	12	0.97	5.827	1.172
179	150.9	-0.96	33.44	9.83	12.45	0.98	7.313	2.46
179	177.3	-0.64	33.61	10.9	13.47	1.01	5.866	2.023
ROV-7	1.5	0.64	30.58	0.65	5.05	0.45	NA	NA
ROV-7	4.9	0.64	30.57	0.48	5.12	0.44	NA	NA
ROV-7	9.9	-0.15	31.62	0.54	5.19	0.43	NA	NA
ROV-7	19.8	-0.71	32.73	0.65	5.56	0.42	NA	NA
ROV-7	30.3	-1.23	33.04	4.02	7.51	0.65	3.491	5.233
ROV-7	40.3	-1.52	33.34	7.13	7.85	0.73	6.684	3.071
ROV-7	50.2	-1.57	33.45	7.29	7.9	0.76	6.073	3.059
ROV-7	60.4	-1.67	33.52	7.72	7.74	0.77	5.119	1.533
ROV-7	70.4	-1.69	33.54	7.99	7.88	0.78	1.643	4.223
ROV-7	79.9	-1.69	33.58	8.4	7.86	0.78	5.742	1.793
ROV-7	100.5	-1.67	33.61	8.87	8.07	0.8	5.521	1.203
ROV-7	126	-0.89	33.74	11.2	11	0.93	5.914	1.885
ROV-7	151.4	0.39	33.96	13.42	13.82	1.04	5.402	1.47
ROV-7	176.4	0.81	34.09	14.29	15.77	1.08	5.57	1.522
ROV-7	201.9	1.37	34.21	14.98	16.37	1.1	5.613	1.189
ROV-7	252.5	2.07	34.39	14.94	15.87	1.07	5.482	2.194
ROV-7	302.9	2.07	34.45	15.21	16.76	1.09	5.278	2.151
ROV-7	404.2	2.21	34.53	15.68	18.76	1.12	5.479	1.766
ROV-7	505.4	1.96	34.54	16.38	22.67	1.18	5.602	1.965
ROV-7	606.7	1.43	34.51	17.02	28.94	1.24	5.595	1.622
ROV-7	708.2	1.3	34.51	17.41	33.29	1.29	6.053	1.99
ROV-7	809.6	1.14	34.51	17.21	36.36	1.32	5.788	1.371
ROV-7	901.7	1.05	34.51	18.1	42.12	1.39	5.782	1.323

BIBLIOGRAPHY

Akenhead, S. A, Petrie, B, Ross, C.K., and D.M Ware (1981), Ocean climate and the marine fisheries of Atlantic Canada: an assessment, Bedford Institute of Oceanography Report Series, BI-R-81-6, 121 p.

Altabet, M. A., & Francois, R. (1994). Sedimentary nitrogen isotopic ratio as a recorder for surface ocean nitrate utilization. *Global Biogeochemical Cycles*, 8(1), 103-116.

Andrews A. H., Cordes E. E., Mahoney M. M., Munk K., Coale K. H., Cailliet G. M., and Heifetz J. (2002). Age, growth and radiometric age validation of a deep-sea, habitat-forming gorgonian (Primnoa resedaeformis) from the Gulf of Alaska. *Hydrobiologia*, 471(1-3), 101-110.

Antia, N. J., Harrison, P. J., & Oliveira, L. (1991). The role of dissolved organic nitrogen in phytoplankton nutrition, cell biology and ecology. *Phycologia*, 30(1), 1-89

Azetsu-Scott, K., Jones, E. P., Yashayaev, I., & Gershey, R. M. (2003). Time series study of CFC concentrations in the Labrador Sea during deep and shallow convection regimes (1991–2000). *Journal of Geophysical Research: Oceans*, 108(C11).

Bacastow, R. B., Keeling, C. D., Lueker, T. J., Wahlen, M., and W.G. Mook (1996), The ^{13}C Suess effect in the world surface oceans and its implications for oceanic uptake of CO2: Analysis of observations at Bermuda, Global Biogeochemical Cycles, 10(2), 335-346.

Baker D. M., Webster K. L., and Kim K. (2010). Caribbean octocorals record changing carbon and nitrogen sources from 1862 to 2005. *Global Change Biology*, 16(10), 2701-2710.

Bishop, J. B. K. (1988), The barite-opal-organic carbon association in oceanic particulate matter, Nature, 332, 341–343, doi:10.1038/332341a0.

Bond Z. A., Cohen A. L., Smith S. R. and W. J. Jenkins (2005), Growth and composition of high-Mg calcite in the skeleton of a Bermudian gorgonian (Plexaurella dichotoma): potential for paleothermometry, *Geochemistry, Geophysics, Geosystems*, 6(8), 10.

Bourke, R. H., Addison, V. G., & Paquette, R. G. (1989). Oceanography of Nares Strait and northern Baffin Bay in 1986 with emphasis on deep and bottom water formation. *Journal of Geophysical Research: Oceans*, 94(C6), 8289-8302.

Buhl-Mortensen, L., Olafsdottir, S. H., Buhl-Mortensen, P., Burgos, J. M., & Ragnarsson, S. A. (2015). Distribution of nine cold-water coral species (Scleractinia and Gorgonacea) in the cold temperate North Atlantic: effects of bathymetry and hydrography. *Hydrobiologia*, 759(1), 39-61.

Cairns, S. D. (2007). Deep-water corals: an overview with special reference to diversity and distribution of deep-water scleractinian corals. *Bulletin of Marine Science*, 81(3), 311-322.

Cairns, S. D., & Bayer, F. M. (2005). A review of the genus Primnoa (Octocorallia: Gorgonacea: Primnoidae), with the description of two new species. *Bulletin of Marine Science*, 77(2), 225-256.

Calvert, S. E., and T. F. Pederson (2007), Elemental proxies for palaeoclimatic and palaeooceanographic variability in marine sediments: Interpretation and application, in *Proxies in the Late Cenozoic Paleoceanography*, edited by C. Hillaire-Marcel, and A. de Vernal, pp. 567–644, Elsevier, Amsterdam, doi:10.1016/S1572-5480(07)01019-6

Casciotti, K. L., Sigman, D. M., Hastings, M. G., Böhlke, J. K., & Hilkert, A. (2002). Measurement of the oxygen isotopic composition of nitrate in seawater and freshwater using the denitrifier method. *Analytical Chemistry*, 74(19), 4905-4912.

Chamberlain C. P., Blum J. D., Holmes R. T., Feng X., Sherry T. W., and Graves G. R. (1996). The use of isotope tracers for identifying populations of migratory birds. *Oecologia*, 109(1), 132-141.

Chan, P., Halfar, J., Adey, W., Hetzinger, S., Zack, T., Moore, G. W. K., Wortmann, U.G,, Williams, B., and A. Hou (2017), Multicentennial record of Labrador Sea primary productivity and sea-ice variability archived in coralline algal barium, *Nature communications*, 8, 15543.

Chapman D. C., anmd Beardsley R. C. (1989). On the origin of shelf water in the Middle Atlantic Bight. *Journal of Physical Oceanography*, 19(3), 384-391.

Cimberg, R. L., Gerrodette, T., & Muzik, K. (1981). Habitat requirements and expected distribution of Alaska coral. Final Report, Research Unit, 601, 207-308.

Clarke, R. A., & Coote, A. R. (1988). The formation of Labrador Sea Water. Part III: The evolution of oxygen and nutrient concentration. *Journal of Physical Oceanography*, 18(3), 469-480.

Cordeiro, R., van Ofwegen, L., and G. Williams (2018), World List of Octocorallia. *Keratoisis grayi* Verrill, 1878, Accessed through: World Register of Marine Species at: http://www.marinespecies.org/aphia.phpδp=taxdetails&id=158285 on 2018-11-17

Csanady, G. T., and P. Hamilton (1988), Circulation of slopewater, *Continental Shelf Research*, 8(5-7), 565-624.

Davenne E. and Masson D. (2001). Water properties in the Straits of Georgia and Juan de Fuca. *Fisheries and Oceans Canada*. Retrieved from www.sci.pac.dfo-mpo.gc.ca/osap/projects/straitofgeorgia/JdFG_e.pdf.

Davies, A. J., Roberts, J. M., & Hall-Spencer, J. (2007). Preserving deep-sea natural heritage: emerging Issues in offshore conservation and management. *Biological* Conservation, 138(3), 299-312.

Dawson, J. (2002). Biogeography of azooxanthellate corals in the Caribbean and surrounding areas. *Coral Reefs*, 21(1), 27-40.

DeGrandpre, M. D., Körtzinger, A., Send, U., Wallace, D. W., & Bellerby, R. G. J. (2006). Uptake and sequestration of atmospheric CO2 in the Labrador Sea deep convection region. *Geophysical Research Letters*, 33(21).

Dehairs, F., Chesselet, R. & Jedwab, J. (1980).Discrete suspended particles of barite and the barium cycle in the open ocean. *Earth and Planetary Science Letters*, 49, 528–550.

DeNiro, M. J., & Epstein, S. (1981). Influence of diet on the distribution of nitrogen isotopes in animals. *Geochimica et Cosmochimica Acta*, 45(3), 341-351.

Deutsch, C., N. Gruber, R. M. Key, J. L. Sarmiento, & A. Ganachaud (2001), Denitrification and N2 fixation in the Pacific Ocean, *Global Biogeochemical Cycles*, 15(2), 483–506, doi: 10.1029/2000GB001291.

Drinkwater K. F. and Gilbert D. (2004). Hydrographic variability in the waters of the Gulf of St. Lawrence, the Scotian Shelf and the eastern Gulf of Maine (NAFO Subarea 4) during 1991–2000. *Journal of Northwest Atlantic Fishery Science*, 34, 83–99.

Drinkwater, K. F., & Harding, G. C. (2001). Effects of the Hudson Strait outflow on the biology of the Labrador Shelf. *Canadian Journal of Fisheries and Aquatic Sciences*, *58*(1), 171-184.

Drinkwater, K. F., Myers, R. A, Pettipas, R. G., and T. L. Wright (1994). Climatic data for the northwest Atlantic: the position of the shelf/slope front and the northern boundary of the Gulf Stream between 50W and 75W, 1973-1992. *Canadian Data Report of Fisheries and Ocean Sciences*, 125, Department of Fisheries and Oceans, Canada.

Drinkwater, K. F. (1986), Physical oceanography of Hudson strait and Ungava Bay, In *Elsevier oceanography series* (Vol. 44, pp. 237-264), Elsevier.

Drinkwater K. and Taylor G. (1982). Monthly means of the temperature, salinity and density along the Halifax Section. *Can. Tech. Rep. Fish. Aquat. Sci*, 1093: 1-67.

Dunbar M. J., (1951). Eastern Arctic Waters, Canada. *Fisheries Research Board Bulletin*, 88, 1-131.

Edinger, E., Baker, K., Devillers, R., & Wareham, V. (2007). Coldwater corals off Newfoundland and Labrador: distribution and fisheries impacts. *WWF-Canada.*

Epstein S., Thompson P., and Yapp C.J. (1977). Oxygen and hydrogen isotopic ratios in plant cellulose. *Science*, 198, 1209-1215

Epstein S., Yapp C. J., and Hall, J. H. (1976). The determination of the d/h ratio of non exchangeable hydrogen in cellulose extracted from aquatic and land plants. *Earth and Planetary Science Letters*, 30(2), 241–251.

Estep M. F. and Hoering T. C. (1981). Stable hydrogen isotope fractionations during autotrophic and mixotrophic growth of microalgae. *Plant Physiology*, 67(3), 474-477.

Estep M. F. and Dabrowski H. (1980). Tracing food webs with stable hydrogen isotopes. *Science*, 209(4464), 1537–1538.

Feng X, Krishnamurthy R. V., and Epstein S. (1993) Determination of D/H ratios of nonexchangeable hydrogen in cellulose: A method based on the cellulose-water exchange reaction. *Geochimica et Cosmochimica Acta*, 57, 4249–56.

Filippelli G.M., Laidlaw M., Latimer, J. C., and R. Raftis (2005), Urban lead poisoning and medical geology: An unfinished story. *GSA Today,* 15, 4–11.

Fisheries and Oceans Canada (2018). Daily sea surface temperature and salinity. Retrieved from http://www.pac.dfo-mpo.gc.ca/science/oceans/data-donnees/lightstations-phares/data/DepartureDailySalTemp.txt.

Fisheries and Oceans Canada, Communications (2018). Facts on Canadian Fisheries. www.dfo-mpo.gc.ca. Retrieved 2018-12-09.

Fratantoni P. S. and Pickart R. S. (2007). The western North Atlantic shelfbreak current system in summer. *Journal of Physical Oceanography*, 37(10), 2509-2533.

Freiwald, A., Wilson, J. B., & Henrich, R. (1999). Grounding Pleistocene icebergs shape recent deep-water coral reefs. *Sedimentary Geology*, 125(1), 1-8.

Fry, B., and E. B. Sherr (1989), $\delta^{13}C$ measurements as indicators of carbon flow in marine and freshwater ecosystems, *Stable isotopes in ecological research* (196-229), Springer, New York, NY.

Fry B. and Sherr E. (1984). δ13C measurements as indicators of carbon flow in marine and freshwater ecosystems. *Contributions to Marine Science*, 27, 13–47.

Fuller, S. D., Picco, C., Ford, J., Tsao, C. F., Morgan, L. E., Hangaard, D., & Chuenpagdee, R. (2008). *How We Fish Matters: Addressing the Ecological Impacts of Canadian Fishing Gear. Ecology Action Centre, Living Oceans Society and Marine Conservation Biology Institute, Canada.* ISBN 978-0-9734181-7-0.

Garrett C. J. R., and Loder J. W. (1981). Dynamical aspects of shallow sea fronts. Phil. Trans. R. Soc. Lond. A, 302(1472), 563-581.

Gass, S. E., & Willison, J. M. (2005). An assessment of the distribution of deep-sea corals in Atlantic Canada by using both scientific and local forms of knowledge. In *Cold-water corals and ecosystems* (pp. 223-245). Springer, Berlin, Heidelberg.

Gili J. M., and Coma R. (1998). Benthic suspension feeders: their paramount role in littoral marine food webs. *Trends in Ecology & Evolution*, 13(8), 316-321.

Granger, J., Sigman, D. M., Needoba, J. A., & Harrison, P. J. (2004). Coupled nitrogen and oxygen isotope fractionation of nitrate during assimilation by cultures of marine phytoplankton. *Limnology and Oceanography, 49*(5), 1763-1773.

Grasshoff, K. (1969). A simultaneous multiple channel system for nutrient analysis in seawater with analog and digital data record. Contribution 2338, Woods Hole Oceanographic Institution.

Greenberg, D. A., and B. D. Petrie (1988), The mean barotropic circulation on the Newfoundland shelf and slope, Journal of Geophysical Research: Oceans, 93(C12), 15541-15550.

Griffin, S., & Druffel, E. R. (1989). Sources of carbon to deep-sea corals. *Radiocarbon*, 31(3), 533-543.

Gruber, N., & J. L. Sarmiento (1997), Global patterns of marine nitrogen fixation and denitrification, *Global Biogeochem. Cycles*, 11(2), 235–266, doi: 10.1029/97GB00077.

Häkkinen, S. and P. B. Rhines (2004), Decline of subpolar North Atlantic circulation during the 1990s, Science, 304(5670), 555-559.

Han, G., Chen, N., and Z. Ma (2014), Is there a north-south phase shift in the surface Labrador Current transport on the interannual-to-decadal scaleδ, Journal of Geophysical Research: Oceans, 119(1), 276-287.

Han, G., Ohashi, K., Chen, N., Myers, P. G., Nunes, N., & Fischer, J. (2010). Decline and partial rebound of the Labrador Current 1993–2004: Monitoring ocean currents from altimetric and conductivity-temperature-depth data. *Journal of Geophysical Research: Oceans*, 115(C12).

Harrison P. J., Fulton J. D., Taylor F. J. R., and Parsons T. R. (1983). Review of the biological oceanography of the Strait of Georgia: pelagic environment. *Canadian Journal of Fisheries and Aquatic Sciences*, 40(7), 1064-1094.

Heikoop J. M., Hickmott D. D., Risk M. J., Shearer C. K., and Atudorei V. (2002). Potential climate signals from the deep-sea gorgonian coral *Primnoa* resedaeformis. *Hydrobiologia*, 471, 117–124.

Hetzinger, S., Halfar, J., Zack, T., Mecking, J. V., Kunz, B. E., Jacob, D. E., and W. H. Adey (2013), Coralline algal Barium as indicator for 20th century northwestern North Atlantic surface ocean freshwater variability, Scientific Reports, 3, 1761.

Hill, T. M., Spero, H. J., Guilderson, T., LaVigne, M., Clague, D., Macalello, S., & Jang, N. (2011). Temperature and vital effect controls on bamboo coral (Isididae) isotope geochemistry: a test of the "lines method". *Geochemistry, Geophysics, Geosystems*, 12(4).

Hurrell, J. W. (1995), Decadal trends in the North Atlantic Oscillation: regional temperatures and precipitation, Science, 269(5224), 676-679.

Johannessen S. C., Macdonald, R.W., and Paton D. W. (2003). A sediment and organic carbon budget for the greater Strait of Georgia. *Estuarine, Coastal and Shelf Science*, 56(3-4), 845-860.

Johannessen S. C., O'Brien M. C., Denman K. L., and Macdonald R. W. (2005). Seasonal and spatial variations in the source and transport of sinking particles in the Strait of Georgia, British Columbia, Canada. *Marine Geology*, 216(1-2), 59-77.

Johnston, D. M. (2002). The Northwest Passage Revisited. *Ocean Development & International Law*, *33*(2), 145-164.

Keigwin, L. D., Sachs, J. P., and Y. Rosenthal (2003), A 1600-year history of the Labrador Current off Nova Scotia, Climate Dynamics, 21(1), 53-62.

Kilham, P., & Hecky, R. E. (1988). Comparative ecology of marine and freshwater phytoplankton 1. *Limnology and Oceanography*, 33, 776-795.

Kiriakoulakis K., Fisher E. L., Wolff G. A., Freiwald A., Grehan A., Roberts J. M., Grehand A., and Roberts J. M. (2005). Lipids and nitrogen isotopes of two deep-water corals from the North-East Atlantic: initial results and implications for their nutrition. *Cold-water Corals and Ecosystems*, 715–729. Springer, Berlin, Heidelberg.

Kollmeyer R. C., McGill D.A., and Corwin N. (1967). Oceanography of the Labrador Sea in the vicinity of Hudson Strait in 1965. U.S. Coast Guard Oceanographic Rep. No. CG373-12, Washington, D.C, 92.

Kramp, P.L. (1939). Octocorallia. *The Zoology of Iceland,* 2(7), 1–13.

LaVigne, M., Grottoli, A. G., Palardy, J. E., & Sherrell, R. M. (2016). Multi-colony calibrations of coral Ba/Ca with a contemporaneous in situ seawater barium record. *Geochimica et Cosmochimica Acta*, 179, 203-216.

Lazar, B., Enmar, R., Schossberger, M., Bar-Matthews, M., Halicz, L., and M. Stein (2004), Diagenetic effects on the distribution of uranium in live and Holocene corals from the Gulf of Aqaba, *Geochimica et Cosmochimica Acta*, 68(22), 4583-4593.

Lea, D., Shen, G. T. & Boyle, E. A (1989b). Coralline barium records temporal variability in equatorial Pacific upwelling. *Nature*, 340, 373–376.

LeBlond P. H. (1983). The Strait of Georgia: functional anatomy of a coastal sea. *Canadian Journal of Fisheries and Aquatic Sciences*, 40(7), 1033-1063.

Liu, K. K., & Kaplan, I. R. (1989). The eastern tropical Pacific as a source of 15N-enriched nitrate in seawater off southern California. *Limnology and Oceanography, 34*(5), 820-830.

Loder J. W., Boicourt W. C., and Simpson J. H. (1998). Western ocean boundary shelves (W). *The Sea*, 11, 3-28.

Maher, P. T. (2007). Arctic tourism: a complex system of visitors, communities, and environments. *Polar Geography*, *30*(1-2), 1-5.

Masson D. & Cummins P. F. (2004). Observations and modeling of seasonal variability in the Straits of Georgia and Juan de Fuca. *Journal of Marine Research*, 62(4), 491-516.

Morrison J., Quick M. C., and Foreman M. G. (2002). Climate change in the Fraser River watershed: flow and temperature projections. *Journal of Hydrology*, 263(1-4), 230-244.

Mortensen P. B. and Buhl-Mortensen L. (2005). Morphology and growth of the deep-water gorgonians Primnoa resedaeformis and Paragorgia arborea. *Marine Biology*, 147(3), 775-788.

Mountain D. G. and Jessen P. F. (1987). Bottom waters of the Gulf of Maine, 1978-1983. *Journal of Marine Research*, 45(2), 319-345.

Muzuka A. N. and Hillaire-Marcel C. (1999). Burial rates of organic matter along the eastern Canadian margin and stable isotope constraints on its origin and diagenetic evolution. *Marine Geology*, 160(3-4), 251270.

Neves, B., Edinger, E., Hillaire-Marcel, C., Saucier, E. H., France, S. C., Treble, M. A., & Wareham, V. E. (2015). Deep-water bamboo coral forests in a muddy Arctic environment. *Marine Biodiversity*, 45(4), 867-871.

Nissenbaum, A. (1974) The organic geochemistry of marine and terrestrial humic substances: implications of carbon and hydrogen isotope studies. *Advances in Organic Geochemistry*, 1973, 39-52.

Noé, S. U., Lembke-Jene, L., & Dullo, W. C. (2008). Varying growth rates in bamboo corals: sclerochronology and radiocarbon dating of a mid-Holocene deep-water gorgonian skeleton (Keratoisis sp.: Octocorallia) from Chatham Rise (New Zealand). *Facies*, 54(2), 151-166.

Nriagu, J. O. (1990), The rise and fall of leaded gasoline, Science of the Total Environment, 92, 13-28.

Paton, C., Hellstrom, J., Paul, B., Woodhead, J., and J. Hergt (2011), Iolite: Freeware for the visualisation and processing of mass spectrometric data, Journal of Analytical Atomic Spectrometry, 26(12), 2508-2518.

Petrie B. (2007). Does the North Atlantic Oscillation affect hydrographic properties on the Canadian Atlantic continental shelf? *Atmosphere-Ocean*, 45(3), 141-151.

Petrie B. and Drinkwater K. (1993). Temperature and salinity variability on the Scotian Shelf and in the Gulf of Maine 1945–1990. *Journal of Geophysical Research: Oceans*, 98(C11), 20079-20089.

Petrie, B., and A. Isenor (1985), The near-surface circulation and exchange in the Newfoundland Grand Banks region, *Atmosphere-Ocean*, 23(3), 209-227

R Core Team (2013), R: A language and environment for statistical computing, R Foundation for Statistical Computing, Vienna, Austria, URL http://www.R-project.org/

Redfield, A. C. (1963). The influence of organisms on the composition of seawater. *The sea*, *2*, 26-77.

Riche O., Johannessen S., and Macdonald R. (2014). Why timing matters in a coastal sea: Trends, variability and tipping points in the strait of georgia, canada. *Journal of Marine Systems*, 131, 36–53.

Risk M. J., Lapointe B. E., Sherwood O. A., and Bedford B. J. (2009). The use of δ15N in assessing sewage stress on coral reefs. *Marine Pollution Bulletin*, 58(6), 793–802.

Risk M. J., Heikoop J. M., Snow M. G., and Beukens R. (2002). Lifespans and growth patterns of two deep-sea corals: Primnoa resedaeformis and Desmophyllum cristagalli. *Hydrobiologia*, 471(1-3), 125-131.

Roark, E. B., Guilderson, T. P., Flood-Page, S., Dunbar, R. B., Ingram, B. L., Fallon, S. J., & McCulloch, M. (2005). Radiocarbon-based ages and growth rates of bamboo corals from the Gulf of Alaska. *Geophysical Research Letters*, 32(4).

Roberts, J. M., & Cairns, S. D. (2014). Cold-water corals in a changing ocean. *Current Opinions in Environmental Sustainability*, 7, 118-126.

Roberts, C. M. (2002). Deep impact: the rising toll of fishing in the deep sea. *Trends in Ecology & Evolution*, 17(5), 242-245.

Salvo, F., Hamoutene, D., Hayes, V. E. W., Edinger, E. N., & Parrish, C. C. (2018). Investigation of trophic ecology in Newfoundland cold-water deep-sea corals using lipid class and fatty acid analyses. *Coral Reefs*, 37(1), 157-171.

Sauer P. E., Schimmelmann A., Sessions A. L., and Topalov K. (2009). Simplified batch equilibration for d/h determination of non-exchangeable hydrogen in solid organic material. *Rapid Communications in Mass Spectrometry,* 23(7), 949–956.

Schimmelmann A., Lewan M. D., and Wintsch R. P. (1999). D/H isotope ratios of kerogen, bitumen, oil, and water in hydrous pyrolysis of source rocks containing kerogen types i, ii, iis, and iii. *Geochimica et Cosmochimica Acta*, 63(22), 3751–3766.

Schimmelmann A. and DeNiro M. J. (1986). Stable isotopic studies on chitin. III. The D/H and 18O/16O ratios in arthropod chitin. *Geochimica et Cosmochimica Acta*, 50(7), 1485-1496.

Seitzinger, S. P., & Sanders, R. W. (1999). Atmospheric inputs of dissolved organic nitrogen stimulate estuarine bacteria and phytoplankton. *Limnology and Oceanography*, 44(3), 721-730.

Seitzinger, S. P. (1988). Denitrification in freshwater and coastal marine ecosystems: ecological and geochemical significance. *Limnology and Oceanography*, 33, 702-724.

Serrato-Marks, G., LaVigne, M., Hill, T. M., Sauthoff, W., Guilderson, T. P., Roark, E. B., Dunbar, R. B., & Horner, T. J. (2017). Reproducibility of Ba/Ca variations recorded by northeast Pacific bamboo corals. *Paleoceanography*, 32(9), 966-979.

Session A.L. (2016). Factors controlling the deuterium contents of sedimentary hydrocarbons. *Organic Geochemistry*, 96, 43–64.

Shearman R. K. and Lentz S. J. (2010). Long-term sea surface temperature variability along the US East Coast. *Journal of Physical Oceanography*, 40(5), 1004-1017.

Shen, G. T., & Boyle, E. A. (1987). Lead in corals: reconstruction of historical industrial fluxes to the surface ocean. *Earth and Planetary Science Letters*, 82(3-4), 289-304.

Sherwood O. A., Guilderson T. P., Batista F. C., Schiff J. T., and McCarthy M. D. (2014). Increasing subtropical north pacific ocean nitrogen fixation since the little ice age. *Nature*, 505(7481), 78–81.

Sherwood O. A., Lehmann M. F., Schubert C. J., Scott D. B., and M. D. McCarthy (2011), Nutrient regime shift in the western north atlantic indicated by compound-specific $\delta^{15}N$ of deep-sea gorgonian corals, *Proceedings of the National Academy of Sciences*, 108(3), 1011–1015.

Sherwood, O. A., and E. N. Edinger, E. N (2009), Ages and growth rates of some deep-sea gorgonian and antipatharian corals of Newfoundland and Labrador, Canadian Journal of Fisheries and Aquatic Sciences, 66(1), 142-152.

Sherwood, O. A., Jamieson, R. E., Edinger, E. N., & Wareham, V. E. (2008). Stable C and N isotopic composition of cold-water corals from the Newfoundland and Labrador continental slope: Examination of trophic, depth and spatial effects. *Deep Sea Research Part I: Oceanographic Research Papers*, 55(10), 1392-1402.

Sherwood O. A., Scott D. B., and Risk M. J. (2006). Late holocene radiocarbon and aspartic acid racemization dating of deep-sea octocorals. *Geochimica et Cosmochimica Acta*, 70(11), 2806–2814.

Sherwood O. A., Heikoop J. M., Scott D. B., Risk M. J., Guilderson T. P., & McKinney R.A. (2005a). Stable isotopic composition of deep-sea gorgonian corals Primnoa spp.: A new archive of surface processes. *Marine Ecology Progress Series*, 301, 135–148

Sherwood O. A., Heikoop J. M., Sinclair D. J., Scott D. B., Risk M. J., Shearer C., and Azetsu-scott K. (2005b). Skeletal Mg / Ca in Primnoa resedaeformis: relationship to temperature? *Cold-water Corals and Ecosystems*. 1061–1079.

Sigman, D. M., Granger, J., DiFiore, P. J., Lehmann, M. M., Ho, R., Cane, G., & van Geen, A. (2005). Coupled nitrogen and oxygen isotope measurements of nitrate along the eastern North Pacific margin. *Global Biogeochemical Cycles*, *19*(4).

Sigman, D. M., Casciotti, K. L., Andreani, M., Barford, C., Galanter, M. B. J. K., & Böhlke, J. K. (2001). A bacterial method for the nitrogen isotopic analysis of nitrate in seawater and freshwater. *Analytical chemistry*, *73*(17), 4145-4153.

Sigman, D. M., Altabet, M. A., McCorkle, D. C., Francois, R., & Fischer, G. (2000). The δ15N of nitrate in the Southern Ocean: Nitrogen cycling and circulation in the ocean interior. *Journal of Geophysical Research: Oceans*, *105*(C8), 19599-19614.

Sinclair, D. J., Sherwood, O. A., Risk, M. J., Hillaire-Marcel, C., Tubrett M., Sylvester, P., McCulloch, M., and L. Kinsley (2005), Testing the reproducibility of Mg/Ca profiles in the deep-water coral Primnoa resedaeformis: putting the proxy through its paces, In *Cold-water corals and ecosystems* (pp. 1039-1060), Springer, Berlin, Heidelberg.

Sinclair, D. J., Williams, B., Allard, G., Ghaleb, B., Fallon, S., Ross, S. W., & Risk, M. (2011). Reproducibility of trace element profiles in a specimen of the deep-water bamboo coral Keratoisis sp. *Geochimica et Cosmochimica Acta*, 75(18), 5101-5121.

Sinclair, D. J., Kinsley, L. P., & McCulloch, M. T. (1998). High resolution analysis of trace elements in corals by laser ablation ICP-MS. *Geochimica et Cosmochimica Acta*, 62(11), 1889-1901.

Smith J. E., Schwarcz H. P., Risk M. J., McConnaughey T. A., and Keller N. (2000). Paleotemperatures from Deep-Sea Corals: Overcoming 'Vital Effects'. *Palaios*, 15(1), 25.

Smith, E. H., Soule, F. M., & Mosby, O. (1937). The Marion and General Greene Expeditions to Davis Strait and Labrador Sea, Under Direction of the United States Coast Guard: 1928-1931-1933-1934-1935: Scientific Results, Part 2: Physical Oceanography. US Government Printing Office.

Sternberg, E., C. Jeandel, J.-C. Miquel, B. Gasser, M. Souhaut, R. Arraes-Mescoff, and R. Francois (2007), Particulate barium fluxes and export production in the northwestern Mediterranean, *Marine Chemistry*, 105, 281–295.

Sutcliffe Jr, W. H., Loucks, R. H., Drinkwater, K. F., & Coote, A. R. (1983). Nutrient Flux onto the Labrador Shelf from Hudson Strait and its Biological Consequences. *Canadian Journal of Fisheries and Aquatic Sciences*, *40*(10), 1692-1701.

Swallow, J. C., & Worthington, L. V. (1969, February). Deep currents in the Labrador Sea. In *Deep Sea Research and Oceanographic Abstracts* (Vol. 16, No. 1, pp. 77-84). Elsevier.

Swart, P. K., Greer, L., Rosenheim, B. E., Moses, C. S., Waite, A. J., Winter, A., Dodge R. E., K. Helmle (2010), The ^{13}C Suess effect in scleractinian corals mirror changes in the anthropogenic CO2 inventory of the surface oceans, Geophysical Research Letters, 37(5).

Tang, C. C., Ross, C. K., Yao, T., Petrie, B., DeTracey, B. M., & Dunlap, E. (2004). The circulation, water masses and sea-ice of Baffin Bay. *Progress in Oceanography*, *63*(4), 183-228.

Thresher R. E., Wilson N. C., MacRae C. M., & Neil H. (2010) Temperature effects on the calcite skeletal composition of deep- water gorgonians (Isididae). *Geochimica et Cosmochimica Acta*, 74(16), 4655–4670.

Thresher R., MacRae C., Wilson N., & Gurney R. (2007) Environmental effects on the skeletal composition of deep- water gorgonians (Keratoisis spp.; Isididae). *Bulletin of Marine Science*, 81, 409–422.

Thresher R., Rintoul S. R., Koslow A. J., Weidman C., Adkins J. F., & Proctor C. (2004) Oceanic evidence of climate change in southern Australia over the last three centuries. *Geophysical Research Letters*, 31, L07212. doi: 10.1029/2003GL018869.

Townsend, D. W., Rebuck, N. D., Thomas, M. A., Karp-Boss, L., and R. M. Gettings (2010), A changing nutrient regime in the Gulf of Maine, Continental Shelf Research, 30(7), 820-832.

Townsend, D. W., Thomas, A. C., Mayer, L. M., Thomas, M. A., and J. A. Quinlan (2006), Oceanography of the northwest Atlantic continental shelf (1, W), The sea: the global coastal ocean: interdisciplinary regional studies and syntheses, 14, 119-168.

Voss B. M., Peucker-Ehrenbrink B., Eglinton T. I., Fiske G., Wang Z. A., Hoering K. A., and Gillies, S. L. (2014). Tracing river chemistry in space and time: Dissolved inorganic constituents of the Fraser River, Canada. *Geochimica et Cosmochimica Acta*, 124, 283-308.

Waldichuk, M. (1957). Physical oceanography of the Strait of Georgia, British Columbia. *Journal of the Fisheries Board of Canada*, 14(3), 321-486.

Wareham, V. E., & Edinger, E. N. (2007). Distribution of deep-sea corals in the Newfoundland and Labrador region, Northwest Atlantic Ocean. *Bulletin of Marine Science*, *81*(3), 289-313.

Wilkinson G. M., Cole J. J., and Pace M. L. (2015). Deuterium as a food source tracer: Sensitivity to environmental water, lipid content, and hydrogen exchange. *Limnology and Oceanography: Methods*, 13(5), 213–223.

Williams B., Thibodeau B., Chikaraishi Y., Ohkouchi N., Walnum A., Grottoli A. G., and Colin P. L. (2017). Consistency in coral skeletal amino acid composition offshore of palau in the western pacific warm pool indicates no impact of decadal variability in nitricline depth on primary productivity. *Limnology and Oceanography*, 62(2), 399–407.

Williams B. and Grottoli A. G. (2011). Solution and laser ablation inductively coupled plasma-mass spectrometry measurements of Br, I, Pb, Mn, Cd, Zn, and B in the organic skeleton of soft corals and black corals. *Geochemistry, Geophysics, Geosystems*, 12(3), 1–16.

Williams, B., & Grottoli, A. G. (2010). Recent shoaling of the nutricline and thermocline in the western tropical Pacific. *Geophysical Research Letters*, 37(22).

Williams B., Risk M. J., Ross S. W., and K. J. Sulak (2006), Deep-water antipatharians: proxies of environmental change, Geology, 34(9), 773–776.

Xu X., Werner M., Butzin M., and Lohmann G. (2012). Water isotope variations in the global ocean model MPI-OM. *Geoscientific Model Development*, 5(3), 809-818.

Yamamoto-Kawai, M., Carmack, E., & McLaughlin, F. (2006). Nitrogen balance and Arctic throughflow. *Nature*, *443*(7107), 43.

Zehr, J. P., & Ward, B. B. (2002). Nitrogen cycling in the ocean: new perspectives on processes and paradigms. *Applied and Environmental Microbiology*, 68(3), 1015-1024.

Zhong, S., & Mucci, A. (1989). Calcite and aragonite precipitation from seawater solutions of various salinities: Precipitation rates and overgrowth compositions. *Chemical Geology*, 78(3-4), 283-299.

Zibrowius, H., & Taviani, M. (2005). Remarkable sessile fauna associated with deep coral and other calcareous substrates in the Strait of Sicily, Mediterranean Sea. In *Cold-water corals and ecosystems* (pp. 807-819). Springer, Berlin, Heidelberg.

Zweng M. M, Reagan J. R, Antonov J. I., Locarnini R. A., Mishonov A. V., Boyer T. P., Garcia H.E., Baranova O. K., Johnson D. R., Seidov D., and Biddle M.M., 2013. *World Ocean Atlas 2013, Volume 2: Salinity*. S. Levitus, Ed., A. Mishonov Technical Ed.; *NOAA Atlas NESDIS,* 74, 39 pp.